

Physics Scotland



# *Review of Coherent SASE Schemes*

Lawrence Campbell<sup>1</sup>, David Dunning<sup>1,2</sup>,  
James Henderson<sup>1</sup>, Brian McNeil<sup>1</sup> & Neil Thompson<sup>2</sup>

<sup>1</sup>University of Strathclyde; <sup>2</sup>STFC ASTeC

We acknowledge STFC MoA 4132361; ARCHIE-WeSt HPC, EPSRC grant EP/K000586/1; John von Neumann Institute for Computing (NIC) on JUROPA at Julich Supercomputing Centre (JSC), under project HHH20



Magnetics and Radiation Sources Group



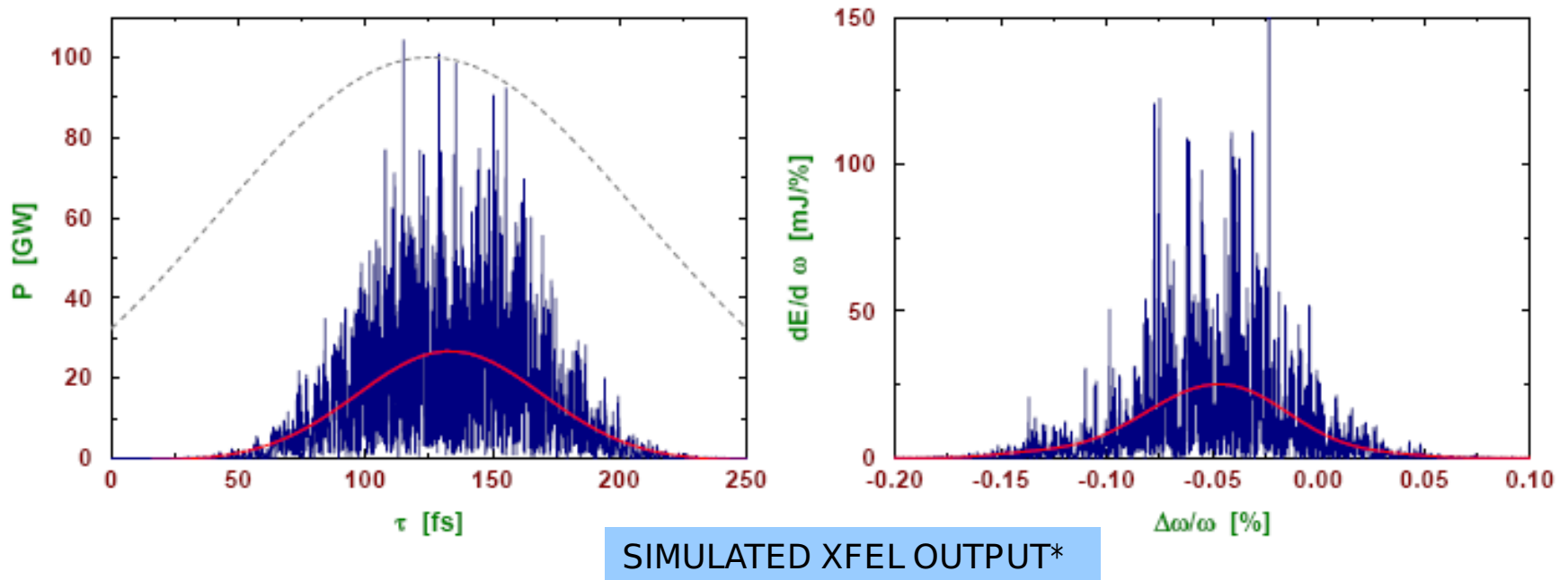
36th International Free Electron Laser Conference, Basel, August 25-29, 2014<sup>1</sup>

# Outline

- Types of Seeding – direct; indirect; self;
- HB-SASE; i-SASE; p-SASE....
- UK CLARA FEL Test Facility

# The issue: SASE photon output

- SASE output is amplified noise
  - Spontaneous emission generated by electron beam in first few gain lengths is the 'seed' which is amplified via an exponential instability.
  - Pulses noisy temporally and spectrally: poor temporal coherence
  - No pulse-to-pulse reproducibility

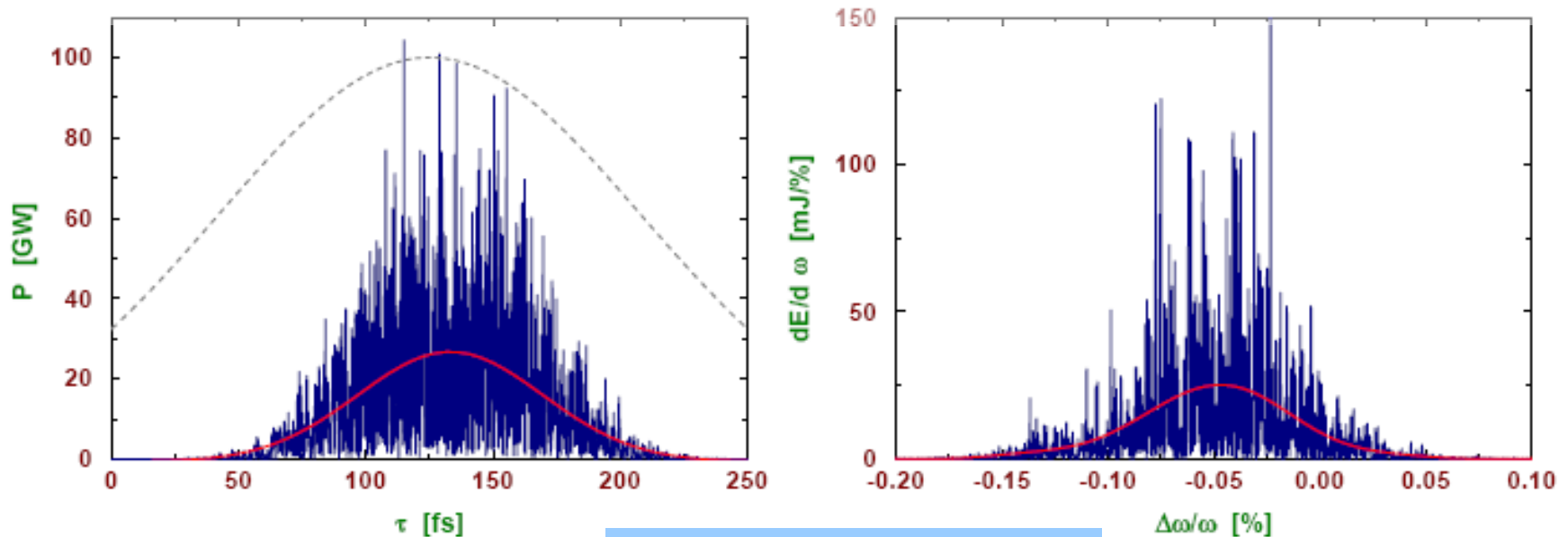


\*Taken from DESY report

# The issue: SASE photon output

- SASE output is amplified noise
  - Spontaneous emission generated by electron beam in first few gain lengths is the 'seed' which is amplified via an exponential instability.
  - Pulses noisy temporally and spectrally: poor temporal coherence
  - No pulse-to-pulse reproducibility

Far from FT limited:  $\Delta\nu \Delta t \gg 1$

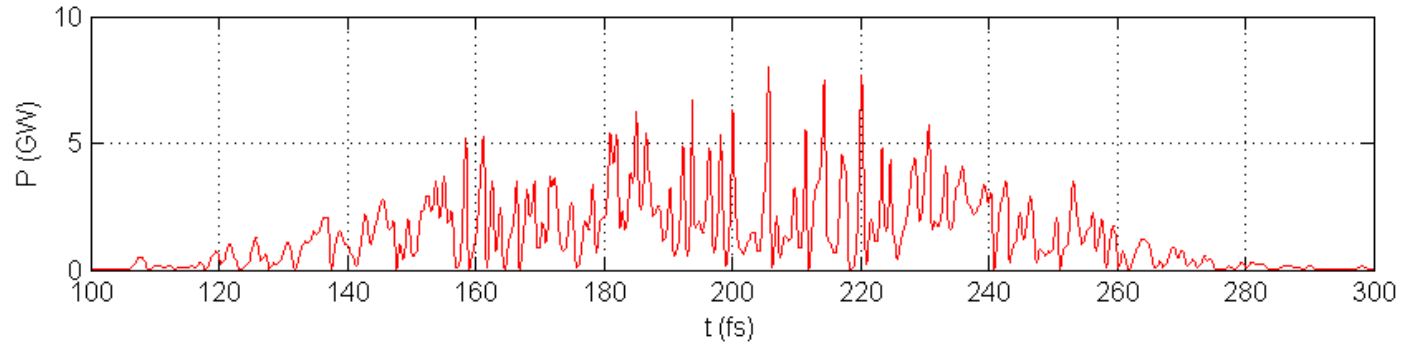


SIMULATED XFEL OUTPUT\*

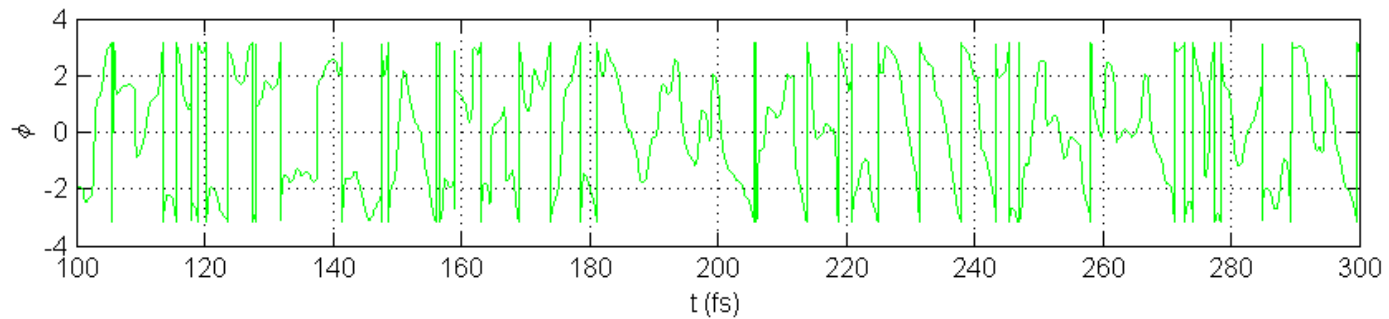
\*Taken from DESY report

# SASE Coherence

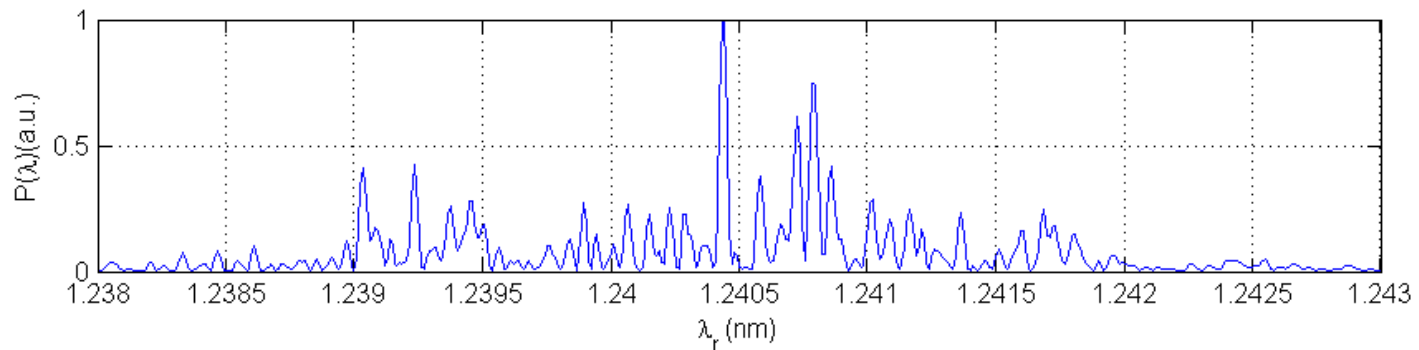
**POWER**



**PHASE**

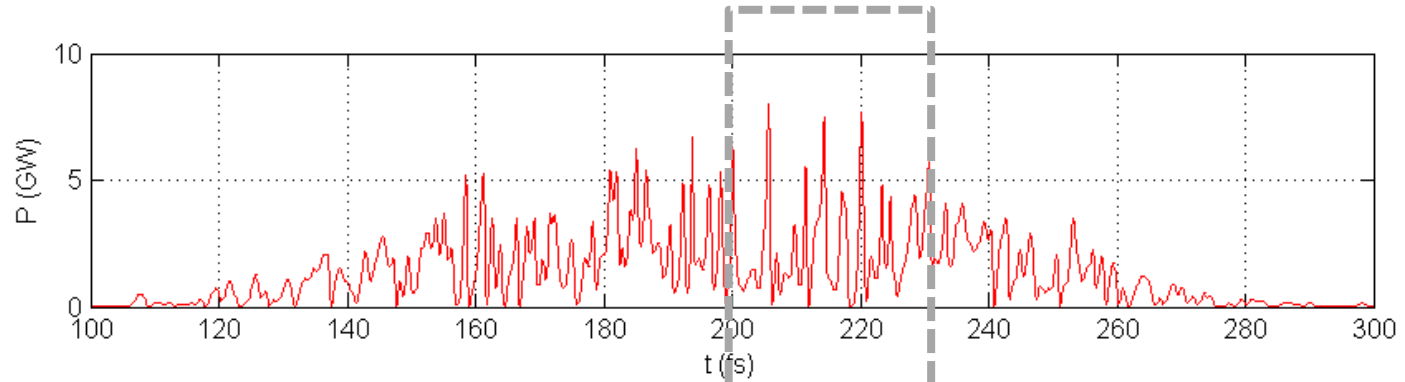


**SPECTRUM**

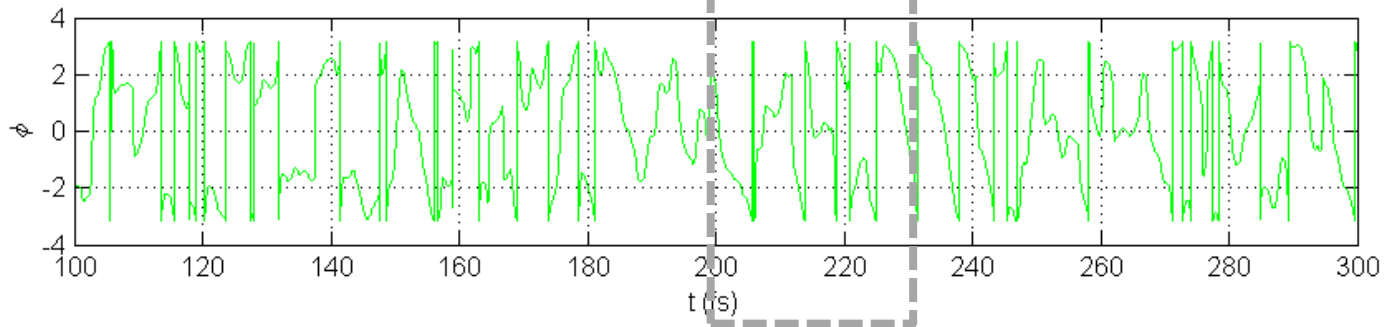


# SASE Coherence

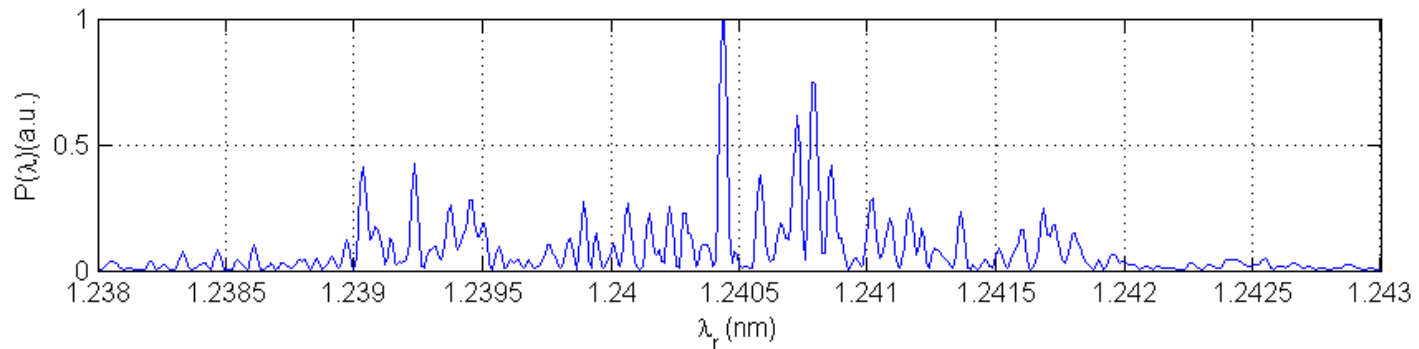
**POWER**



**PHASE**

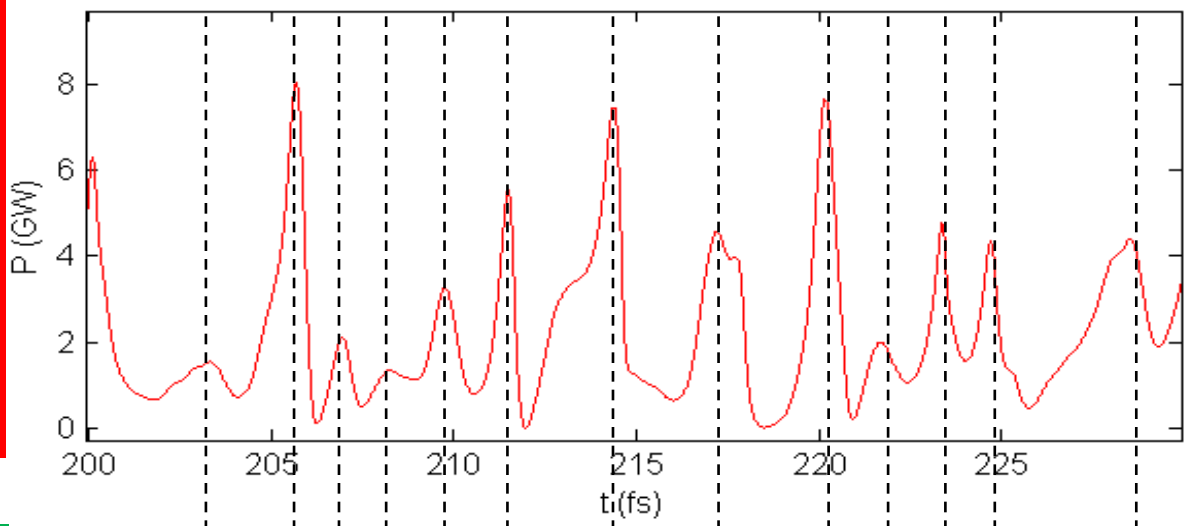


**SPECTRUM**

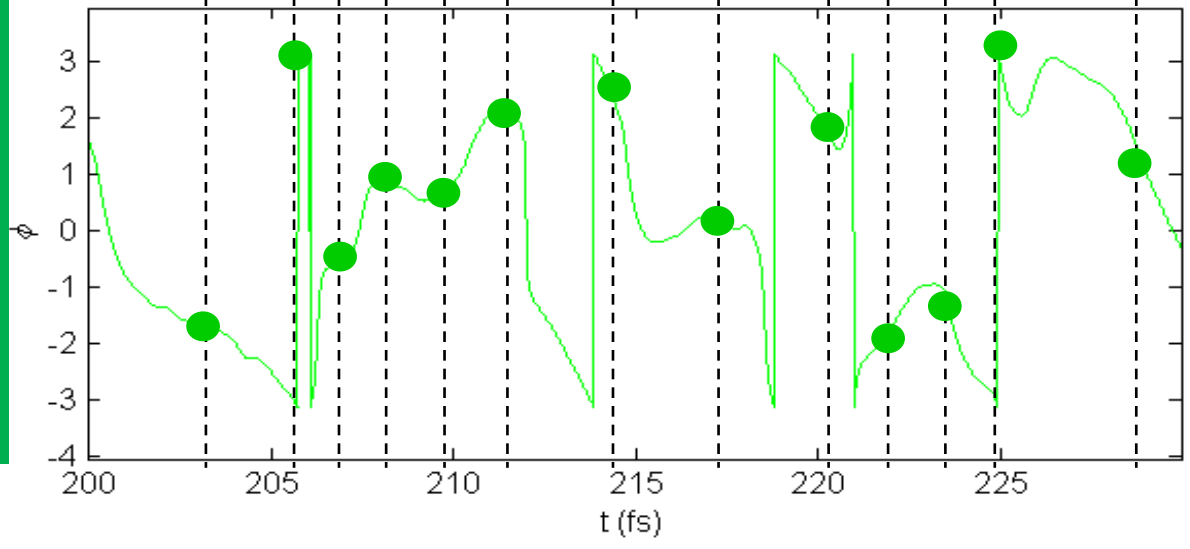


# CASE 2

**POWER**



**PHASE**



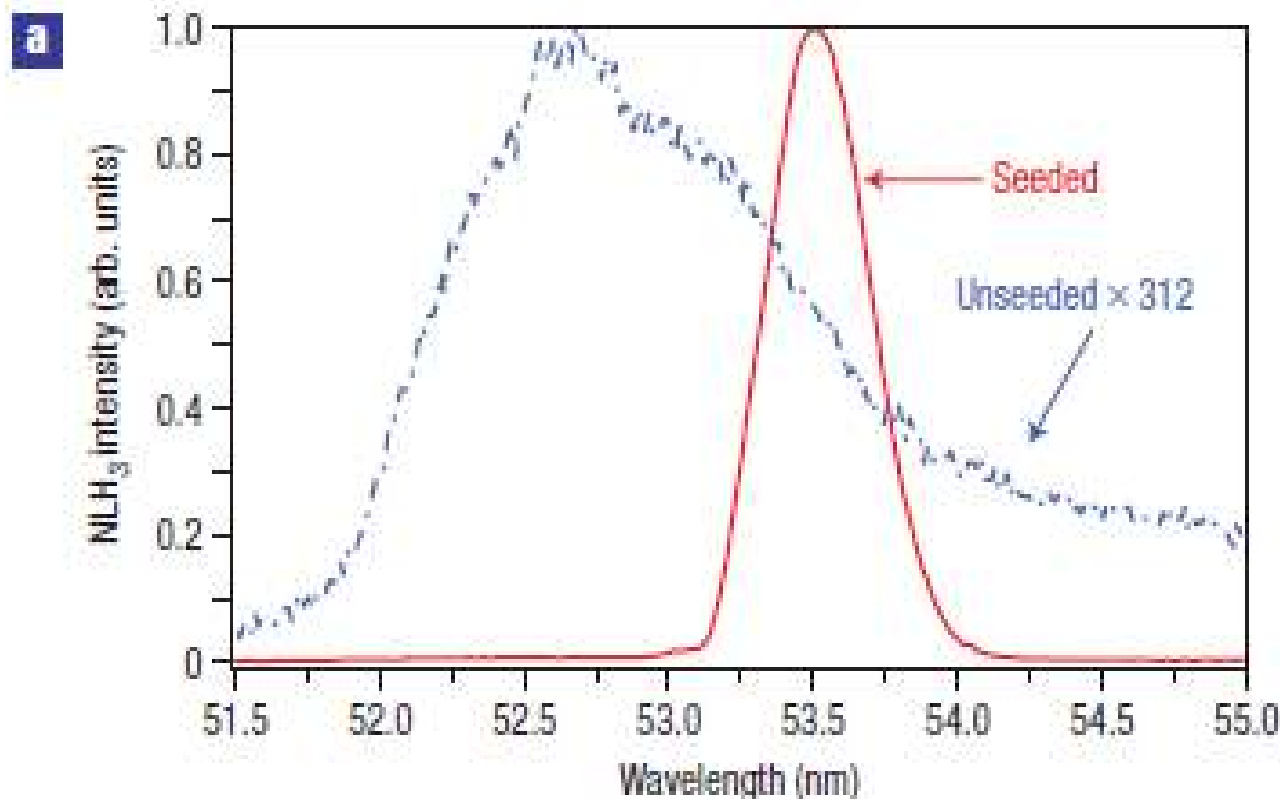
Direct seeding at fundamental



# Injection of harmonics generated in gas in a free-electron laser providing intense and coherent extreme-ultraviolet light

G. LAMBERT<sup>1,2,3\*</sup>, T. HARA<sup>2,4</sup>, D. GARZELLA<sup>1</sup>, T. TANIKAWA<sup>2</sup>, M. LABAT<sup>1,3</sup>, B. CARRE<sup>1</sup>, H. KITAMURA<sup>2,4</sup>, T. SHINTAKE<sup>2,4</sup>, M. BOUGEARD<sup>1</sup>, S. INOUE<sup>4</sup>, Y. TANAKA<sup>2,4</sup>, P. SALIERES<sup>1</sup>, H. MERDJI<sup>1</sup>, O. CHUBAR<sup>3</sup>, O. GOBERT<sup>1</sup>, K. TAHARA<sup>2</sup> AND M.-E. COUPRIE<sup>3</sup>

nature physics | VOL 4 | APRIL 2008



Injection of harmonics generated in gas in a free-electron laser providing intense and coherent extreme-ultraviolet light

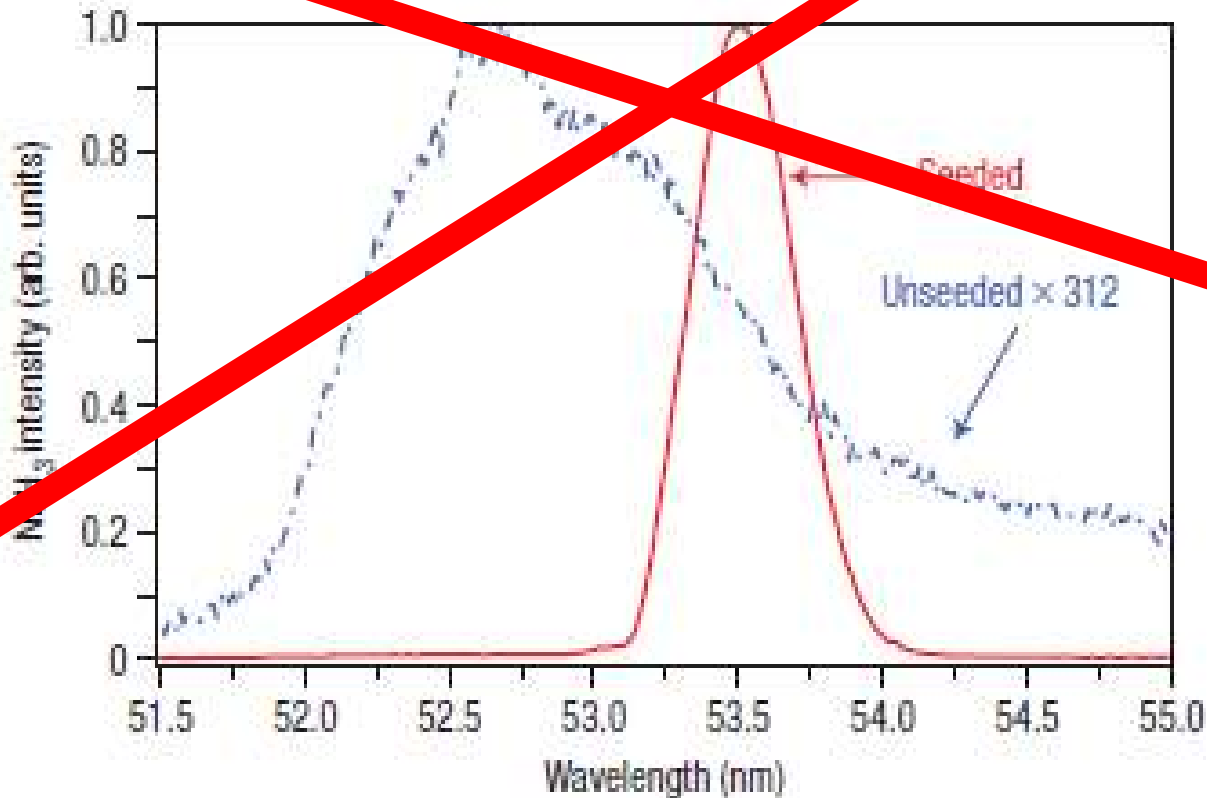
**No seeds**

**in X-ray**

G. LAMBERT<sup>1,2,3\*</sup>, T. HARA<sup>2,4</sup>, D. GARZELI<sup>1</sup>, T. TANIKAWA<sup>2</sup>, M. LABAT<sup>1,3</sup>, B. CARRE<sup>1</sup>, H. MIYAMURA<sup>2,4</sup>, T. SHINTAKE<sup>2,4</sup>, M. BOUGEREAU<sup>1</sup>, S. SINOUE<sup>4</sup>, T. TANAKA<sup>1</sup>, P. SAUERB<sup>5</sup>, H. MERDJI<sup>1</sup>, S. CHUBAR<sup>3</sup>, O. GOBERT<sup>1</sup>, K. TAHARA<sup>2</sup>, AND M.-J. COUILLIE

nature physics | VOL 4 | APRIL 2008

**a**



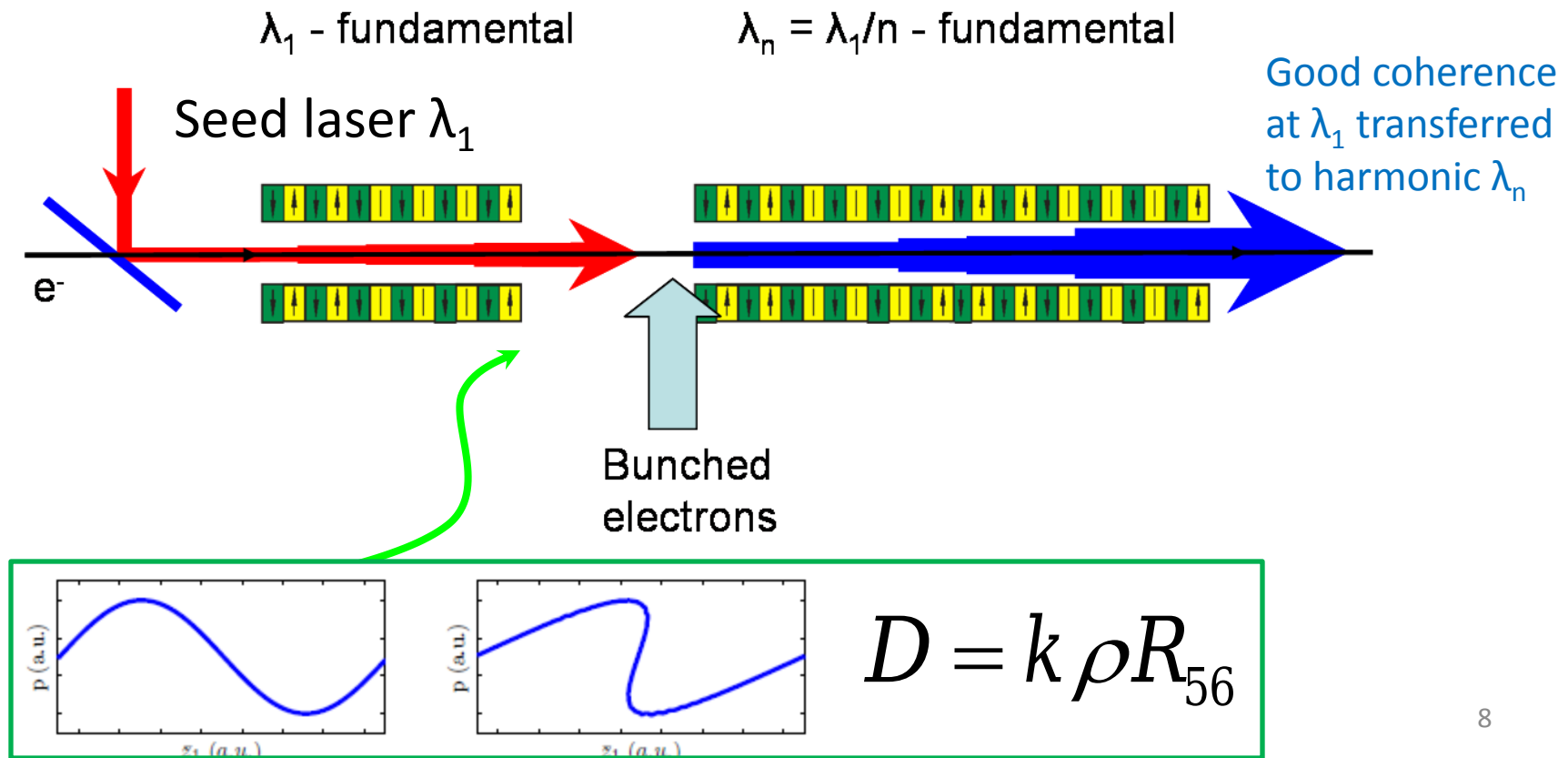
# Indirect Seeding Using Harmonics

‘Use good temporal coherence of a longer wavelength to seed coherence at shorter harmonic wavelength ’

# Harmonic Generation via a longer wavelength seeded beam

R. Bonifacio, L. De Salvo Souza, P. Pierini, and E. T. Scharlemann, NIM A **296**, 787 (1990).

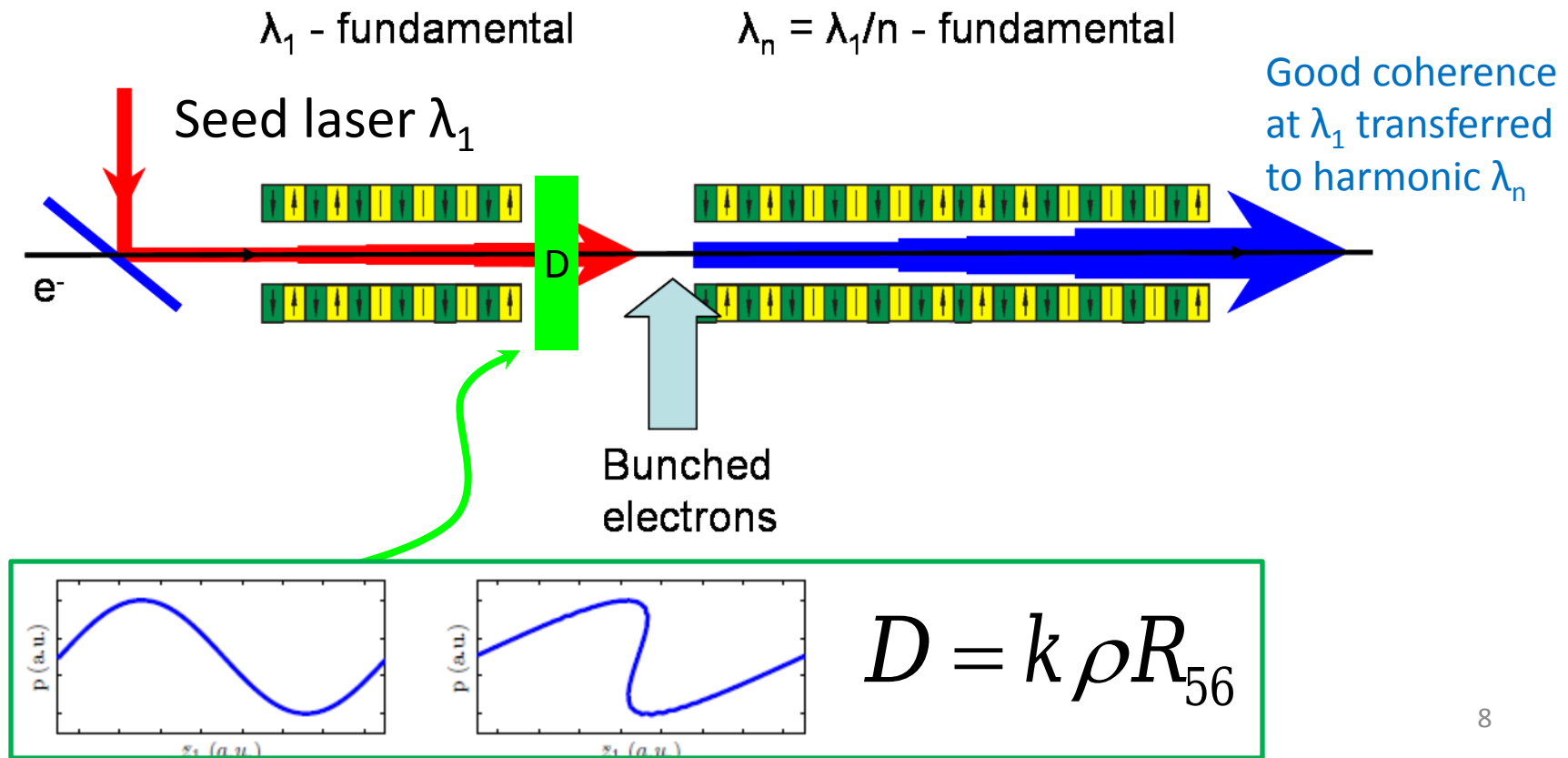
L.-H. Yu *et al.*, Science **289**, 932 (2000).



# Harmonic Generation via a longer wavelength seeded beam

R. Bonifacio, L. De Salvo Souza, P. Pierini, and E. T. Scharlemann, NIM A **296**, 787 (1990).

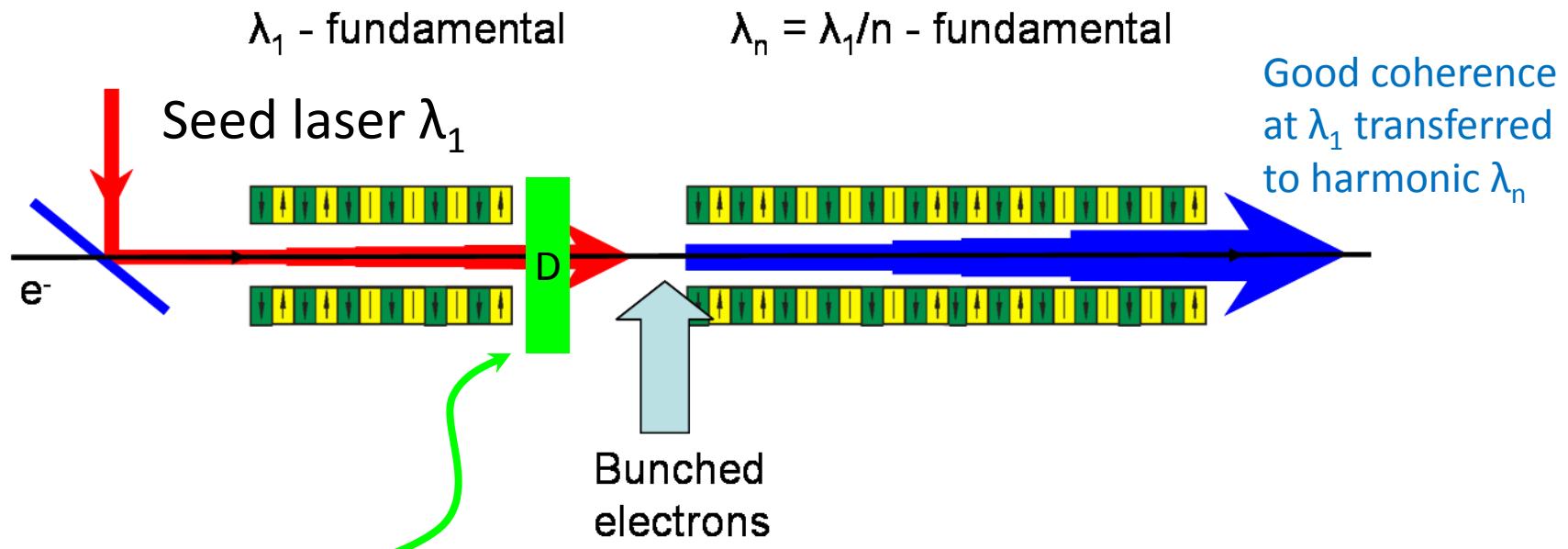
L.-H. Yu *et al.*, Science **289**, 932 (2000).



# Harmonic Generation via a longer wavelength seeded beam

R. Bonifacio, L. De Salvo Souza, P. Pierini, and E. T. Scharlemann, NIM A **296**, 787 (1990).

L.-H. Yu *et al.*, Science **289**, 932 (2000).



$$\frac{\Delta\gamma}{\rho\gamma} < \frac{1}{nD} \quad D = k\rho R_{56}$$

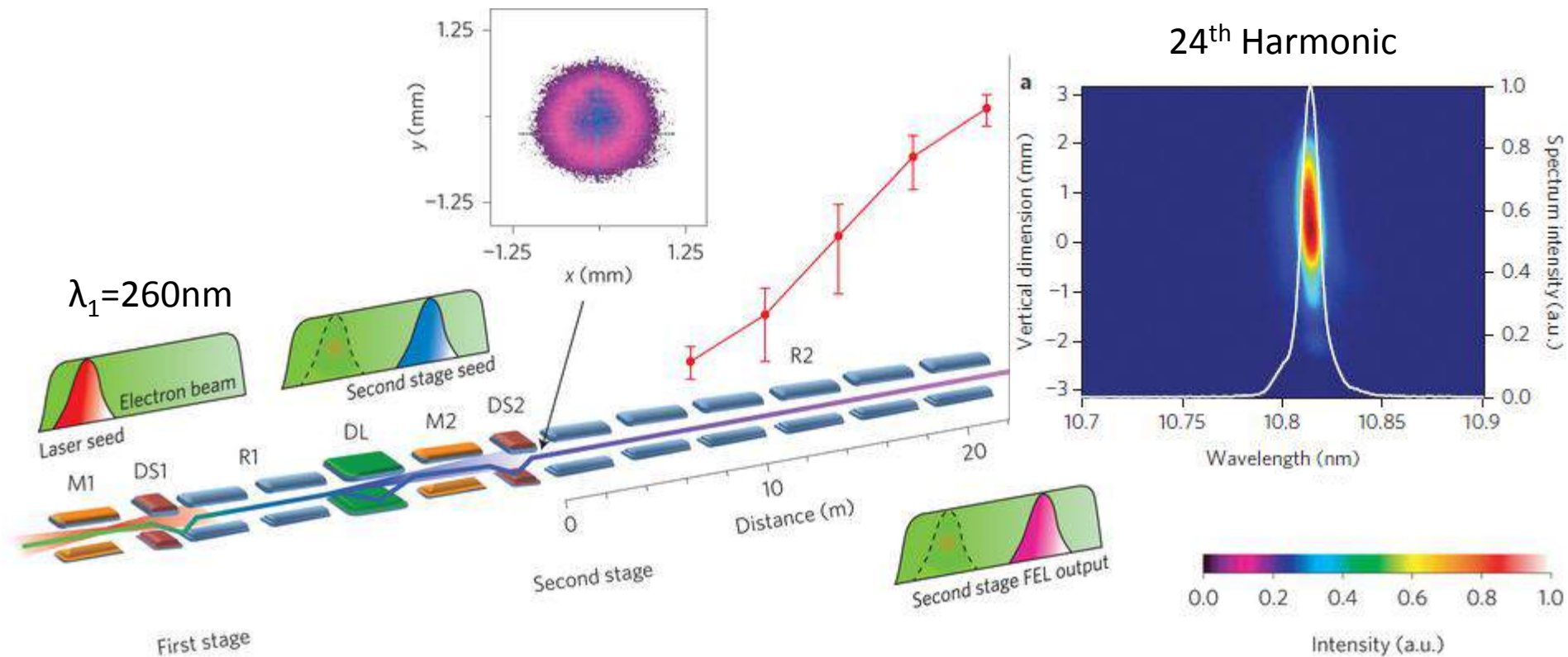
# X-rays require a HGHG Cascade

From

Two-stage seeded soft-X-ray free-electron laser

E. Allaria, D. Castronovo, P. Cinquegrana, P. Craievich, M. Dal Forno, M. B. Danailov, G. D'Auria, A. Demidovich, G. De Ninno, S. Di Mitri, B. Diviacco, W. M. Fawley, M. Ferianis, E. Ferrari, L. Froehlich, G. Gaio, D. Gauthier, L. Giannessi, R. Ivanov, B. Mahieu, N. Mahne, I. Nikolov, F. Parmigiani, G. Penco, L. Raimondi *et al.*

*Nature Photonics* 7, 913–918 (2013) | doi:10.1038/nphoton.2013.277



# However...

## Study of a noise degradation of amplification process in a multistage HGHG FEL

E.L. Saldin<sup>a,\*</sup>, E.A. Schneidmiller<sup>a</sup>, M.V. Yurkov<sup>b</sup>

Optics Communications 202 (2002) 169–187

always been an important problem. The majority of communication and radar engineers are familiar with the fact that inserting the amplifier prior to frequency multiplication has the disadvantage that the phase noise contribution of the amplifier is multiplied by  $n^2$ , where  $n$  is a frequency multiplication factor (see, for example [19]). In the case of HGHG FEL this means that the effect of frequency multiplication by a factor of  $N$  multiplies the first FEL amplifier noise power to carrier ratio by  $N^2$ . This prevents operation of HGHG FEL at very short wavelength range. The results presented in this paper have demonstrated that the HGHG FEL approach is quite adequate for a 10–100 nm coherent source, but not scalable to an X-ray device.

Recently, various HGHG schemes have been proposed to improve the performance of X-ray FEL. The basic theory of these schemes does not take into account the shot noise effect, meanwhile it leads to a dramatic degradation of the quality of the output radiation when applying frequency multiplication schemes. The arguments discussed above, based on our results of numerical simulations, seem to be strong enough to suggest that the HGHG FEL schemes for reaching hard X-rays proposed in the literature so far will not work.



# However...

## Study of a noise degradation of amplification process in a multistage HGHG FEL

E.L. Saldin<sup>a,\*</sup>, E.A. Schneidmiller<sup>a</sup>, M.V. Yurkov<sup>b</sup>

Optics Communications 202 (2002) 169–187

always been an important problem. The majority of communication and radar engineers are familiar with the fact that inserting the amplifier prior to frequency multiplication has the disadvantage that the phase noise contribution of the amplifier is multiplied by  $n^2$ , where  $n$  is a frequency multiplication factor (see, for example [19]). In the case of HGHG FEL this means that the effect of frequency multiplication by a factor of  $N$  multiplies the first FEL amplifier noise power to carrier ratio by  $N^2$ . This prevents operation of HGHG FEL at very short wavelength range. The results presented in this paper have demonstrated that the HGHG FEL approach is quite adequate for a 10–100 nm coherent source, but not scalable to an X-ray device.

Recently, various HGHG schemes have been proposed to improve the performance of X-ray FEL. The basic theory of these schemes does not take into account the shot noise effect, meanwhile it leads to a dramatic degradation of the quality of the output radiation when applying frequency multiplication schemes. The arguments discussed above, based on our results of numerical simulations, seem to be strong enough to suggest that the HGHG FEL schemes for reaching hard X-rays proposed in the literature so far will not work.

# However...

## Study of a noise degradation of amplification process in a multistage HGHG FEL

E.L. Saldin<sup>a,\*</sup>, E.A. Schneidmiller<sup>a</sup>, M.V. Yurkov<sup>b</sup>

Optics Communications 202 (2002) 169–187

always been an important problem. The majority of communication and radar engineers are familiar with the fact that inserting the amplifier prior to frequency multiplication has the disadvantage that the phase noise contribution of the amplifier is multiplied by  $n^2$ , where  $n$  is a frequency multiplication factor (see, for example [19]). In the case of HGHG FEL this means that the effect of frequency multiplication by a factor of  $N$  multiplies the first FEL amplifier noise power to carrier ratio by  $N^2$ . This prevents operation of HGHG FEL at very short wavelength range. The results presented in this paper have demonstrated that the HGHG FEL approach is quite adequate for a 10–100 nm coherent source, but not scalable to an X-ray device.

Recently, various HGHG schemes have been proposed to improve the performance of X-ray FEL. The basic theory of these schemes does not take into account the shot noise effect, meanwhile it leads to a dramatic degradation of the quality of the output radiation when applying frequency multiplication schemes. The arguments discussed above, based on our results of numerical simulations, seem to be strong enough to suggest that the HGHG FEL schemes for reaching hard X-rays proposed in the literature so far will not work.

# However...

## Study of a noise degradation of amplification process in a multistage HGHG FEL

E.L. Saldin<sup>a,\*</sup>, E.A. Schneidmiller<sup>a</sup>, M.V. Yurkov<sup>b</sup>

Optics Communications 202 (2002) 169–177

always been an important problem. The majority of communication and radar engineers are familiar with the fact that inserting the amplifier prior to frequency multiplication has the disadvantage that the phase noise contribution of the amplifier is multiplied by  $N^2$ , when  $N$  is a frequency multiplication factor (see, for example [19]). In the case of HGHG FEL this means that the effect of frequency multiplication by a factor of  $N$  multiplies the first FEL amplifier noise power to carrier ratio by  $N^2$ . This prevents operation of HGHG FEL at very short wavelength range. The results presented in this paper have demonstrated that the HGHG FEL approach is quite adequate for a 10–100 nm coherent source, but not scalable to an X-ray device.

Recently, various HGHG schemes have been proposed to improve the performance of X-ray FEL. The basic theory of these schemes does not take into account the shot noise effect, meanwhile it leads to a dramatic degradation of the quality of the output radiation when applying frequency multiplication schemes. The arguments discussed above, based on our results of numerical simulations, seem to be strong enough to suggest that the HGHG FEL schemes for reaching hard X-rays proposed in the literature so far will not work.

Problems in X-ray

# Indirect Seeding: Echo Enabled Harmonic Gain

## Using the Beam-Echo Effect for Generation of Short-Wavelength Radiation

G. Stupakov

*SLAC National Accelerator Laboratory, Menlo Park, California 94025, USA*

(Received 22 October 2008; published 17 February 2009)

---

PHYSICAL REVIEW SPECIAL TOPICS - ACCELERATORS AND BEAMS 12, 030702 (2009)

---

## Echo-enabled harmonic generation free electron laser

Dao Xiang and Gennady Stupakov

*SLAC National Accelerator Laboratory, Menlo Park, California 94025, USA*

(Received 2 December 2008; published 4 March 2009)



# First lasing of an echo-enabled harmonic generation free-electron laser

Z. T. Zhao, D. Wang, J. H. Chen, Z. H. Chen, H. X. Deng, J. G. Ding, C. Feng, Q. Gu, M. M. Huang, T. H. Lan, Y. B. Leng, D. G. Li, G. Q. Lin, B. Liu, E. Prat, X. T. Wang, Z. S. Wang, K. R. Ye, L. Y. Yu, H. O. Zhang, J. Q. Zhang, Me. Zhang, Mi. Zhang, T. Zhang, S. P. Zhong  *et al.*

[Affiliations](#) | [Contributions](#) | [Corresponding author](#)

*Nature Photonics* **6**, 360–363 (2012) | doi:10.1038/nphoton.2012.105

Received 09 January 2012 | Accepted 04 April 2012 | Published online 13 May 2012

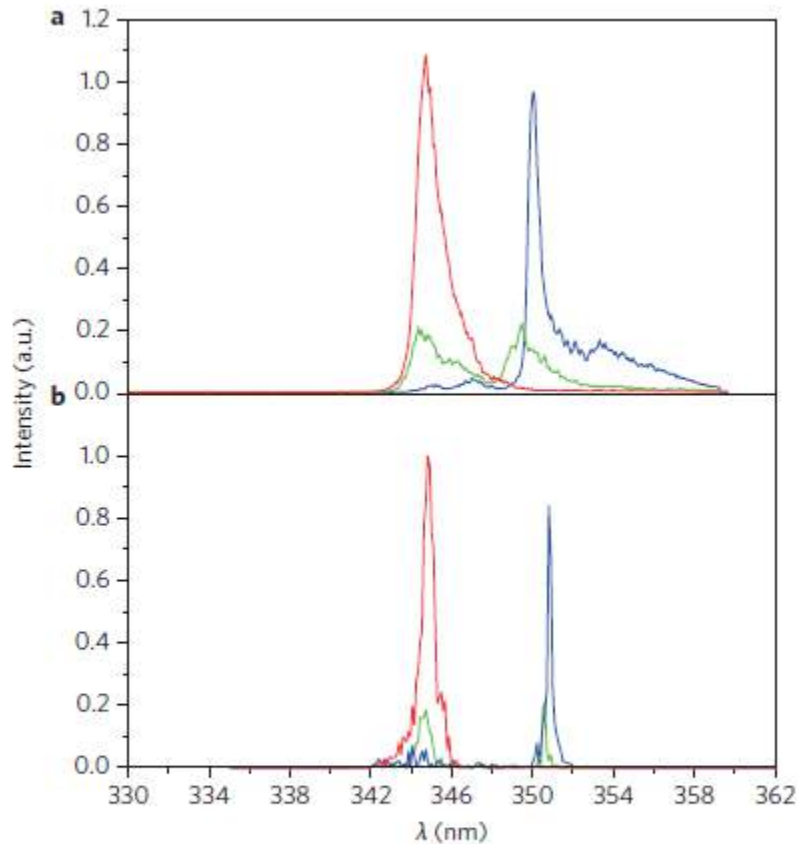


**Figure 3 | Spectra for FEL radiation.** **a**, Experimental results (red line, HGFG; blue line, EEHG; green line, intermediate state between HGFG and EEHG). **b**, Simulation results (red line, HGFG; blue line, EEHG; green line, intermediate state between HGFG and EEHG).

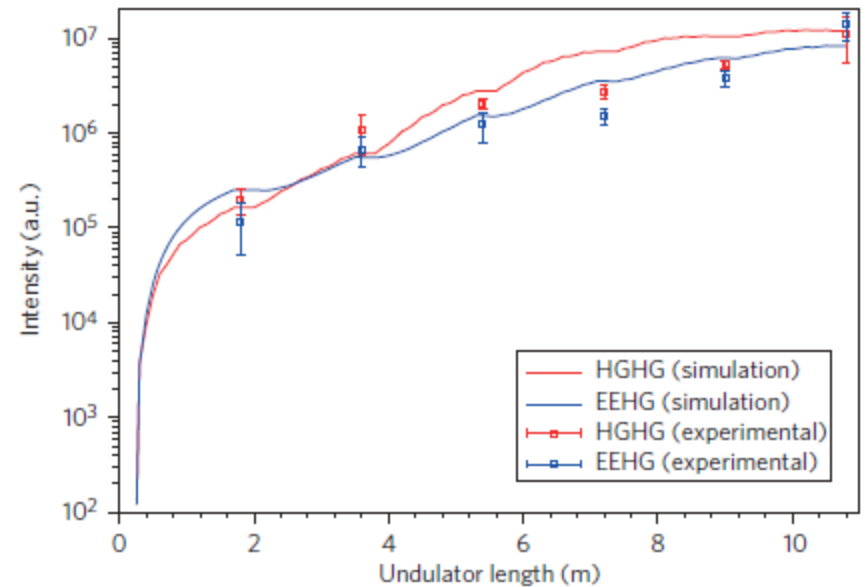


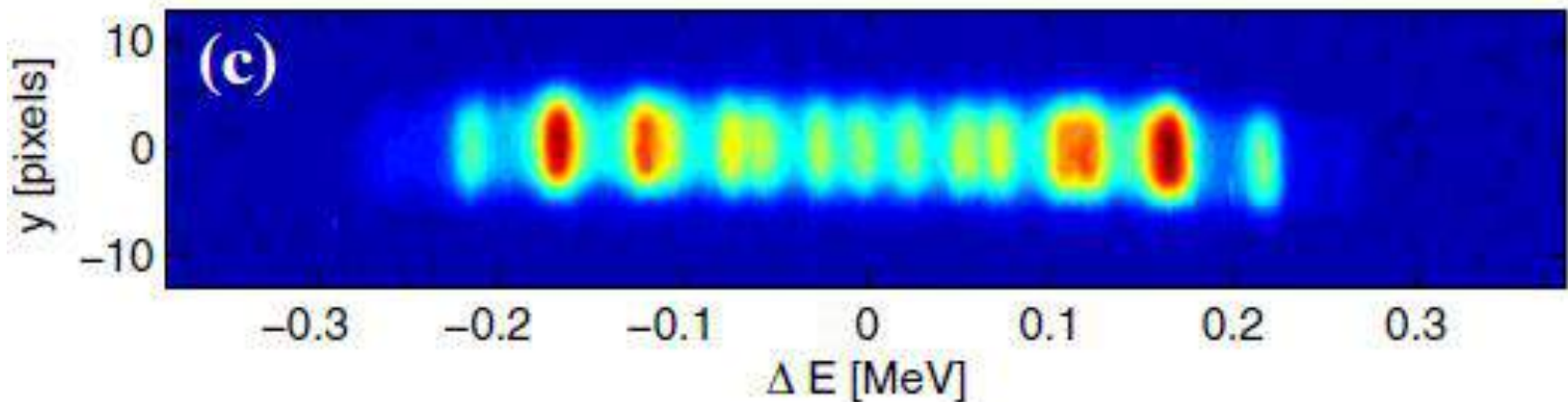
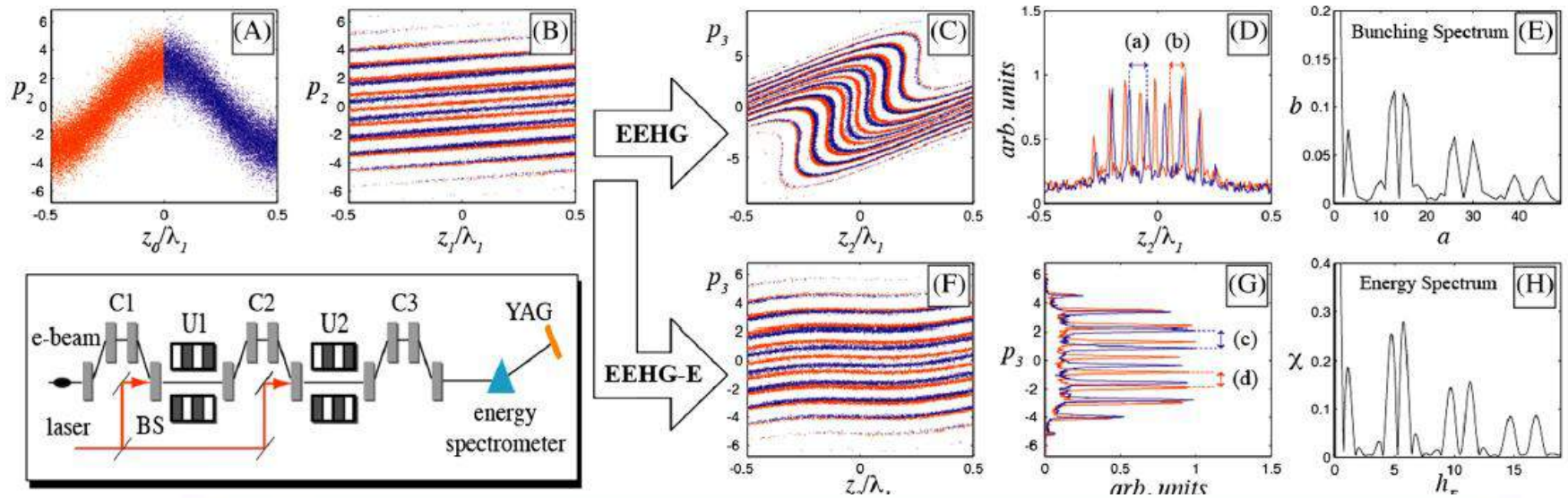
**Figure 5 | Gain curves of the EEHG and HGFG FEL at SDUV-FEL.** Intensity is measured with a calibrated CCD at the end of the radiator (red open squares, HGFG; blue open squares, EEHG). Error bars correspond to the peak-to-peak intensity statistics of 100 measurements. Simulation results are shown as a red line (HGFG) and a blue line (EEHG).

## Direct observation of fine-scale energy banding in echo-enabled harmonic generation

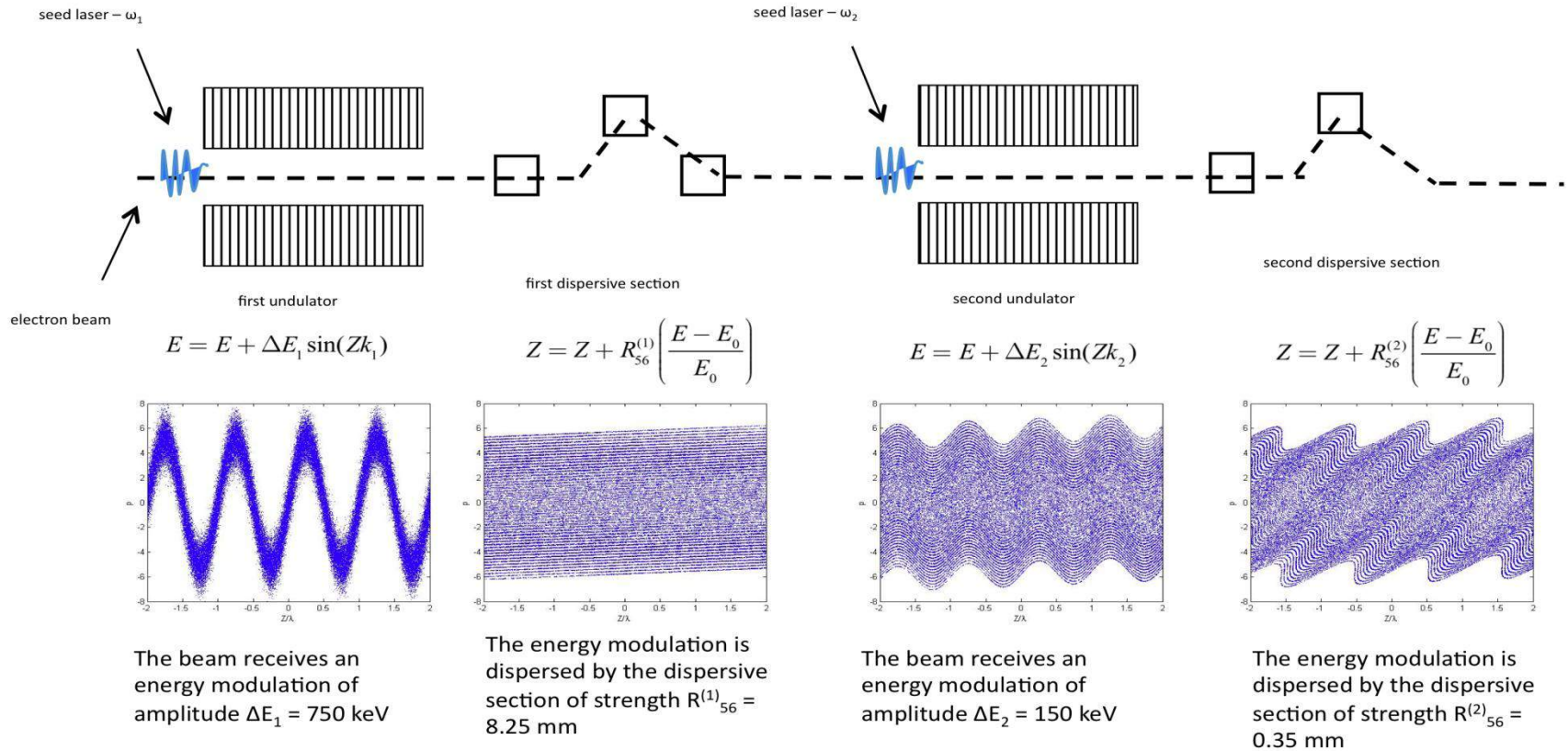
E. Hemsing, D. Xiang, M. Dunning, S. Weathersby, C. Hast, and T. Raubenheimer

*SLAC National Accelerator Laboratory, Menlo Park, California 94025, USA*

(Received 5 July 2013; published 30 January 2014)

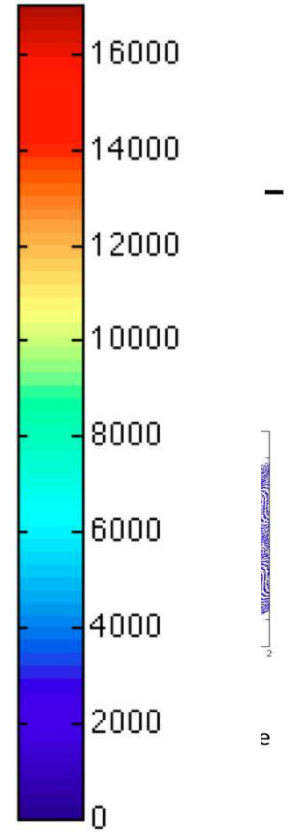
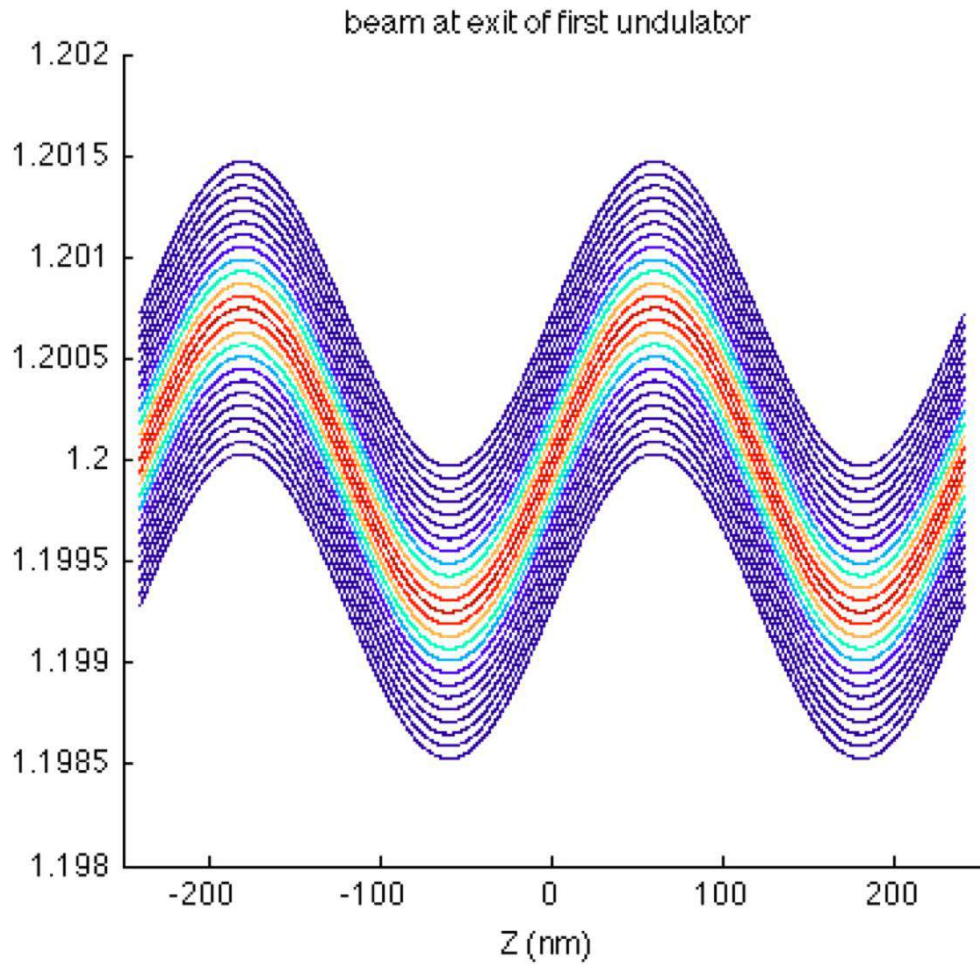
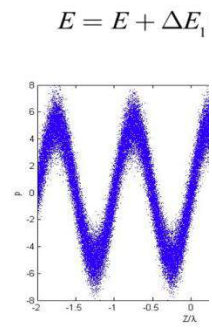
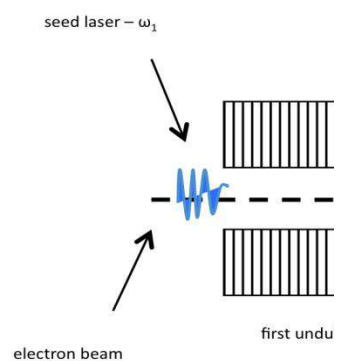


# Mechanism

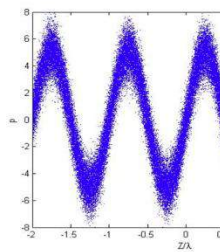
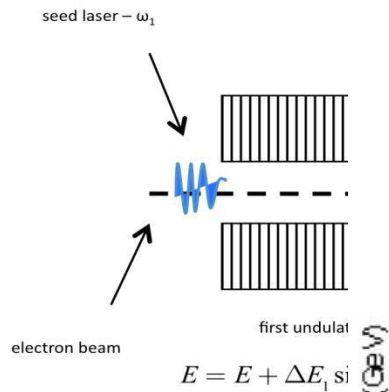




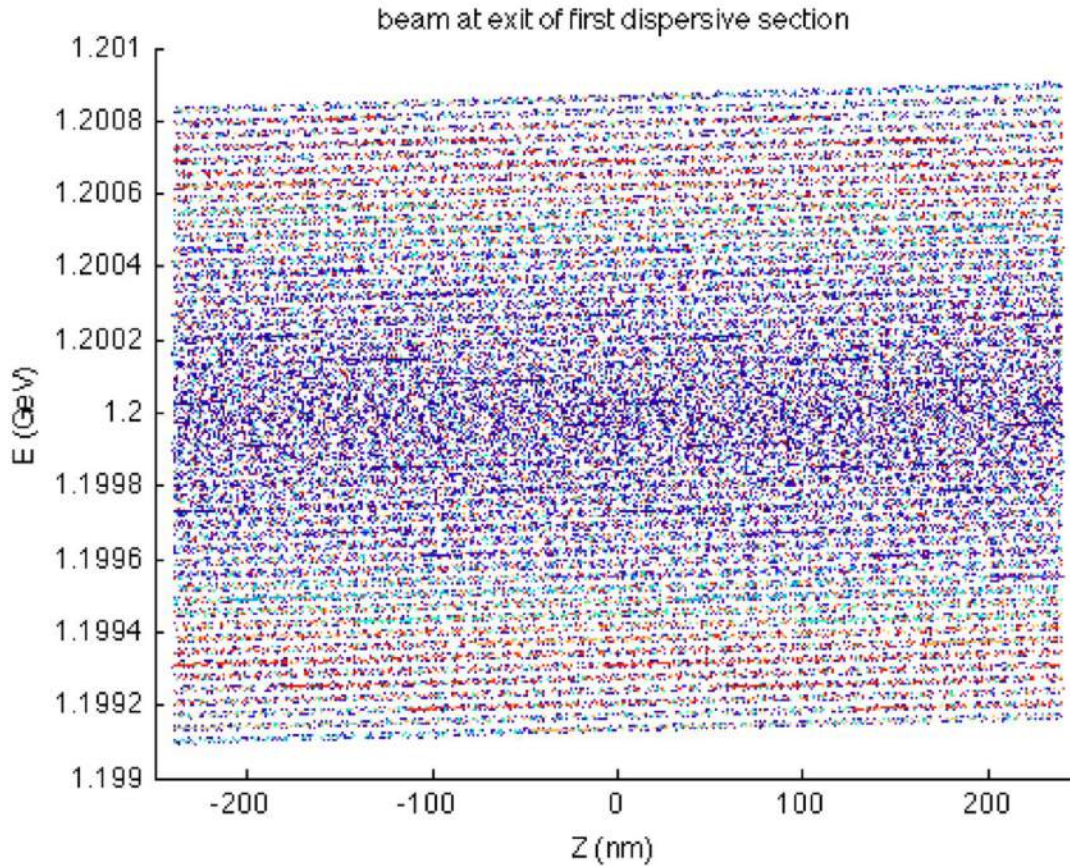
# Mechanism



# Mechanism

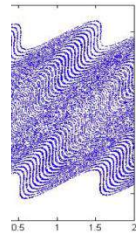


The beam receive energy modulation amplitude  $\Delta E_1 = 7$



ion

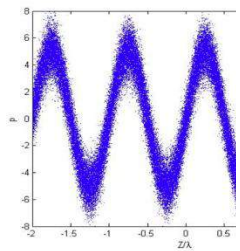
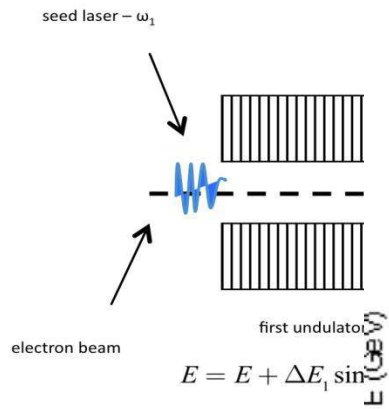
$$\frac{E - E_0}{E_0}$$



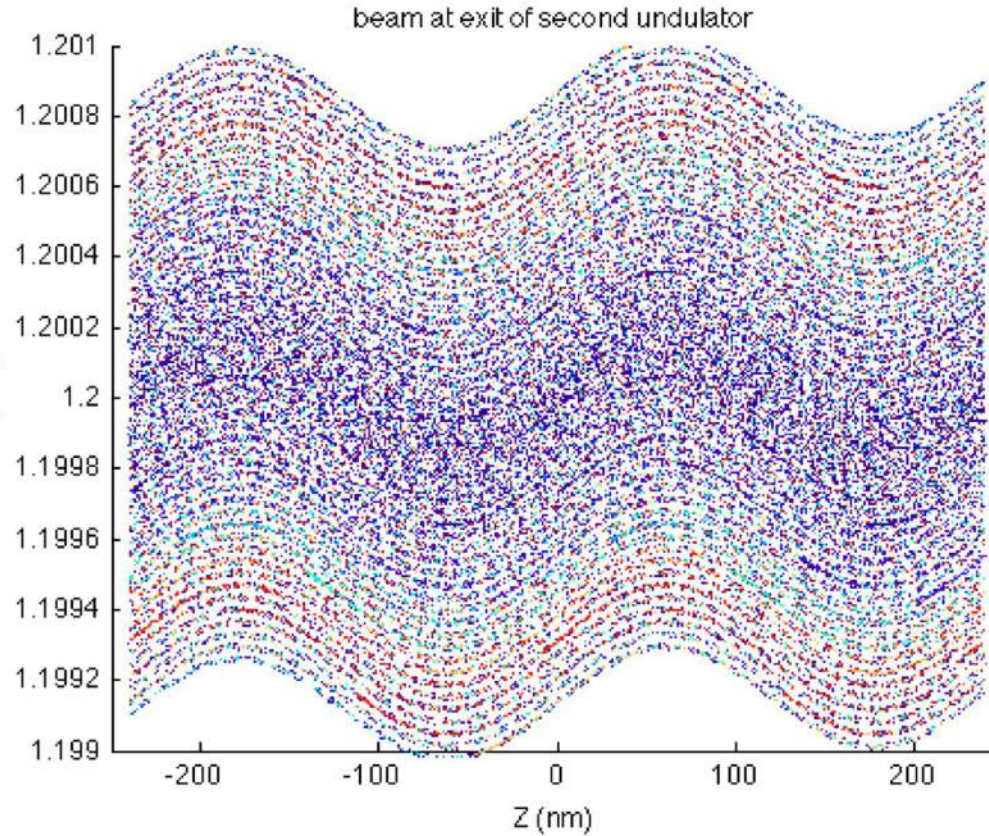
ulation is  
dispersive  
gth  $R_{56}^{(2)} =$



# Mechanism

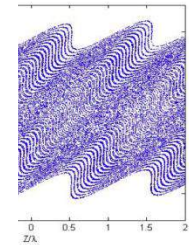


The beam receives energy modulation amplitude  $\Delta E_1 = 75$



e section

$$\chi_{56}^{(2)} \left( \frac{E - E_0}{E_0} \right)$$

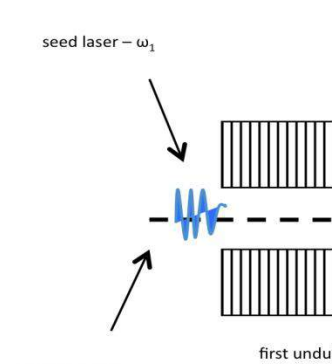


modulation is / the dispersive length  $R_{56}^{(2)} =$

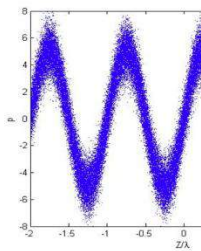
0.55 mm

# Mechanism

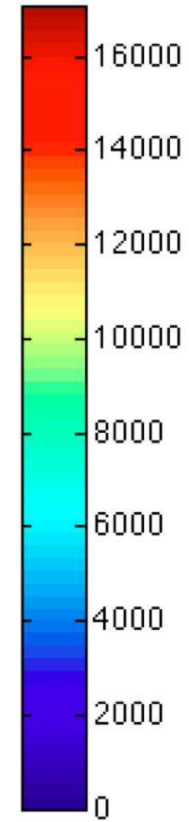
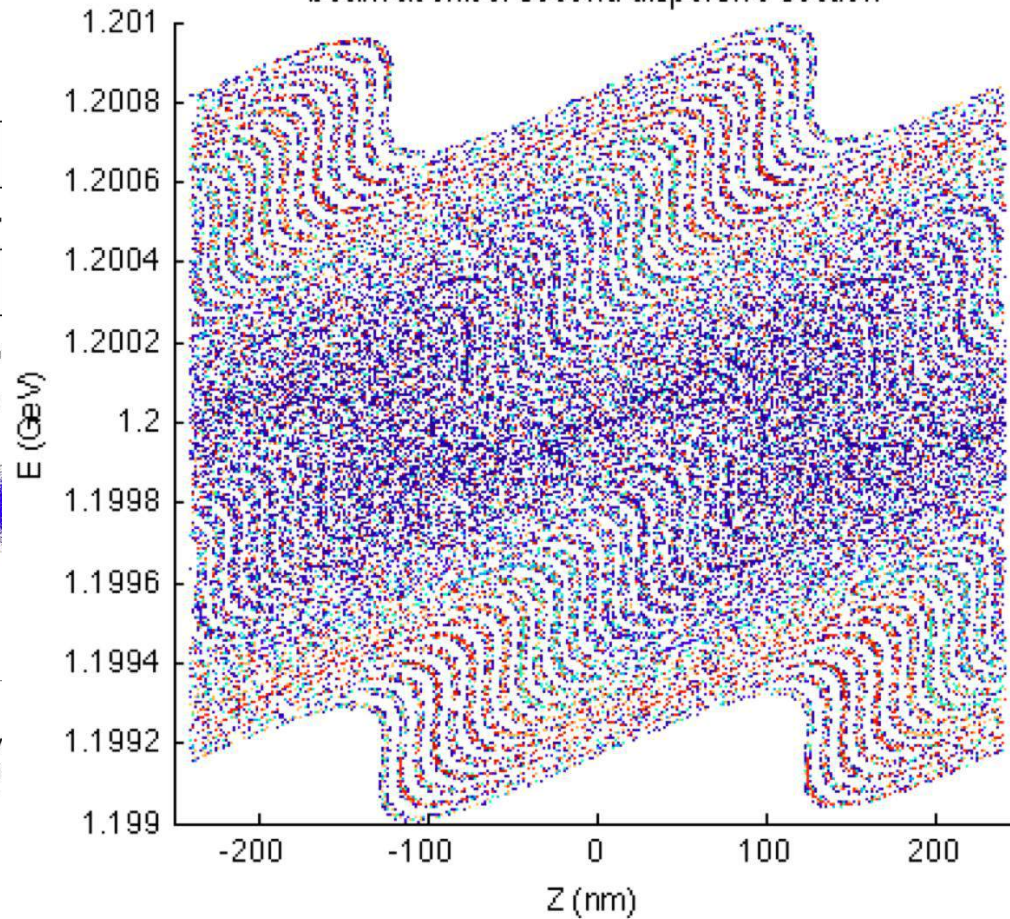
beam at exit of second dispersive section



$$E = E_0 + \Delta E_1$$



The beam receive energy modulation amplitude  $\Delta E_1 =$



# Indirect Seeding: Echo Enabled Harmonic Gain - Also results in modal bunching

---

EPL, 100 (2012) 64001  
doi: 10.1209/0295-5075/100/64001

[www.epljournal.org](http://www.epljournal.org)

**Echo enabled harmonic generation free electron laser  
in a mode-locked configuration**

J. R. HENDERSON<sup>1,2</sup> and B. W. J. McNEIL<sup>1</sup>

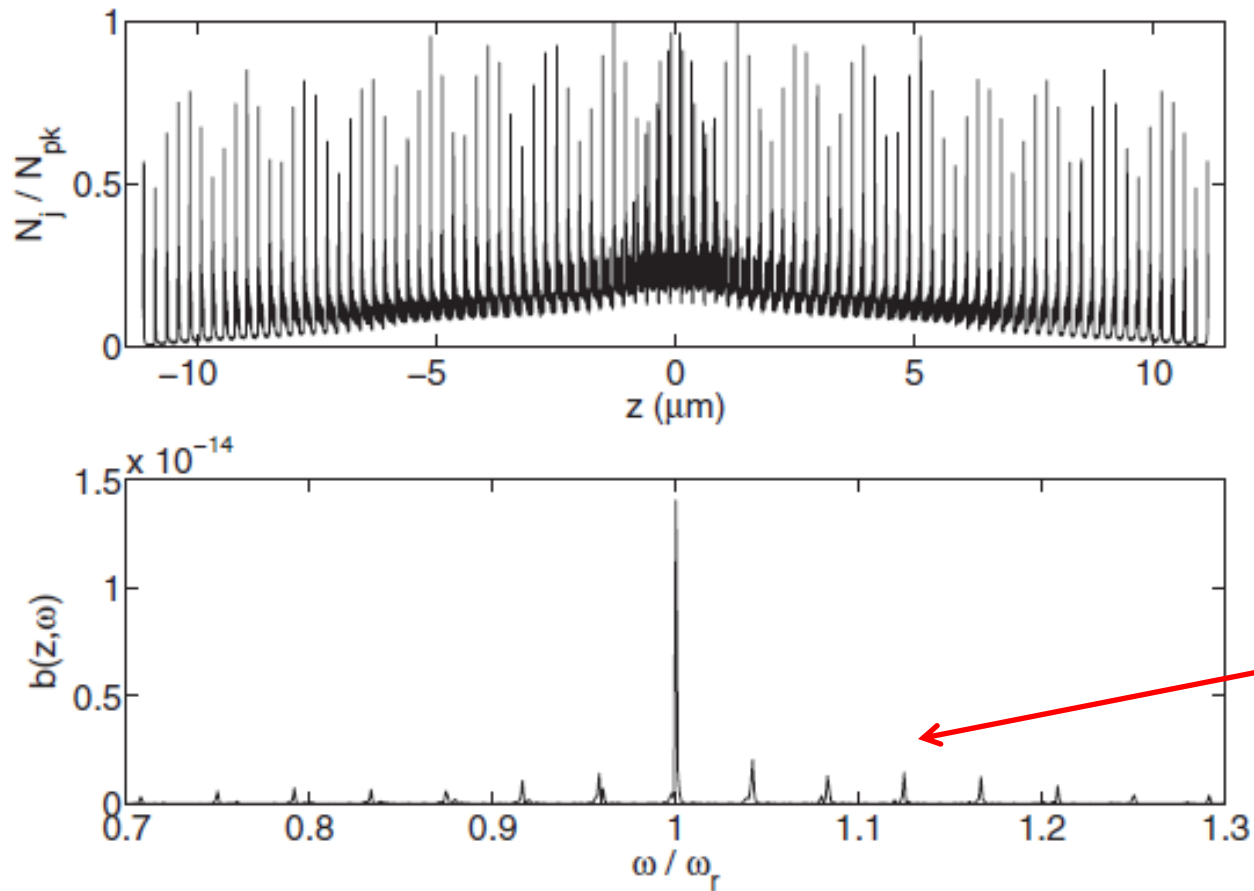


Fig. 4: Histogram of electron numbers (top) normalised with respect to the peak, and the Fourier transform of the bunching parameter  $b(z, \omega)$  for the full electron beam distribution showing the modal structure at the end of the EEHG pre-bunching process.



# Mode locked FEL interaction

$$\lambda_r \approx 10 \text{ nm}$$

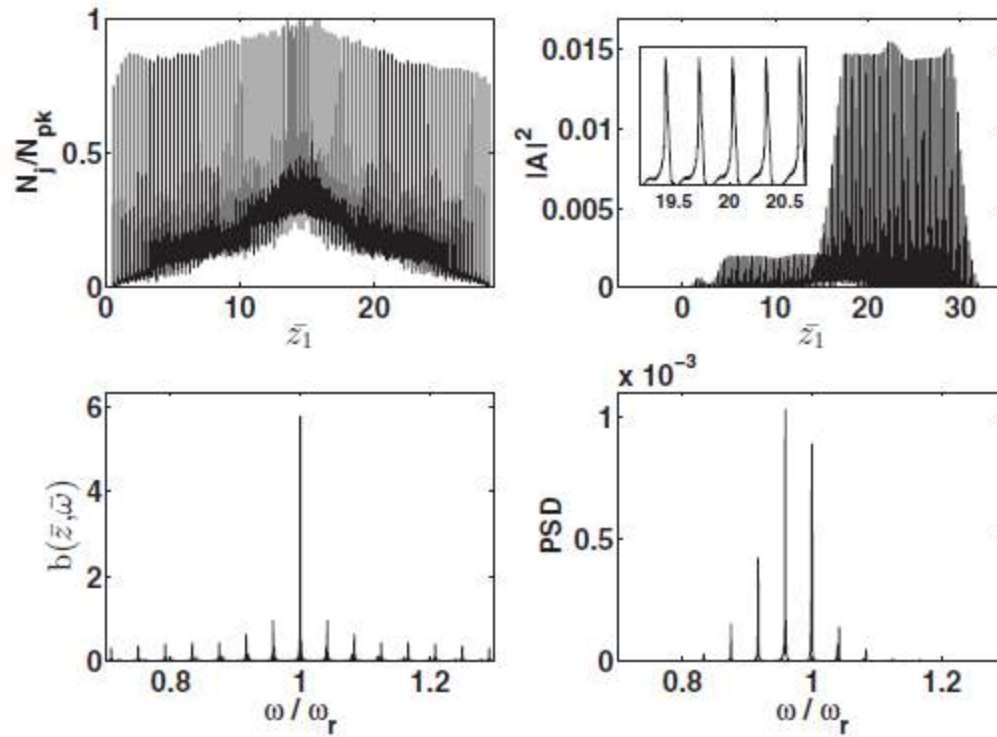


Fig. 6: As fig. 5, but for the MLOK undulator at saturation ( $\bar{z} \approx 0.6$ ). The inset (top, right) shows more detail expanded in  $\bar{z}_1$ . A well-defined set of phase-matched radiation modes has developed resulting in a train of short radiation pulses. In unscaled units the individual pulse widths are  $\sim 106$  attoseconds (FWHM) and separated by  $\sim 0.8$  femtoseconds corresponding to  $\bar{s} = 0.3$  in scaled units of  $\bar{z}_1$ .

# Self-Seeding



# Self-seeding

## Demonstration of self-seeding in a hard-X-ray free-electron laser

J. Amann<sup>1</sup>, W. Berg<sup>2</sup>, V. Blank<sup>3</sup>, F.-J. Decker<sup>1</sup>, Y. Ding<sup>1</sup>, P. Emma<sup>4\*</sup>, Y. Feng<sup>1</sup>, J. Frisch<sup>1</sup>, D. Fritz<sup>1</sup>, J. Hastings<sup>1</sup>, Z. Huang<sup>1</sup>, J. Krzywinski<sup>1</sup>, R. Lindberg<sup>2</sup>, H. Loos<sup>1</sup>, A. Lutman<sup>1</sup>, H.-D. Nuhn<sup>1</sup>, D. Ratner<sup>1</sup>, J. Rzepiela<sup>1</sup>, D. Shu<sup>2</sup>, Yu. Shvyd'ko<sup>2</sup>, S. Spampinati<sup>1</sup>, S. Stoupin<sup>2</sup>, S. Terentyev<sup>3</sup>, E. Trakhtenberg<sup>2</sup>, D. Walz<sup>1</sup>, J. Welch<sup>1</sup>, J. Wu<sup>1</sup>, A. Zholents<sup>2</sup> and D. Zhu<sup>1</sup>

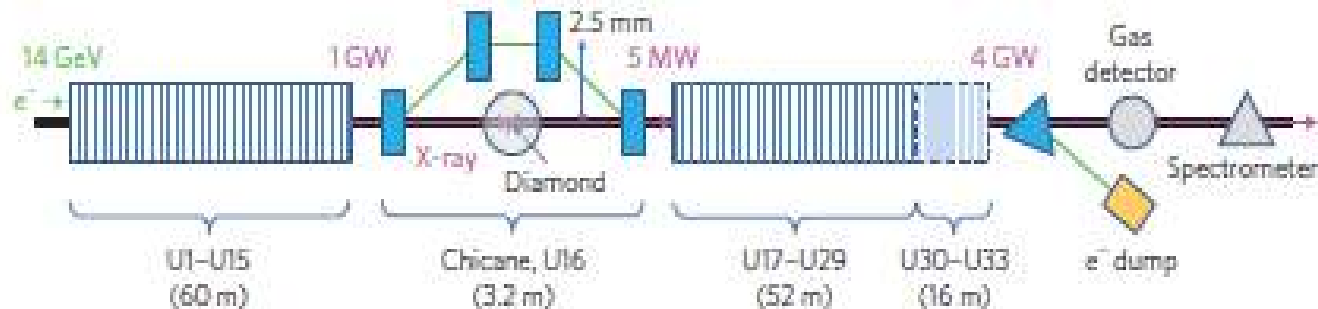


**Figure 1** | Layout of the LCLS undulator with a self-seeding chicane, diamond monochromator, gas detector and hard-X-ray spectrometer. The chicane is greatly exaggerated in scale. The last four LCLS undulators (U30-U33) were previously modified as second-harmonic afterburners<sup>15</sup> and were not used in this experiment.

Feldhaus, J., Saldin, E. L., Schneider, J. R., Schneidmiller, E. A. & Yurkov, M.V. *Opt. Commun.* **140**, 341 (1997)

A novel self-seeding scheme for hard X-ray FELs *Journal of Modern Optics*

Gianluca Geloni<sup>a\*</sup>, Vitali Kocharyan<sup>b</sup> and Evgeni Saldin<sup>b</sup> Vol. 58, No. 16, 20 September 2011

# Self-seeding\*

## Demonstration of self-seeding in a hard-X-ray free-electron laser

J. Amann<sup>1</sup>, W. Berg<sup>2</sup>, V. Blank<sup>3</sup>, F.-J. Decker<sup>1</sup>, Y. Ding<sup>1</sup>, P. Emma<sup>4\*</sup>, Y. Feng<sup>1</sup>, J. Frisch<sup>1</sup>, D. Fritz<sup>1</sup>, J. Hastings<sup>1</sup>, Z. Huang<sup>1</sup>, J. Krzywinski<sup>1</sup>, R. Lindberg<sup>2</sup>, H. Loos<sup>1</sup>, A. Lutman<sup>1</sup>, H.-D. Nuhn<sup>1</sup>, D. Ratner<sup>1</sup>, J. Rzepiela<sup>1</sup>, D. Shu<sup>2</sup>, Yu. Shvyd'ko<sup>2</sup>, S. Spampinati<sup>1</sup>, S. Stoupin<sup>2</sup>, S. Terentyev<sup>3</sup>, E. Trakhtenberg<sup>2</sup>, D. Walz<sup>1</sup>, J. Welch<sup>1</sup>, J. Wu<sup>1</sup>, A. Zholents<sup>2</sup> and D. Zhu<sup>1</sup>

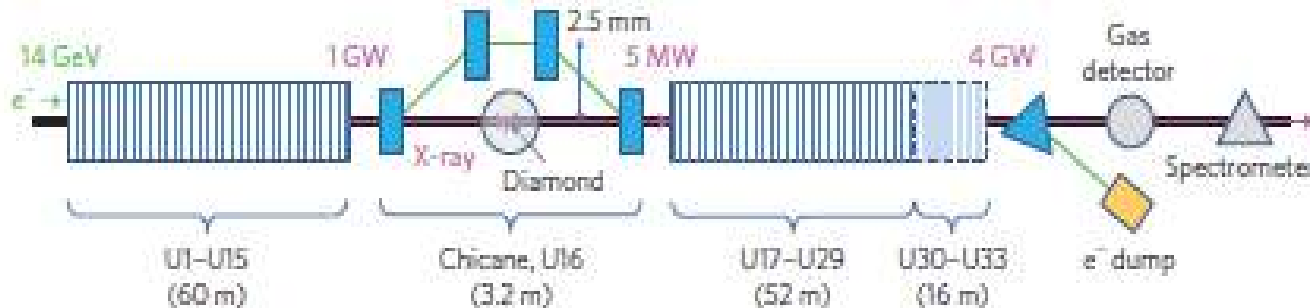


**Figure 1** | Layout of the LCLS undulator with a self-seeding chicane, diamond monochromator, gas detector and hard-X-ray spectrometer. The chicane is greatly exaggerated in scale. The last four LCLS undulators (U30-U33) were previously modified as second-harmonic afterburners<sup>15</sup> and were not used in this experiment.

\* Feldhaus, J., Saldin, E. L., Schneider, J. R., Schneidmiller, E. A. & Yurkov, M.V. *Opt. Commun.* **140**, 341 (1997)

A novel self-seeding scheme for hard X-ray FELs *Journal of Modern Optics*

Gianluca Geloni<sup>a\*</sup>, Vitali Kocharyan<sup>b</sup> and Evgeni Saldin<sup>b</sup> Vol. 58, No. 16, 20 September 2011

# Self-seeding\*

## Demonstration of self-seeding in a hard-X-ray free-electron laser

J. Amann<sup>1</sup>, W. Berg<sup>2</sup>, V. Blank<sup>3</sup>, F.-J. Decker<sup>1</sup>, Y. Ding<sup>1</sup>, P. Emma<sup>4\*</sup>, Y. Feng<sup>1</sup>, J. Frisch<sup>1</sup>, D. Fritz<sup>1</sup>, J. Hastings<sup>1</sup>, Z. Huang<sup>1</sup>, J. Krzywinski<sup>1</sup>, R. Lindberg<sup>2</sup>, H. Loos<sup>1</sup>, A. Lutman<sup>1</sup>, H.-D. Nuhn<sup>1</sup>, D. Ratner<sup>1</sup>, J. Rzepiela<sup>1</sup>, D. Shu<sup>2</sup>, Yu. Shvyd'ko<sup>2</sup>, S. Spampinati<sup>1</sup>, S. Stoupin<sup>2</sup>, S. Terentyev<sup>3</sup>, E. Trakhtenberg<sup>2</sup>, D. Walz<sup>1</sup>, J. Welch<sup>1</sup>, J. Wu<sup>1</sup>, A. Zholents<sup>2</sup> and D. Zhu<sup>1</sup>

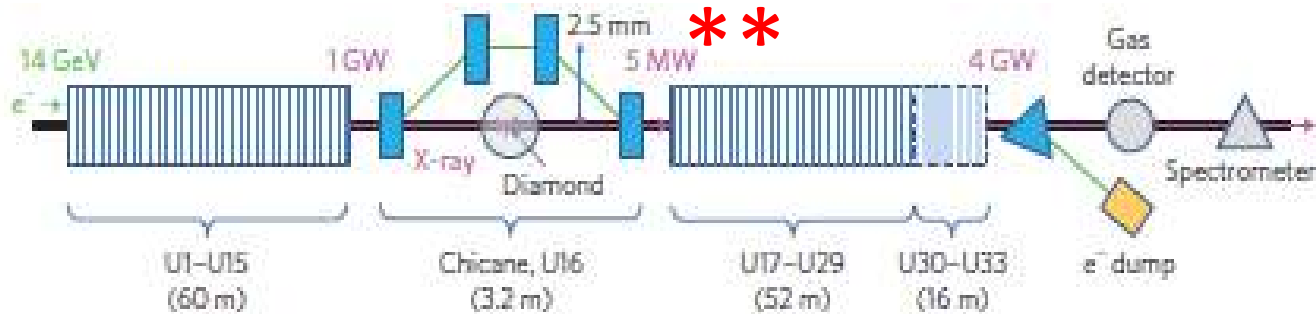


**Figure 1 | Layout of the LCLS undulator with a self-seeding chicane, diamond monochromator, gas detector and hard-X-ray spectrometer. The chicane is greatly exaggerated in scale. The last four LCLS undulators (U30-U33) were previously modified as second-harmonic afterburners<sup>15</sup> and were not used in this experiment.**

\* Feldhaus, J., Saldin, E. L., Schneider, J. R., Schneidmiller, E. A. & Yurkov, M.V. *Opt. Commun.* **140**, 341 (1997)

\*\* A novel self-seeding scheme for hard X-ray FELs *Journal of Modern Optics*

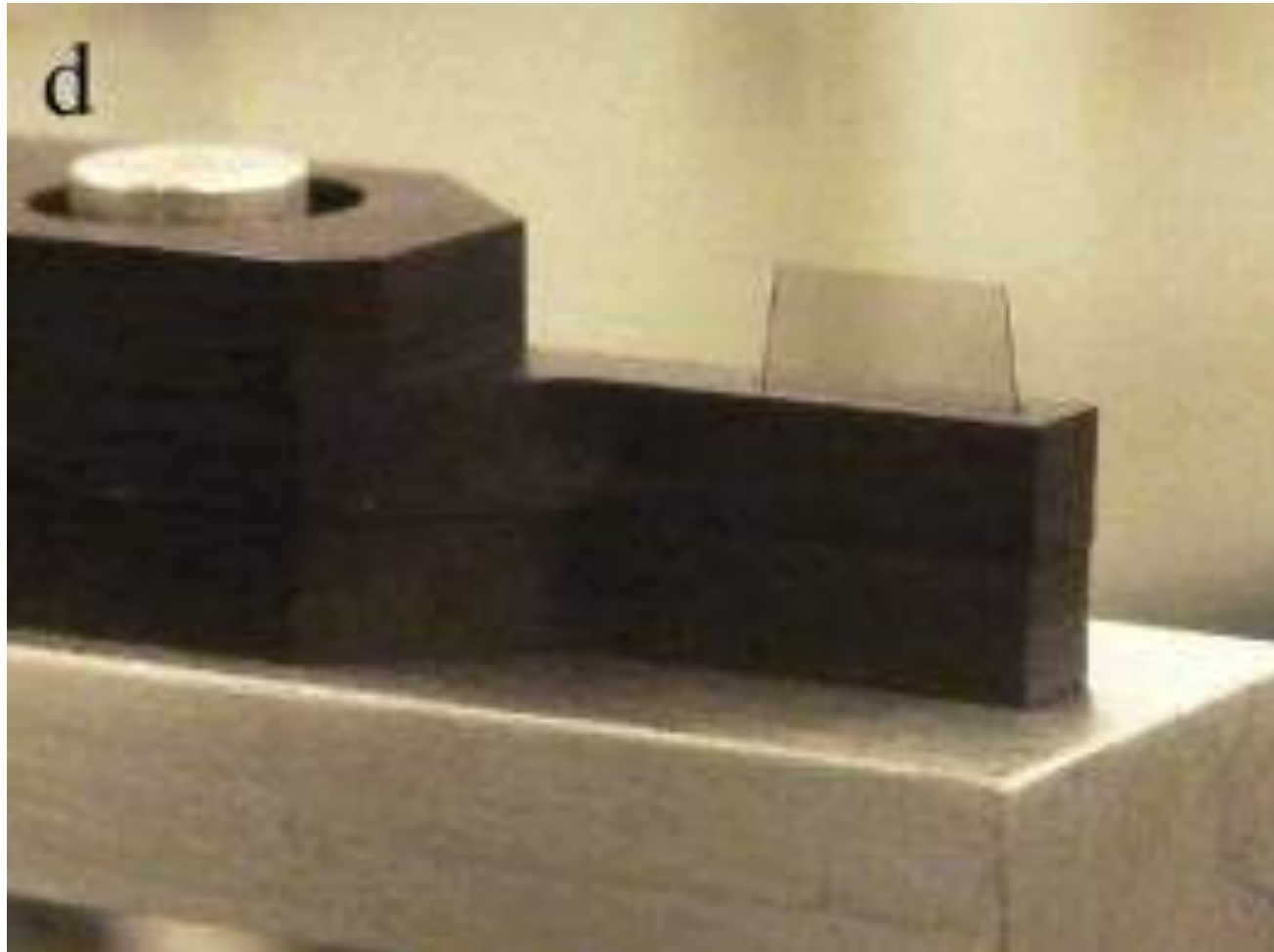
Gianluca Geloni<sup>a\*</sup>, Vitali Kocharyan<sup>b</sup> and Evgeni Saldin<sup>b</sup> Vol. 58, No. 16, 20 September 2011

# Diamond and Related Materials

Volume 33, March 2013, Pages 1–4

## Diamond crystal optics for self-seeding of hard X-rays in X-ray free-electron lasers

S. Stoupin<sup>a</sup>,  , V.D. Blank<sup>b</sup>, S.A. Terentyev<sup>b</sup>, S.N. Polyakov<sup>b</sup>, V.N. Denisov<sup>b</sup>, M.S. Kuznetsov<sup>b</sup>, Yu.V. Shvyd'ko<sup>a</sup>, D. Shu<sup>a</sup>, P. Emma<sup>c</sup>, J. Maj<sup>a</sup>, J. Katsoudas<sup>d</sup>



# Results from LCLS Experiment\* based

on: A novel self-seeding scheme for hard X-ray FELs *Journal of Modern Optics*  
Gianluca Geloni<sup>a\*</sup>, Vitali Kocharyan<sup>b</sup> and Evgeni Saldin<sup>b</sup> Vol. 58, No. 16, 20 September 2011

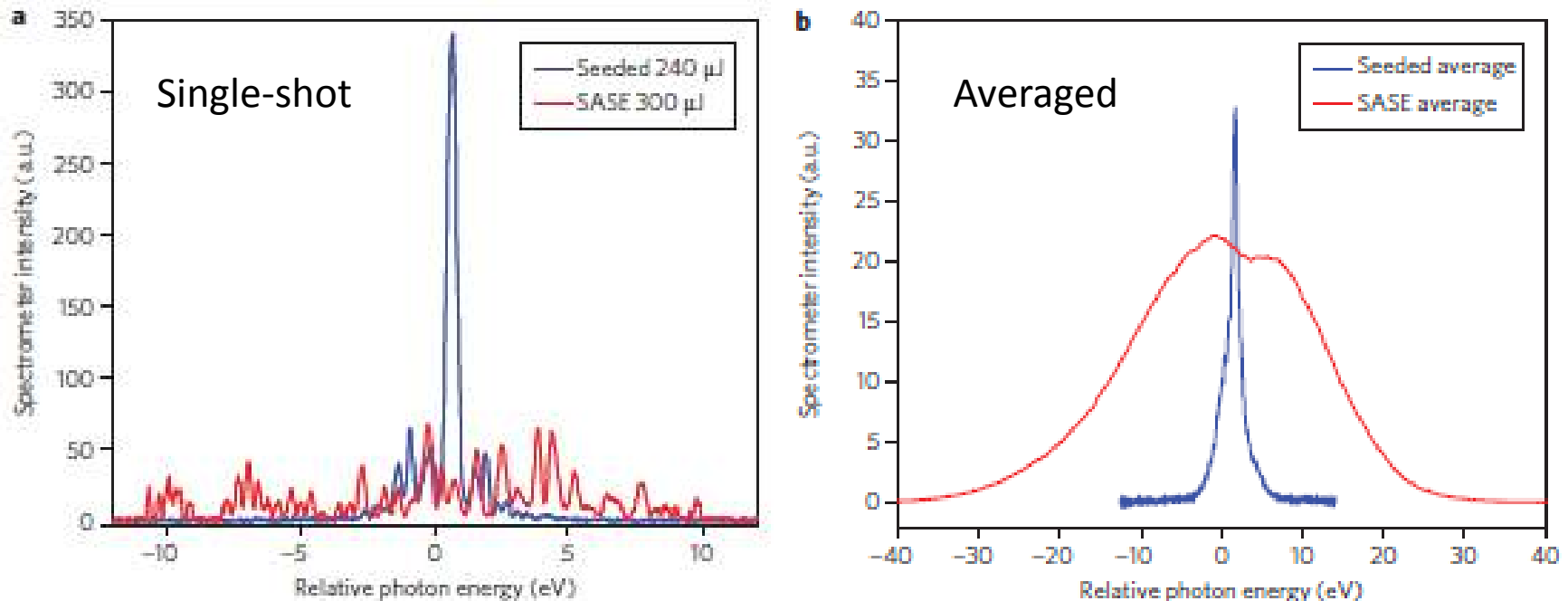


**Figure 5 | Measured X-ray spectra. a,b**, Single-shot (a) and averaged (b) X-ray spectrum in SASE mode (red) and self-seeded mode (blue). The FWHM single-shot seeded bandwidth is 0.4 eV, whereas the SASE FWHM bandwidth is  $\sim 20$  eV. Vertical scales have the same arbitrary units in both a and b. The chicane is turned off for the SASE measurements, but necessarily switched on for the self-seeded mode.

# Results from LCLS Experiment\* based

on: A novel self-seeding scheme for hard X-ray FELs *Journal of Modern Optics*  
Gianluca Geloni<sup>a\*</sup>, Vitali Kocharyan<sup>b</sup> and Evgeny Solov'ev<sup>b</sup> Vol. 58, No. 16, 20 September 2011



Figure 5 | Measured X-ray spectra. **a,b**, Single-shot (**a**) and averaged (**b**) X-ray spectrum in SASE mode (red) and self-seeded mode (blue). The FWHM single-shot seeded bandwidth is 0.4 eV, whereas the SASE FWHM bandwidth is  $\sim 20$  eV. Vertical scales have the same arbitrary units in both **a** and **b**. The chicane is turned off for the SASE measurements, but necessarily switched on for the self-seeded mode.

\* J. Amann et al, NATURE PHOTONICS 6, 693 (2012)

HB-SASE; i-SASE; p-SASE....

HB-SASE; i-SASE; p-SASE....

?? HiBp-SASE ??





HB-SASE developed from  
numerical experiments on studies  
of phase shifting in the FEL

Small shifts  $< \lambda_r$   
(Phase shifts)

## INDUCING STRONG DENSITY MODULATION WITH SMALL ENERGY DISPERSION IN PARTICLE BEAMS AND THE HARMONIC AMPLIFIER FREE ELECTRON LASER

B. W. J. McNeil, G. R. M. Robb, Department of Physics, University of Strathclyde, Glasgow, UK  
M. W. Poole, ASTeC, Daresbury Laboratory, Warrington WA4 4AD, UK

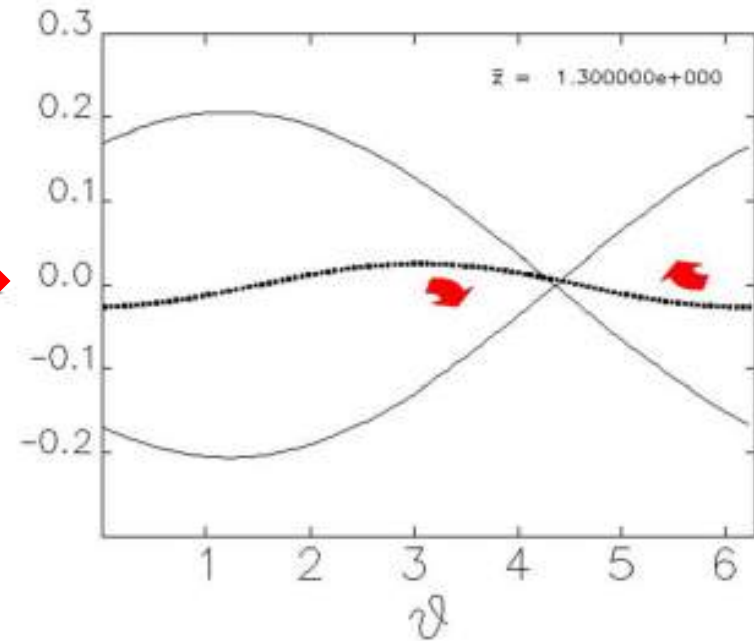
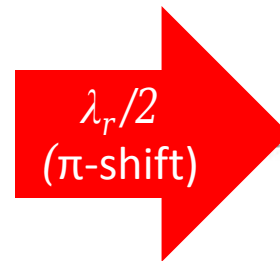
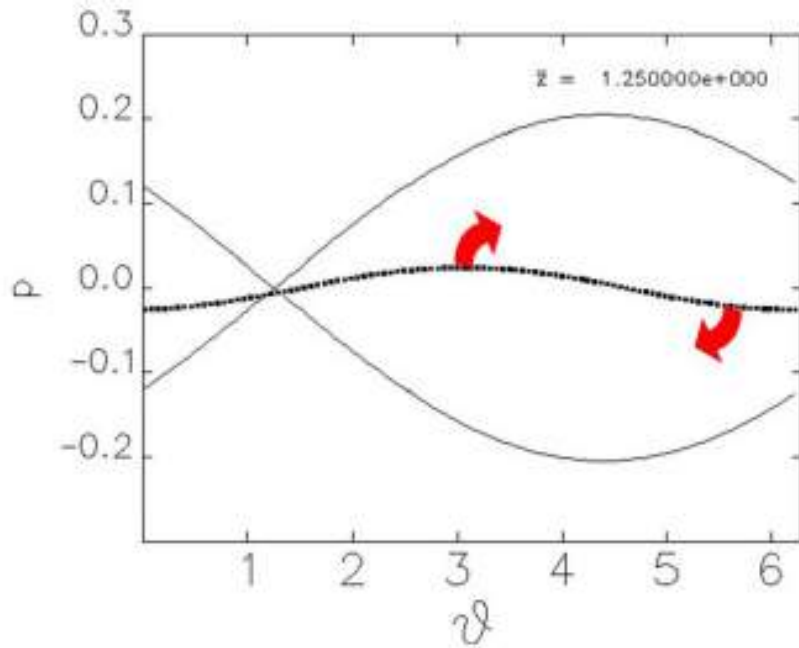
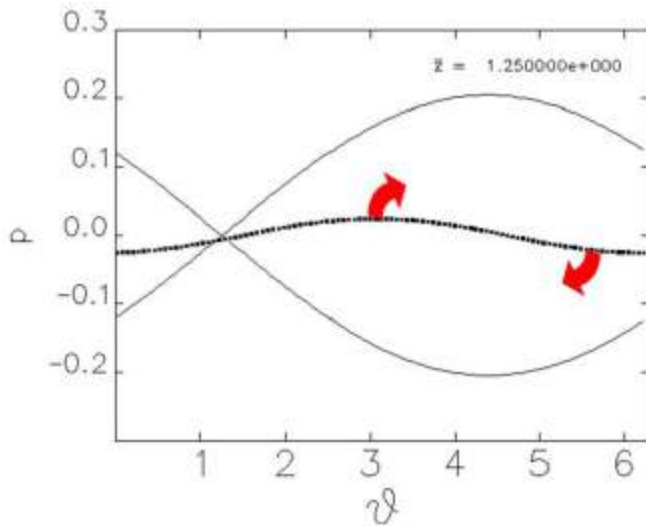
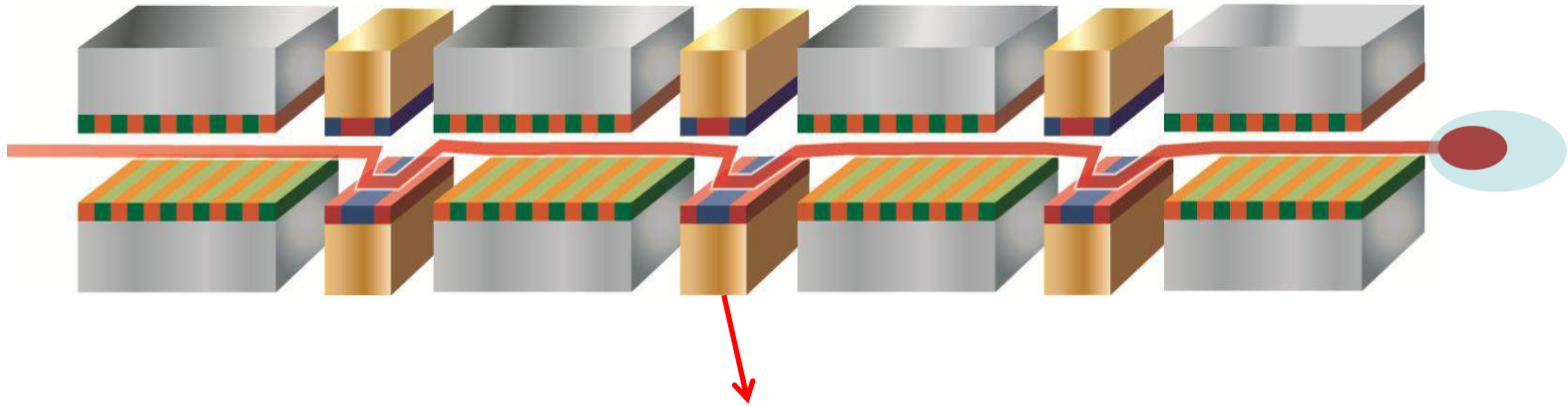


Figure 1: Electron trajectories in phase-space ( $\vartheta, p$ ) at beginning of FEL-type interaction. The solid line is the instantaneous separatrix and the red arrows indicate the direction of electron phase flow.

Figure 2: Electron trajectories in phase-space at beginning of FEL-type interaction as Fig. 1 but immediately following a relative  $\Delta\vartheta = \pi$  phase change between electrons and radiation.

# Phase shifting

Electron delay



$\pi$ -shift

Use chicanes to delay electrons

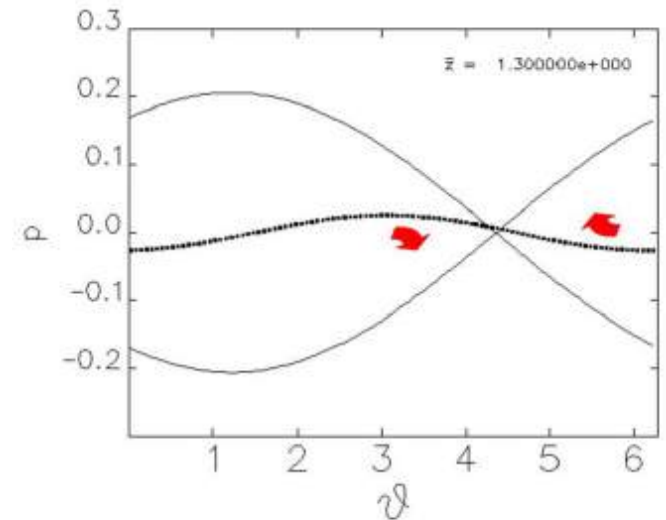


Figure 1: Electron trajectories in phase-space  $(\vartheta, p)$  at beginning of FEL-type interaction. The solid line is the instantaneous separatrix and the red arrows indicate the direction of electron phase flow.

Figure 2: Electron trajectories in phase-space at beginning of FEL-type interaction as Fig. 1 but immediately following a relative  $\Delta\vartheta = \pi$  phase change between electrons and radiation.

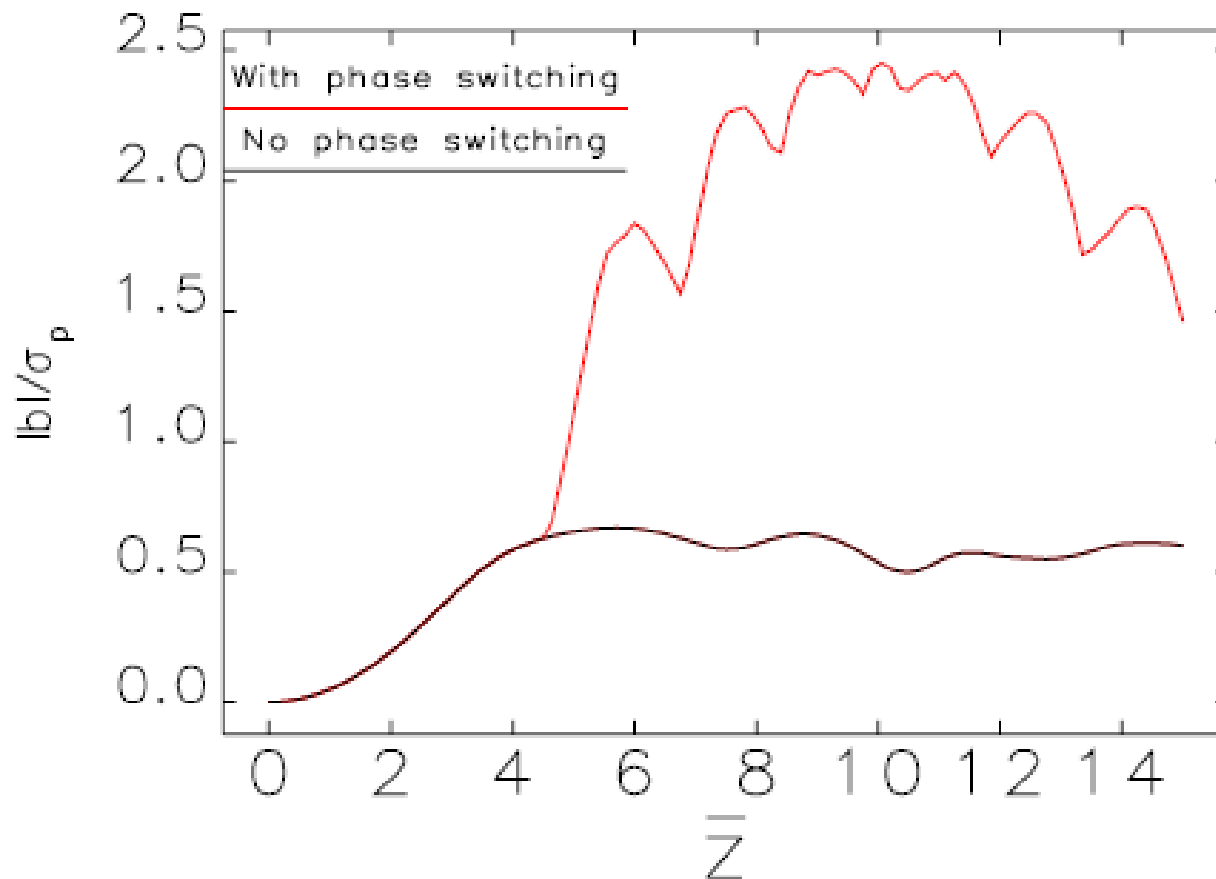
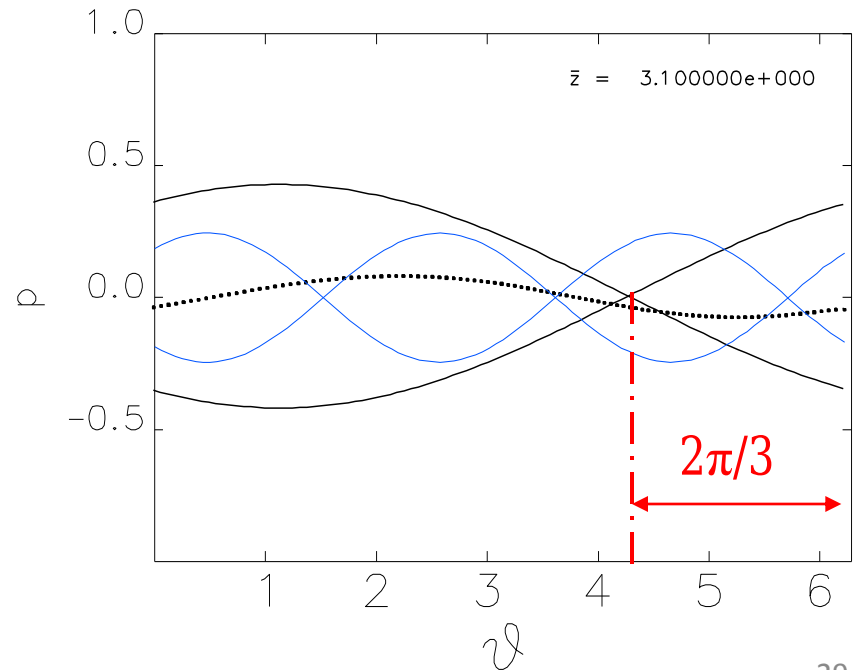
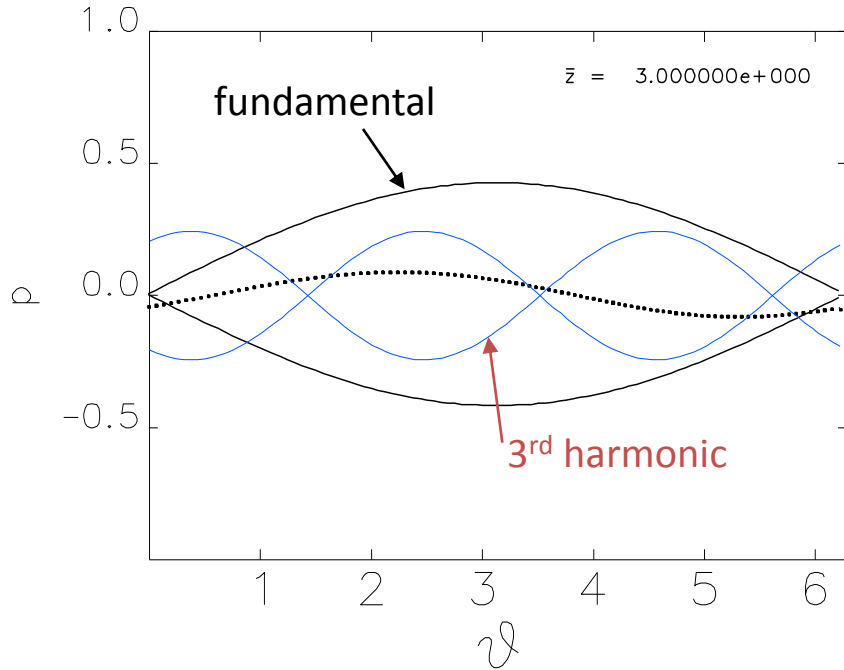


Figure 5: FEL type evolution of the quantity  $|b|/\sigma_p$  as a function of scaled distance,  $\bar{z}$ , through the interaction region.

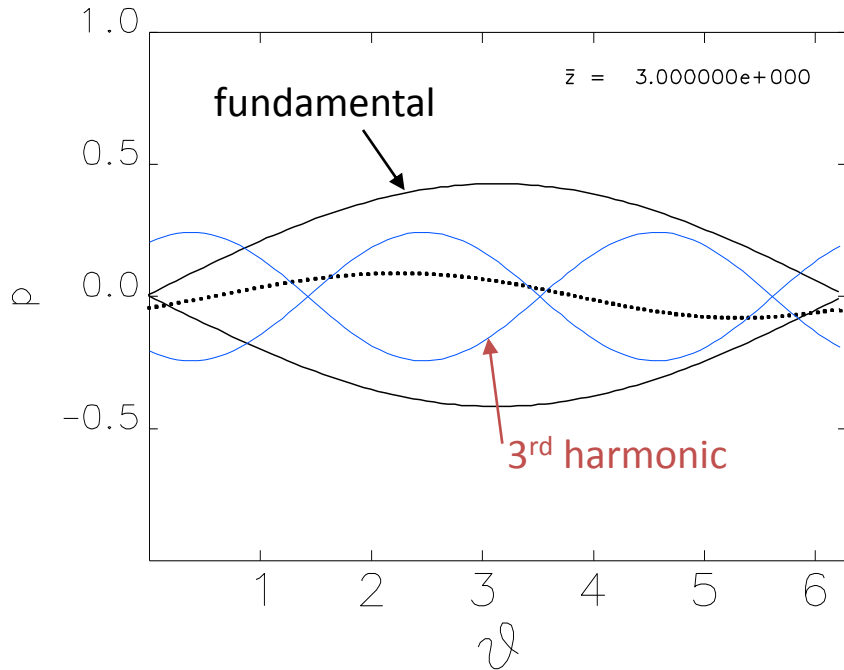
**Result: bunching with reduced energy spread**

# Can also get Harmonic Amplifier FEL\*

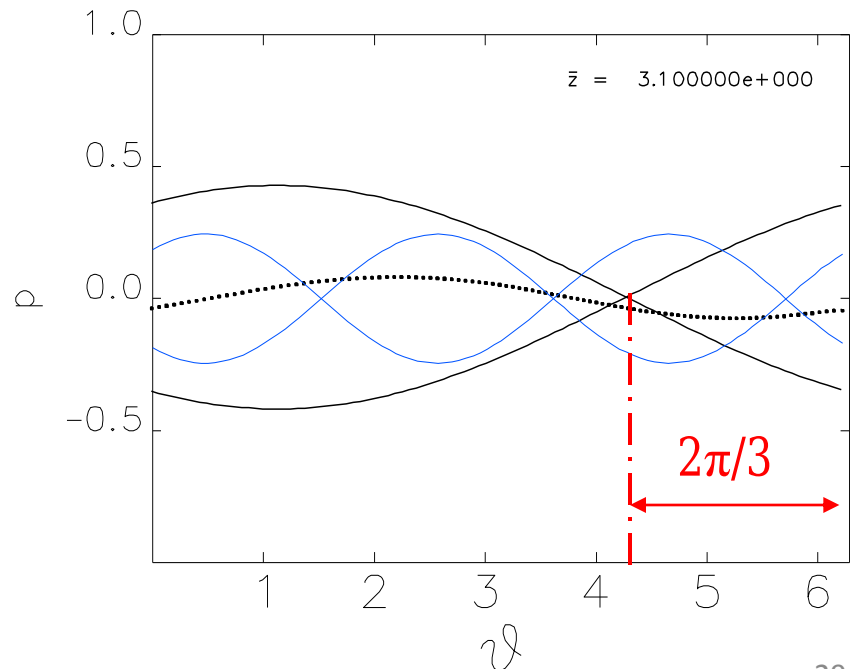


\*McNeil, Robb & Poole, PAC 2005, Knoxville, Tennessee, 1718-20

# Can also get Harmonic Amplifier FEL\*

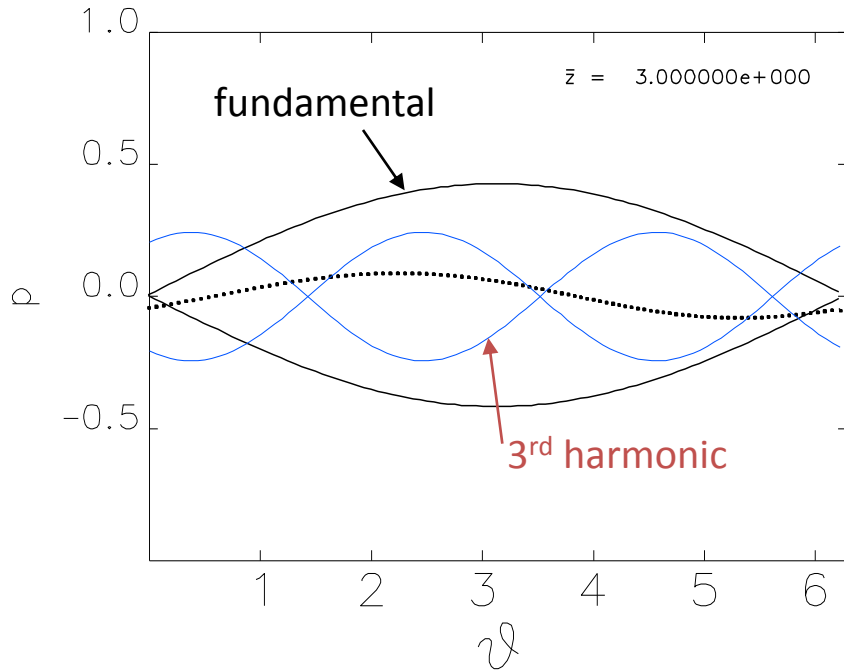


A relative phase change between electrons and fundamental radiation of  $n2\pi/3$  ( $n$  - integer) will disrupt the fundamental-electron coupling and so the fundamental's growth.



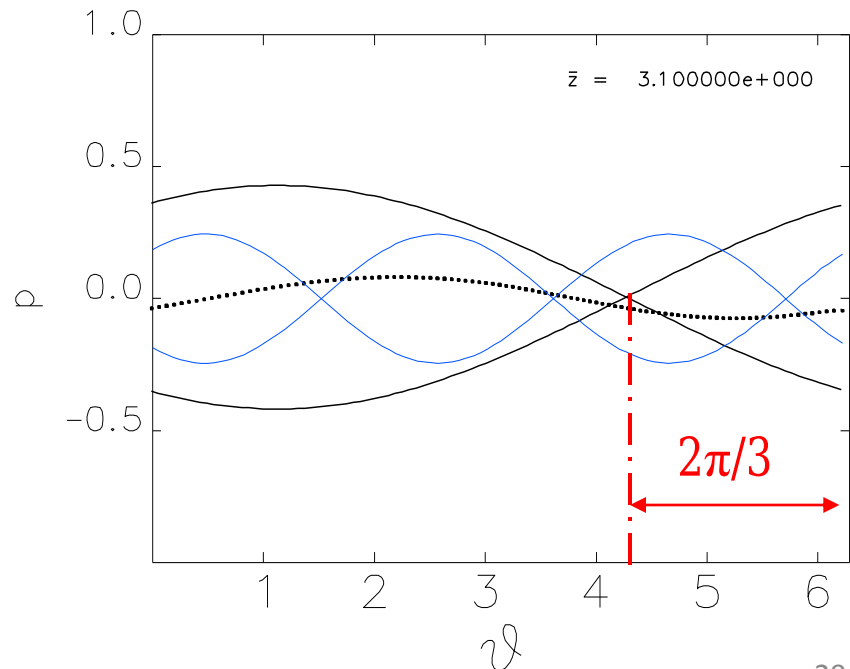
\*McNeil, Robb & Poole, PAC 2005, Knoxville, Tennessee, 1718-20

# Can also get Harmonic Amplifier FEL\*



However, a  $n2\pi/3$  phase change for the fundamental is a  $n2\pi$  phase change for the 3<sup>rd</sup> harmonic – The 3<sup>rd</sup> harmonic interaction therefore suffers no disruption.

A relative phase change between electrons and fundamental radiation of  $n2\pi/3$  ( $n$  - integer) will disrupt the fundamental-electron coupling and so the fundamental's growth.





Using a seeded steady-state model\* (i.e. no pulses effects):

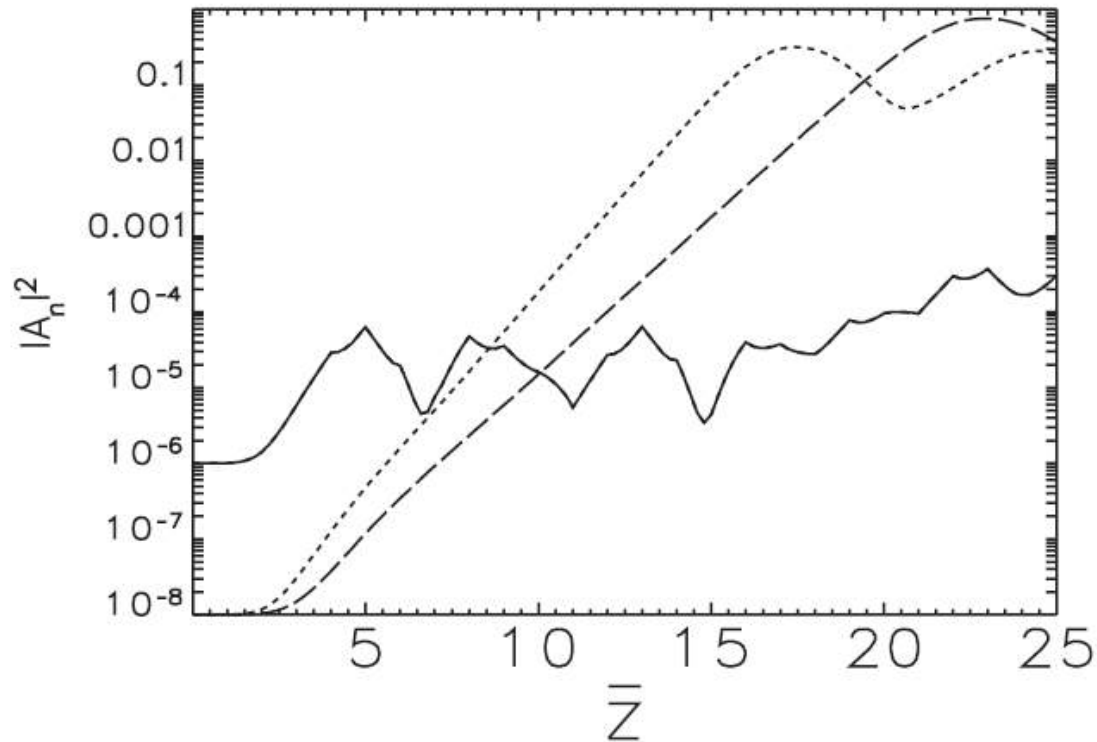


FIG. 2. Scaled powers of fundamental  $|A_1|^2$  (solid line) and third harmonic  $|A_3|^2$  (dotted line) for wiggler parameter  $a_1 = 4$  demonstrating the effects of relative phase changes of  $\Delta\theta = 2\pi/3$  at  $\bar{z} = 4, 5, 6, \dots, 24$ . For the wiggler parameter retuned to  $a_3 = 2.16$ ,  $A_3$  is the fundamental and a separate simulation shows how  $|A_3|^2$  (dashed line) evolves.

\*McNeil, Robb, Poole & Thompson, PRL **96**, 084801 (2006)  
Schneidmiller & Yurkov, PRST-AB **15**, 080702 (2012) - For SASE

Using a seeded steady-state model\* (i.e. no pulses effects):

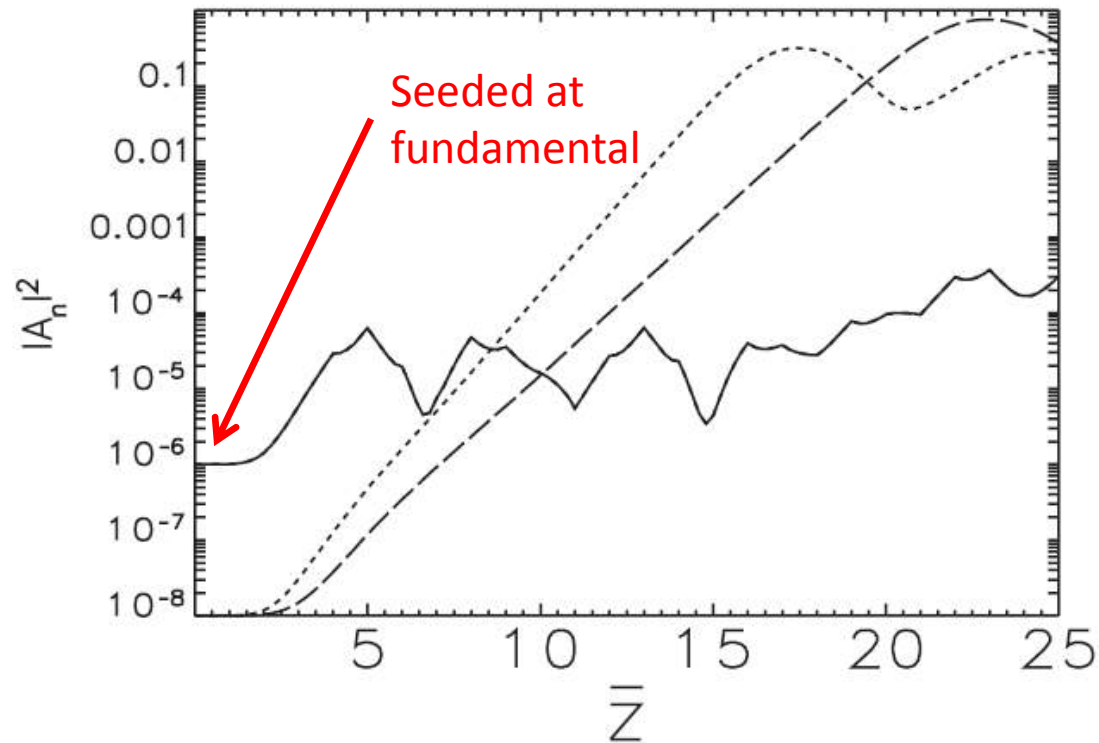


FIG. 2. Scaled powers of fundamental  $|A_1|^2$  (solid line) and third harmonic  $|A_3|^2$  (dotted line) for wiggler parameter  $a_1 = 4$  demonstrating the effects of relative phase changes of  $\Delta\theta = 2\pi/3$  at  $\bar{z} = 4, 5, 6, \dots, 24$ . For the wiggler parameter retuned to  $a_3 = 2.16$ ,  $A_3$  is the fundamental and a separate simulation shows how  $|A_3|^2$  (dashed line) evolves.

\*McNeil, Robb, Poole & Thompson, PRL **96**, 084801 (2006)  
Schneidmiller & Yurkov, PRST-AB **15**, 080702 (2012) - For SASE

Large shifts  $\gg \lambda_r$   
(But no phase shifting)

The introduction of longer shifts,  $\gg \lambda_r$  over many wavelengths, was subject of PhD study from Oct. 2005 to improve SASE coherence:

## Year One/Two Report

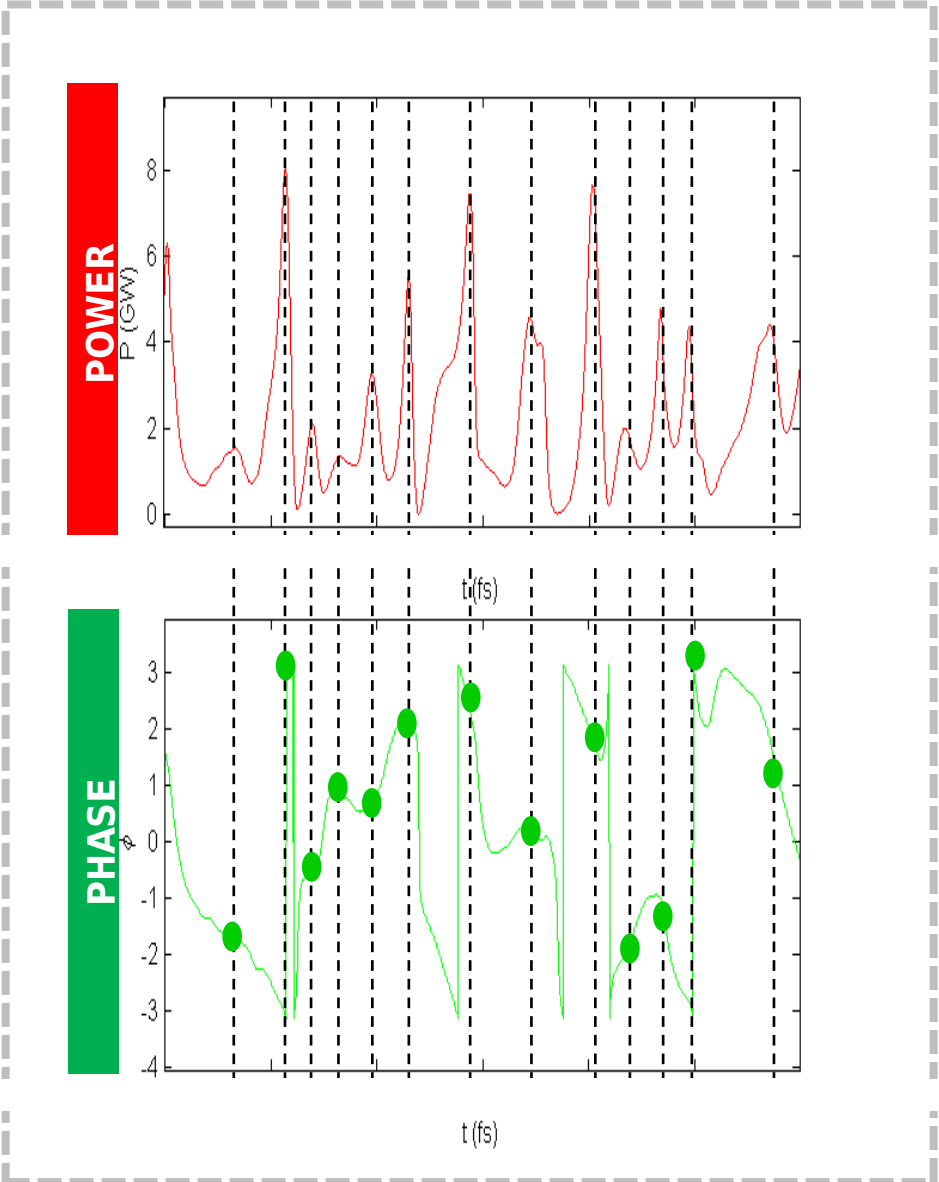
N. R. Thompson

13 January 2007

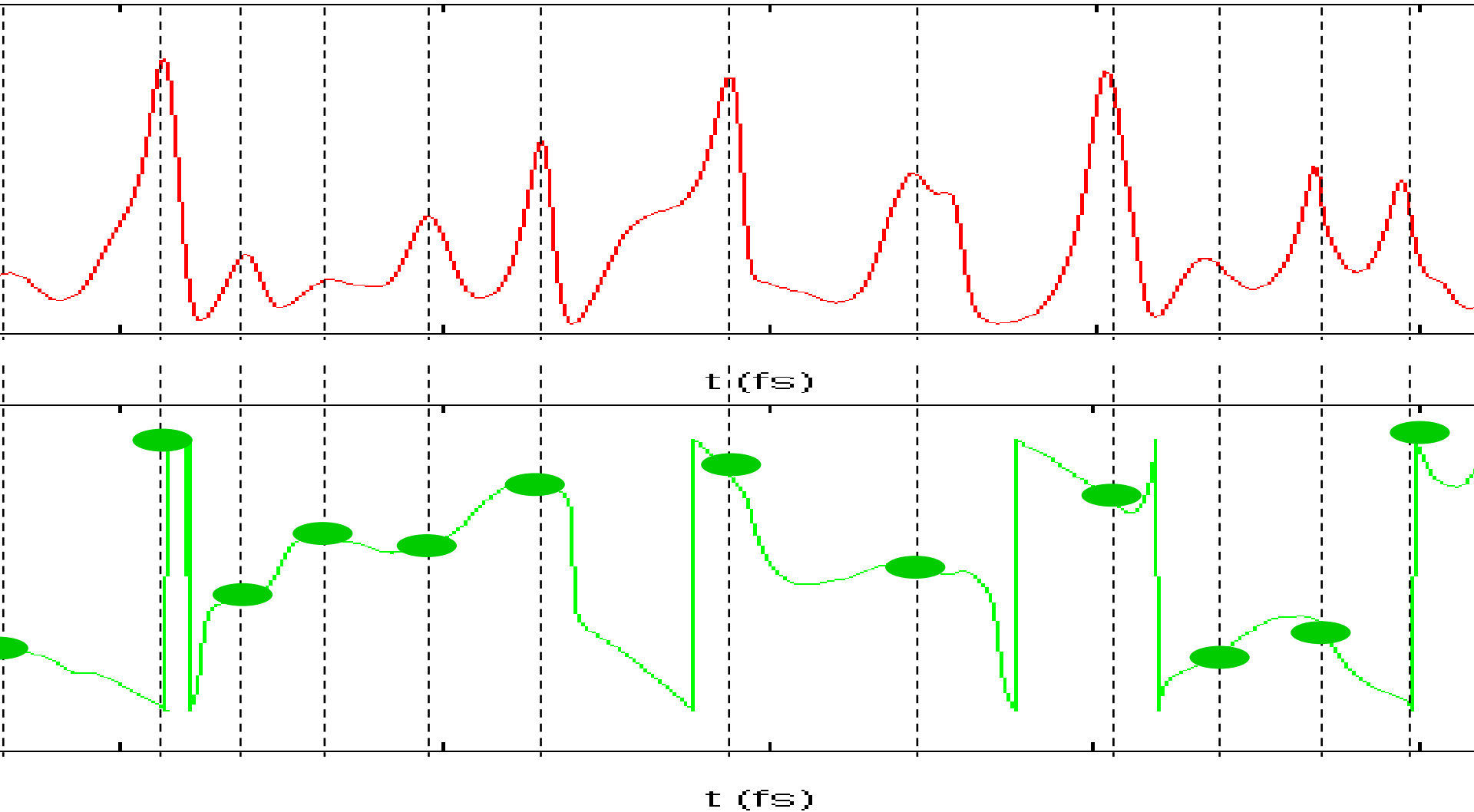
### Abstract

This report summarises the research carried out until January 2007. The main thrust has been the development of techniques and ideas to improve the longitudinal (or temporal) coherence of Self-Amplified Spontaneous Emission (SASE) Free-Electron Lasers. Some satisfactory progress has been made in this area, as well as observation of new phenomena which are not yet understood but which promise to be interesting fields for future research.

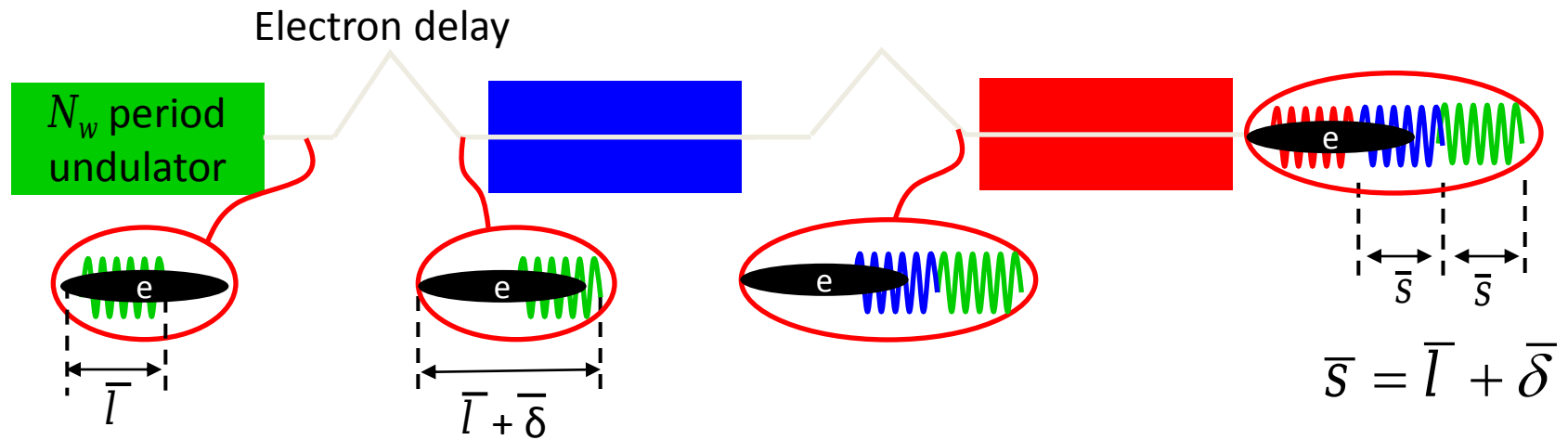
# Method: Stretch out the interaction and the coherence length:



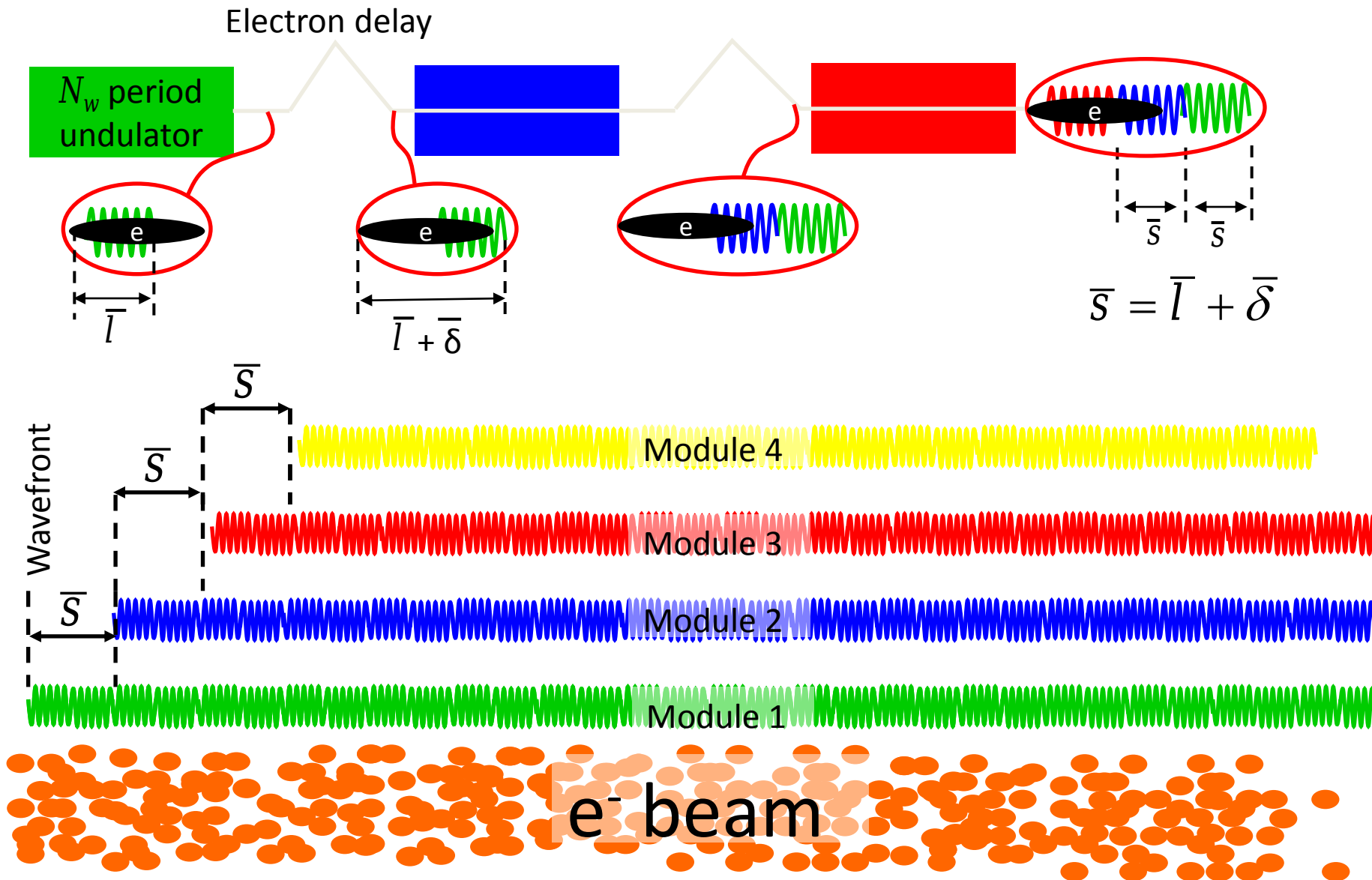
Method: Stretch out the interaction and the coherence length:



# Large shifts $\gg \lambda_r$ ,

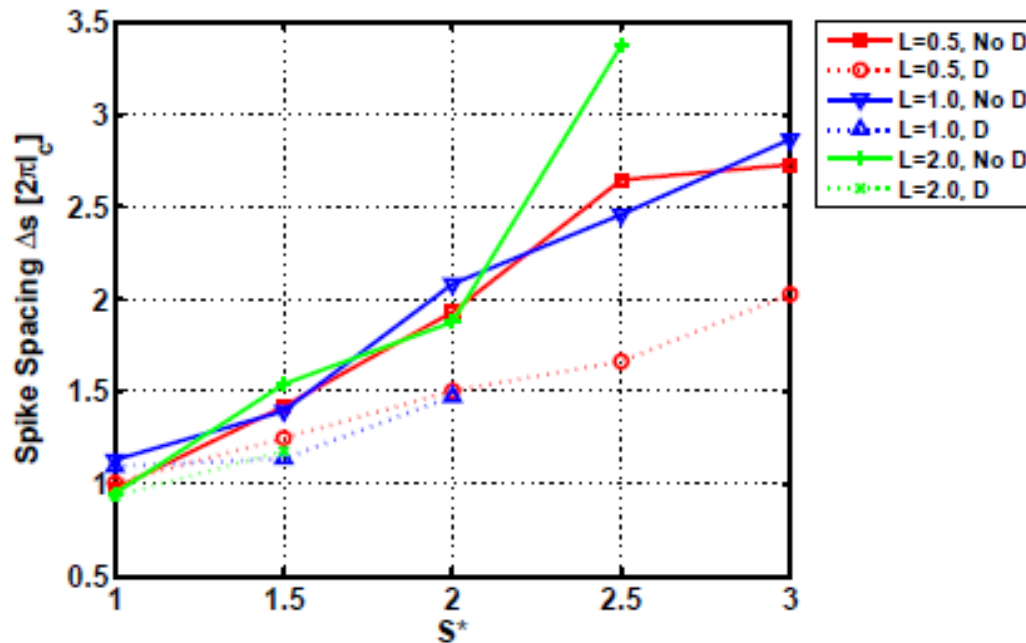
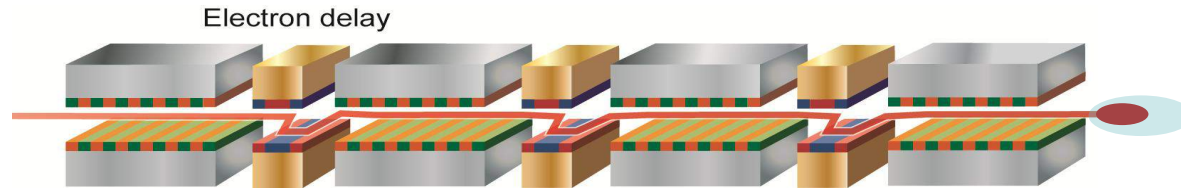


# Large shifts $\gg \lambda_r$ ,





# Chicanes with equal electron delays $\gg \lambda_r$



Increased cooperation length:

$$\hat{l}_c \simeq l_c S_e$$

$$S_e = (l + \delta) / l$$

↑  
Undulator  
slippage

↑  
Chicane  
slippage

Figure 2: The mean spacing between spikes in units of  $2\pi l_c$  for rectangular electron bunch current profile, as a function of the slippage enhancement factor  $S^*$ .

Summarising:

Increasing spike separation  $\Rightarrow$  Increasing cooperation length  
 $\Rightarrow$  Improved temporal coherence

# Chicanes with equal electron delays $\gg \lambda_r$

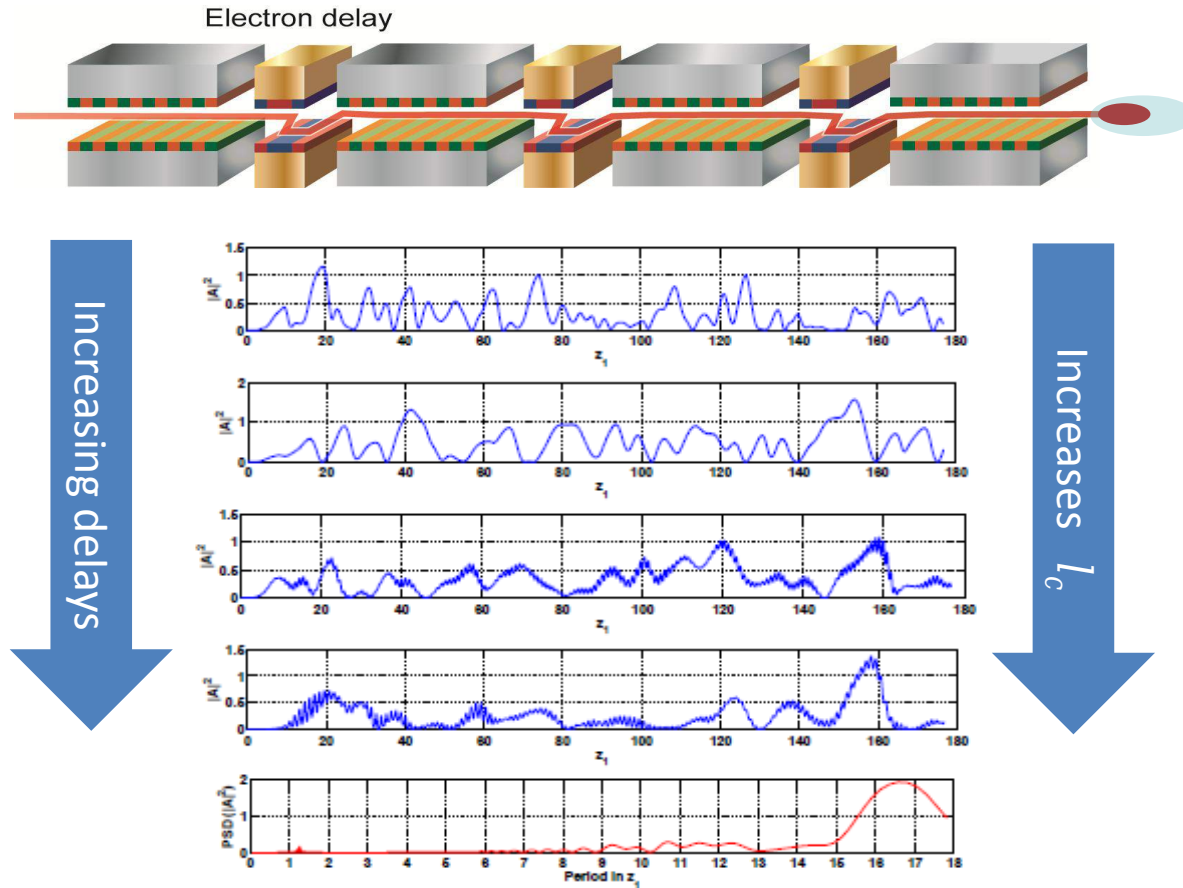


Figure 1: Pulse intensity profiles for a rectangular electron bunch, with undulator section length  $L = 0.5$ . The  $z$ -shifts are non-dispersive, with  $S^* = 1$  (i.e. SASE) at the top, then  $S^* = 1.5$ ,  $S^* = 2.0$ ,  $S^* = 2.5$ . It is clear that the spikes broaden and separate as  $S^*$  increases, accompanied by the appearance of small-period oscillations. The bottom plot shows the Fourier transform of the pulse intensity for the case  $S^* = 2.5$  where  $\delta_c = 1.25$ . It is seen that the small oscillations on the intensity plot have a period of 1.25 and that the longer scale oscillation has a period of  $\sim 16.5$  which is close to  $2\pi S^* = 15.7$ .

# Chicanes with equal electron delays $\gg \lambda_r$

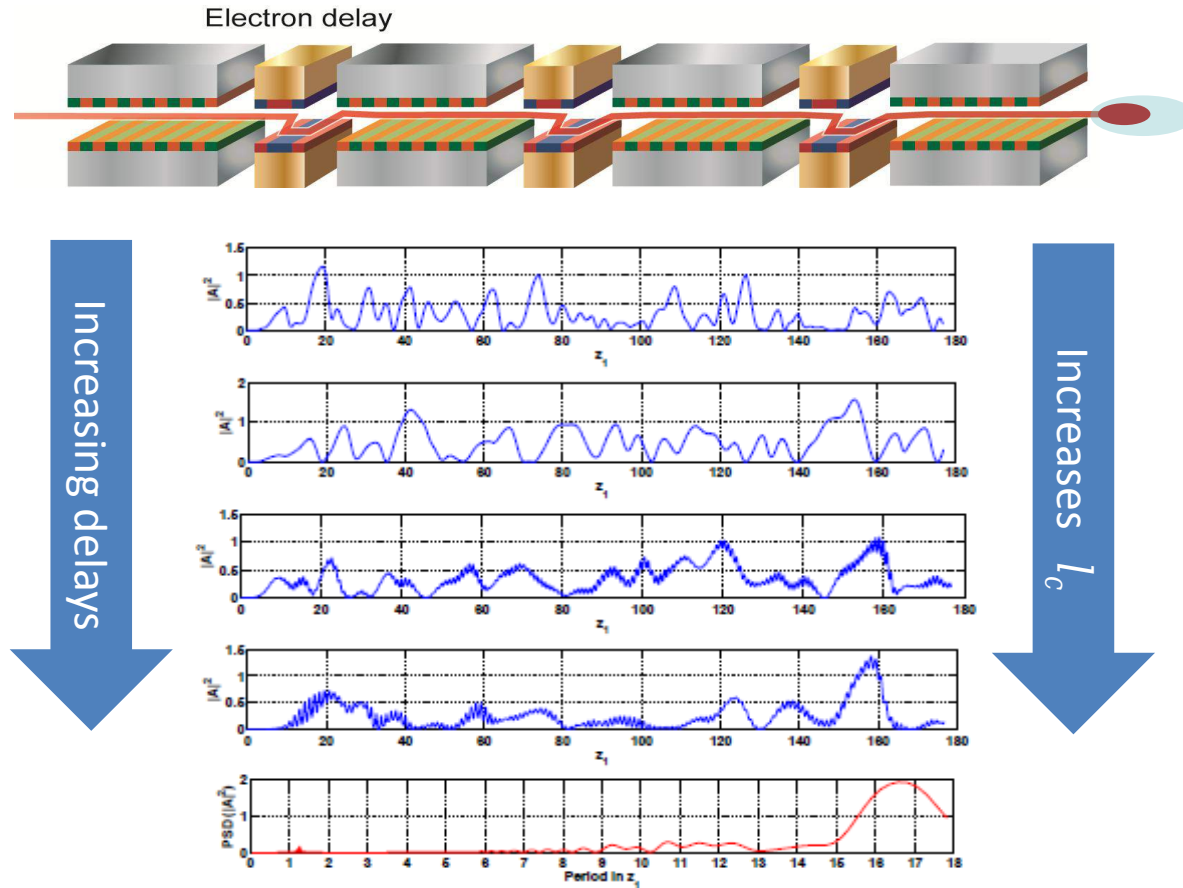


Figure 1: Pulse intensity profiles for a rectangular electron bunch, with undulator section length  $L = 0.5$ . The  $z$ -shifts are non-dispersive, with  $S^* = 1$  (i.e. SASE) at the top, then  $S^* = 1.5$ ,  $S^* = 2.0$ ,  $S^* = 2.5$ . It is clear that the spikes broaden and separate as  $S^*$  increases, accompanied by the appearance of small-period oscillations. The bottom plot shows the Fourier transform of the pulse intensity for the case  $S^* = 2.5$  where  $\xi_0 = 0.95$ . It is clear that the small oscillations on the intensity plot have a period of 1.25 and that the longer scale oscillation has a period of  $\sim 16.5$  which is close to  $2\pi S^* = 15.7$ .

**Some success!**

# Chicanes with equal electron delays $\gg \lambda_r$

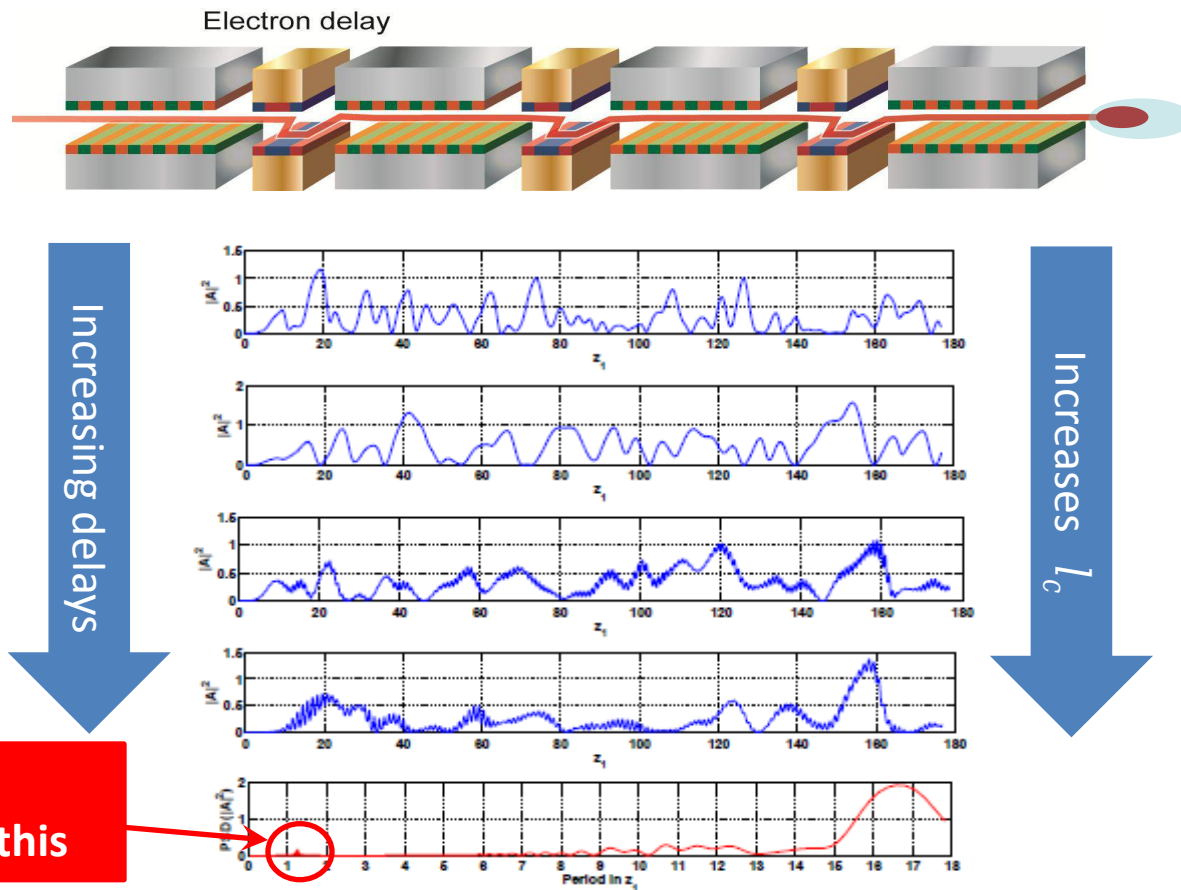


Figure 1: Pulse intensity profiles for a rectangular electron bunch, with undulator section length  $L = 0.5$ . The  $z$ -shifts are non-dispersive, with  $S^* = 1$  (i.e. SASE) at the top, then  $S^* = 1.5$ ,  $S^* = 2.0$ ,  $S^* = 2.5$ . It is clear that the spikes broaden and separate as  $S^*$  increases, accompanied by the appearance of small-period oscillations. The bottom plot shows the Fourier transform of the pulse intensity for the case  $S^* = 2.5$  where  $\omega_0 = 0.95$ . It is clear that the small oscillations on the intensity plot have a period of 1.25 and that the longer scale oscillation has a period of  $\sim 16.5$  which is close to  $2\pi S^* = 15.7$ .

**Some success!**

## COHERENCE OF E-BEAM RADIATION SOURCES AND FELS – A THEORETICAL OVERVIEW

Avi Gover, Egor Dyunin, Tel-Aviv University, Ramat Aviv, Israel.

A third scheme that should be considered for phase locking and increasing the coherence of the radiation in a SASE FEL consists of imposing periodic perturbation on the wiggler (e.g. periodic dispersive sections) [20]. The filtering effect of the periodic structure may be viewed as the analogue of linewidth narrowing of radiation emitted in a Fabri-Perot resonator. It is speculated (but needs further study) that if the SASE FEL in such a structure arrives to saturation within the wiggler length, nonlinear process of mode competition between the filtered spikes will lead to further increase of coherence and stability in analogy to the CW FEL oscillator case discussed previous.

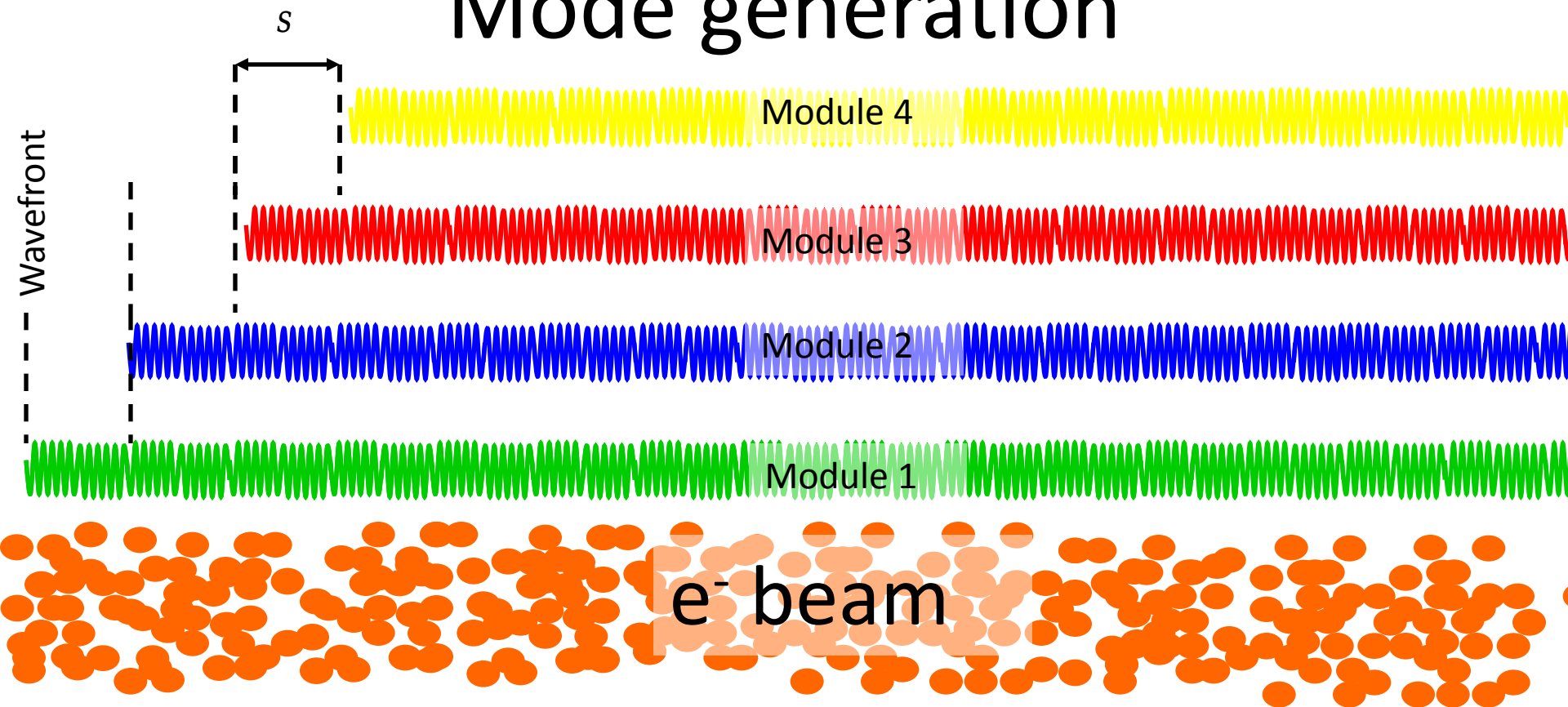
Also get  
'cavity' modes

Linear process

Clearly thinking along the same lines, but did not pursue further?

# Generating Modes

# Mode generation

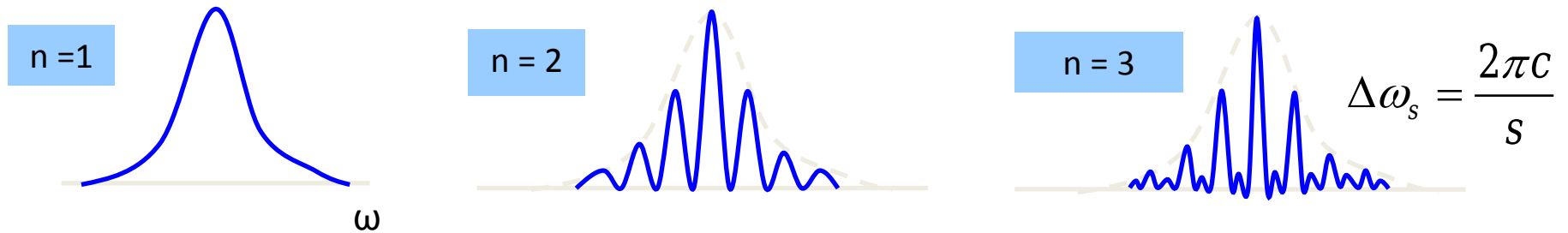
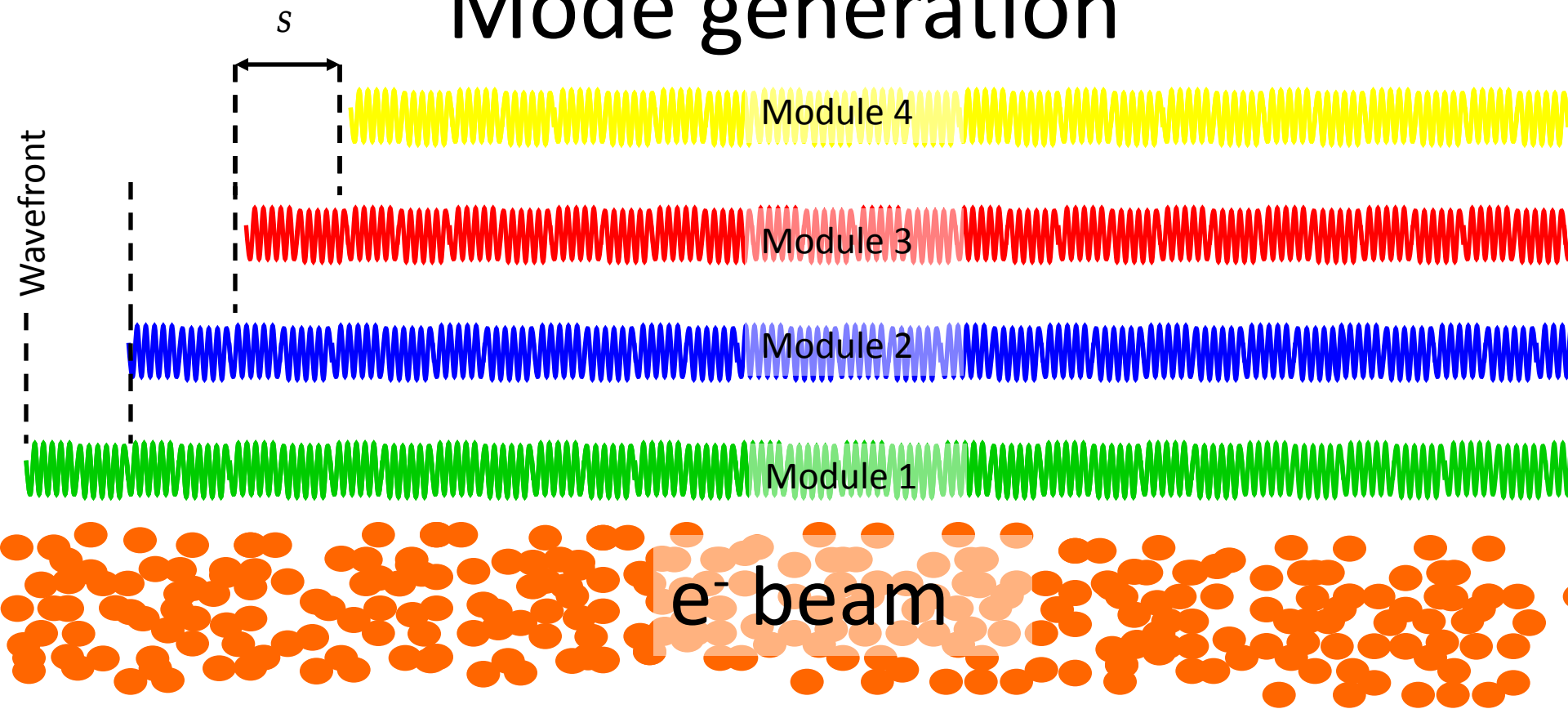


For continued slips of distance  $s$ , only those wavelengths with an integer number of periods in distance  $s$  will survive after many such slips. For  $s$  an integer of  $\lambda_j$ :

$$s = N\lambda_j = (N + 1)\lambda_{j-1}$$

$$\Rightarrow \omega_j = \frac{2\pi c N}{s}; \omega_{j-1} = \frac{2\pi c (N + 1)}{s} \Rightarrow \Delta\omega_s = \omega_{j-1} - \omega_j = \frac{2\pi c}{s}$$

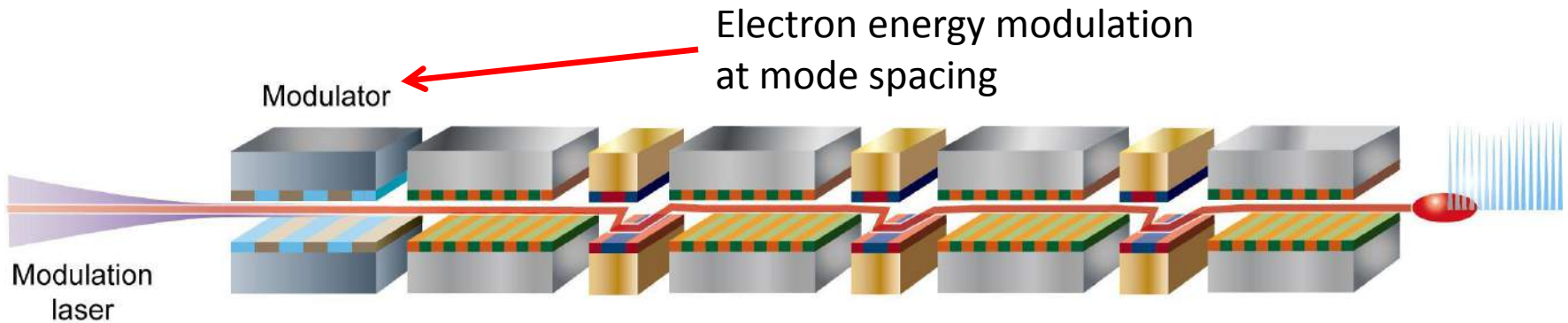
# Mode generation



*The spectrum is the same as a ring cavity of length  $S$ . A ring cavity of length equal to the total slippage in each undulator/chicane module has been synthesized*



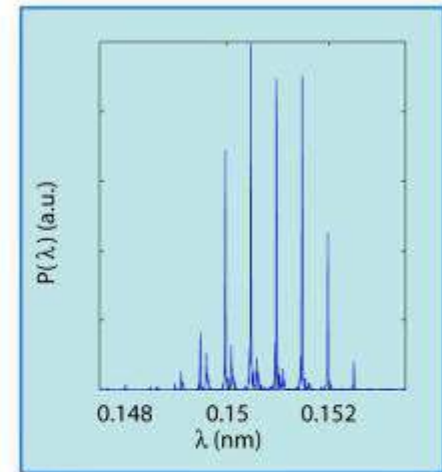
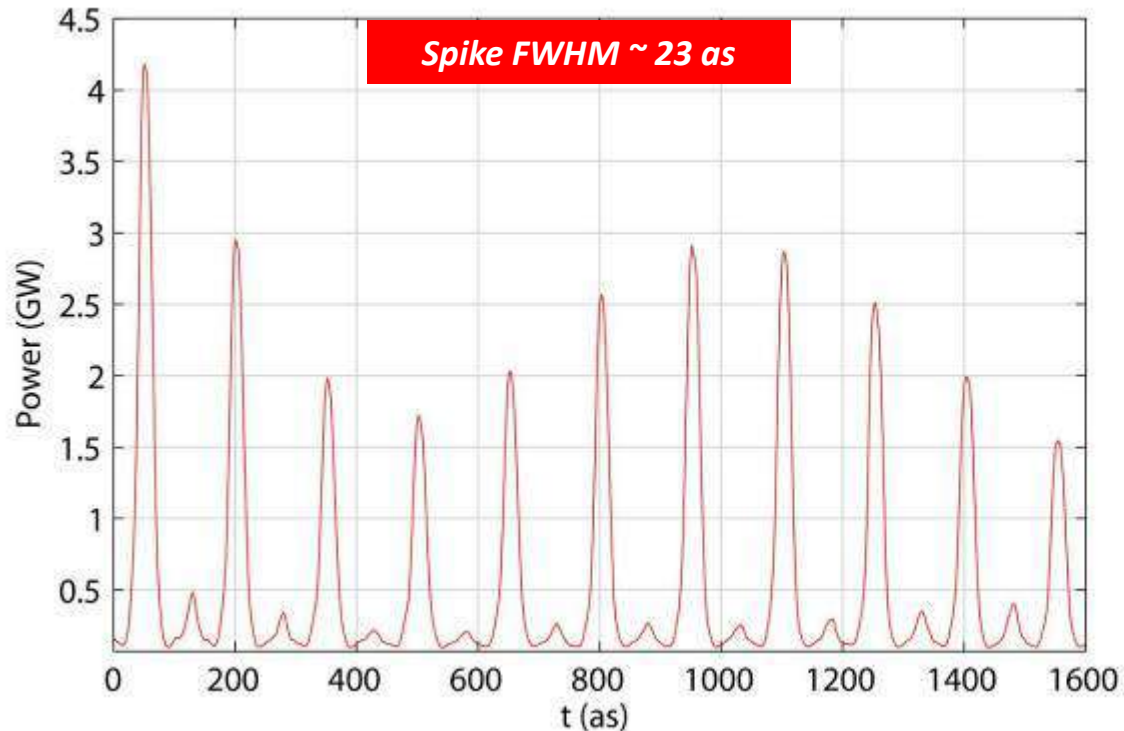
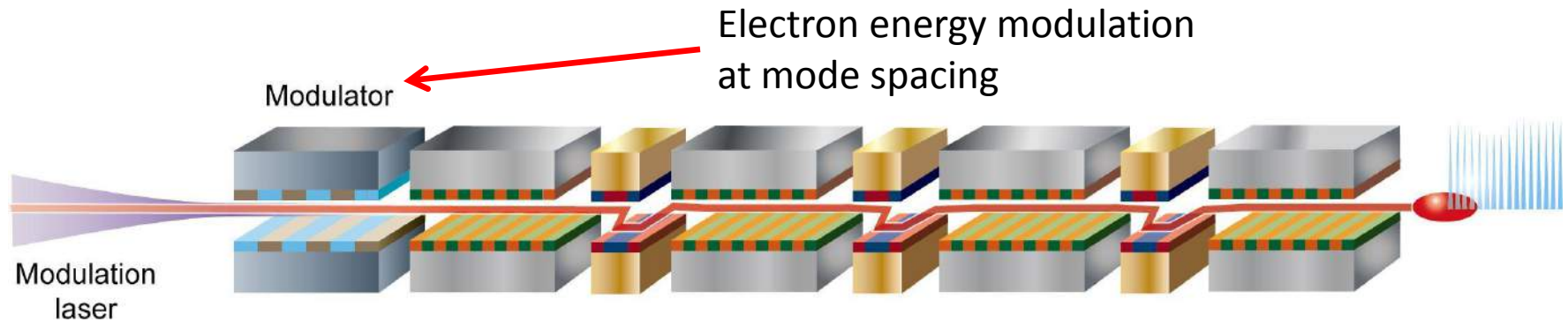
# X-ray FEL amplifier with mode-locking\*



\*Thompson, McNeil, PRL **100**, 203901 (2008)

Kur, Dunning, McNeil, Wurtele & Zholents, NJP **13**, 063012 (2011)

# X-ray FEL amplifier with mode-locking\*

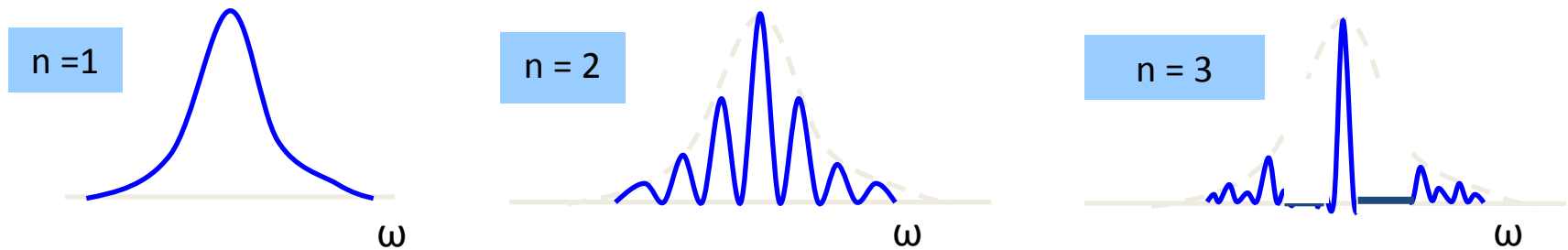
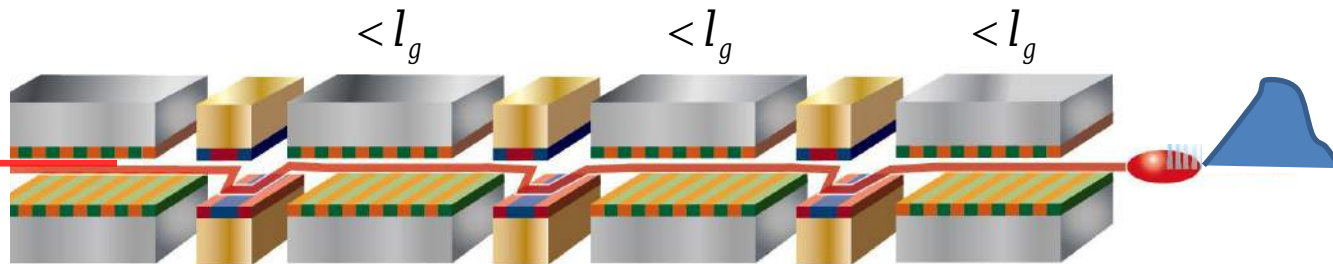


\*Thompson, McNeil, PRL **100**, 203901 (2008)  
Kur, Dunning, McNeil, Wurtele & Zholents, NJP **13**, 063012 (2011)

# Removing the modes

Different chicane delays\* introduce **different** integer resonant wavelength delay to  $e^-$ :

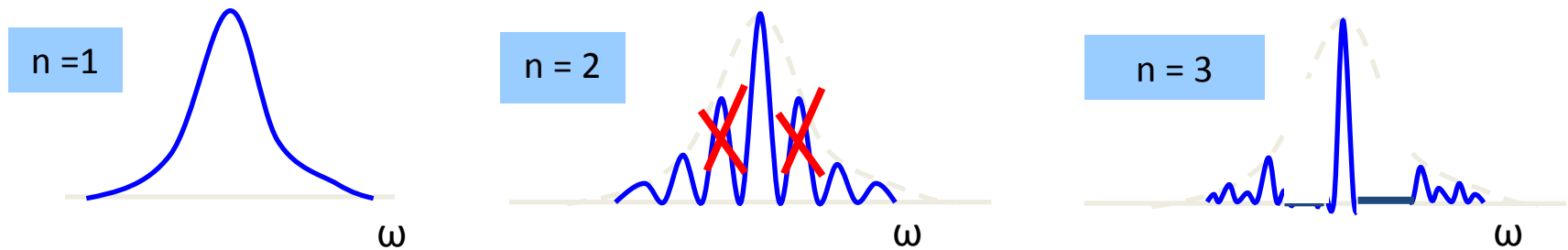
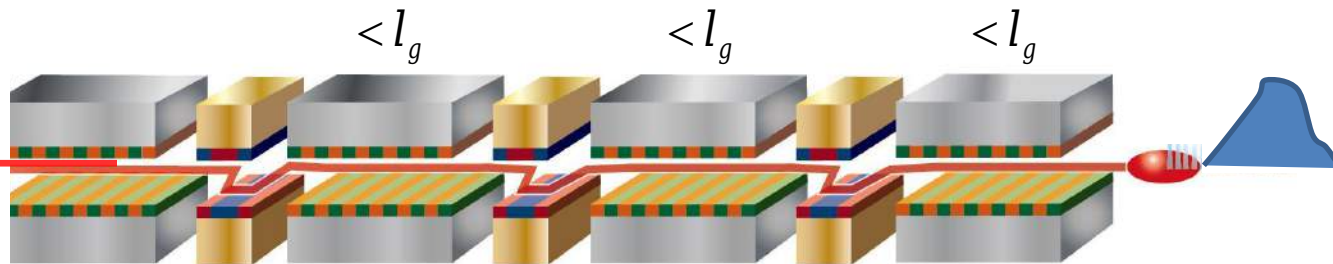
$\Rightarrow \Delta\omega_s = \frac{2\pi c}{S_n}$  is different for each module, to leave only the central resonant wavelength.



\*Thompson, Dunning & McNeil, 'Improved temporal coherence in SASE FELs', TUPE050, Proceedings of IPAC'10, Kyoto, Japan

Different chicane delays\* introduce **different** integer resonant wavelength delay to  $e^-$ :

$\Rightarrow \Delta\omega_s = \frac{2\pi c}{S_n}$  is different for each module, to leave only the central resonant wavelength.



\*Thompson, Dunning & McNeil, 'Improved temporal coherence in SASE FELs', TUPE050, Proceedings of IPAC'10, Kyoto, Japan

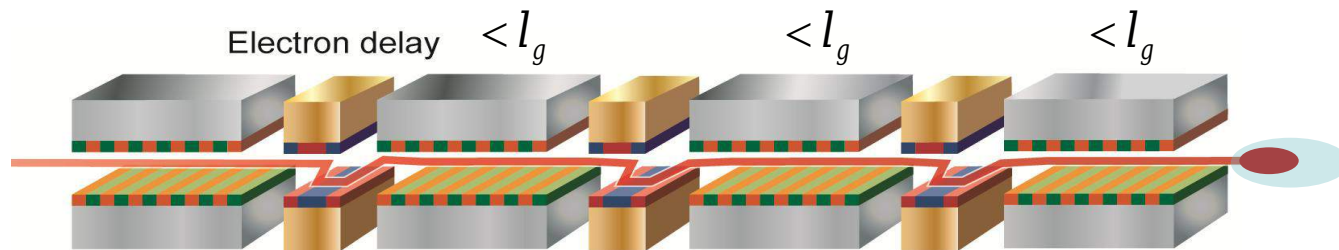
# High-Brightness SASE – Stage I\*

Proceedings of IPAC'10, Kyoto, Japan

TUPE050

## IMPROVED TEMPORAL COHERENCE IN SASE FELS

N.R. Thompson and D. J. Dunning, ASTeC/CI, STFC Daresbury Laboratory, UK  
B. W. J. McNeil, University of Strathclyde, Scotland, UK



To remove the modes, a randomness in the chicane delays was introduced :

$$\bar{\delta}_n = \bar{\delta} + \bar{\delta}_r$$

where:  $\bar{\delta}$  is a constant and  $\bar{\delta}_r$  is a uniform random variate  $|\bar{\delta}_r| < \bar{\delta}$



# High-Brightness SASE – Stage I\*

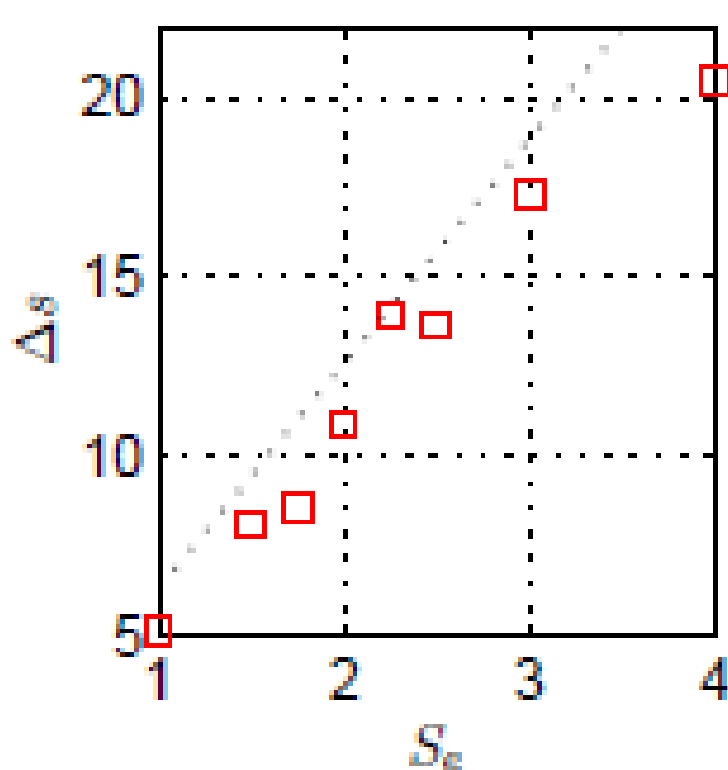
Proceedings of IPAC'10, Kyoto, Japan

TUPE050

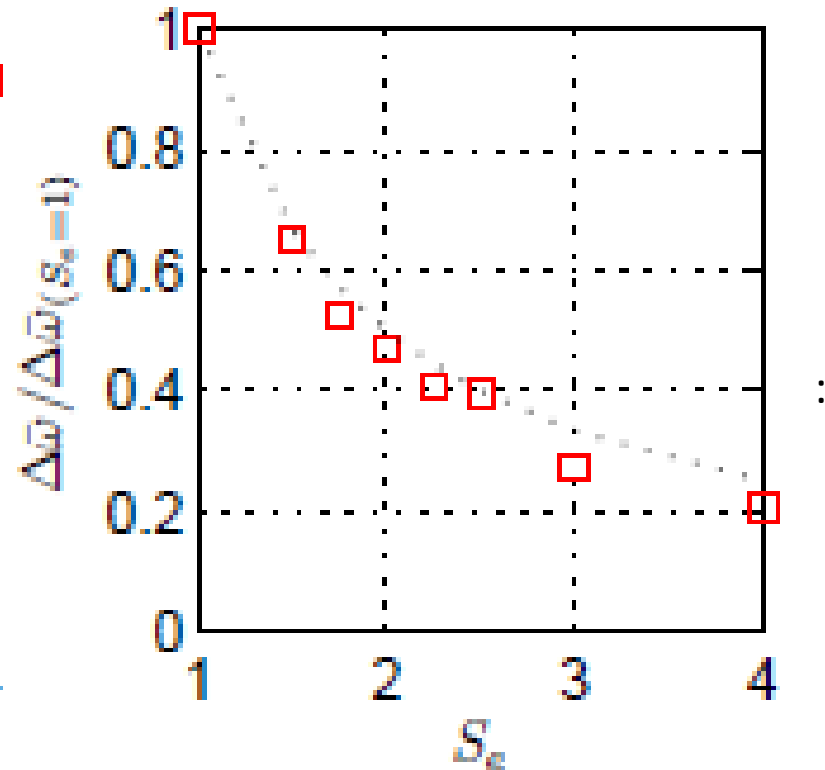
## IMPROVED TEMPORAL COHERENCE IN SASE FELS

N.R. Thompson and D. J. Dunning, ASTeC/CI, STFC Daresbury Laboratory, UK

B. W. J. McNeil, University of Strathclyde, Scotland, UK



Mean spike spacing



Bandwidth reduction

# High-Brightness SASE – Stage II

- The following results are for a delay sequence based on **Prime Numbers**, as a method of prohibiting the sidebands:

As the frequency spacing of the axial modes is inversely proportional to the delay  $s$ :

- ***no common supported sidebands between any two delays***
- The prime delay sequence is defined as

$$\bar{s}_n = \mathbb{P}_n \bar{s}_1 / 2 \quad \mathbb{P}_n \text{ is sequence of primes beginning with } \mathbb{P}_1 = 2$$

- Setting  $s_1$  scales the whole sequence.

## Transform-Limited X-Ray Pulse Generation from a High-Brightness Self-Amplified Spontaneous-Emission Free-Electron Laser

B. W. J. McNeil,<sup>1,\*</sup> N. R. Thompson,<sup>1,2,†</sup> and D. J. Dunning<sup>1,2,‡</sup>

<sup>1</sup>University of Strathclyde (SUPA), Glasgow G4 0NG, United Kingdom

<sup>2</sup>ASTeC, Daresbury Laboratory, Warrington WA4 4AD, United Kingdom

(Received 23 December 2012; published 26 March 2013)

- The following results are for a delay sequence based on **Prime Numbers**, as a method of prohibiting the sidebands:

As the frequency spacing of the axial modes is inversely proportional to the delay  $s$ :

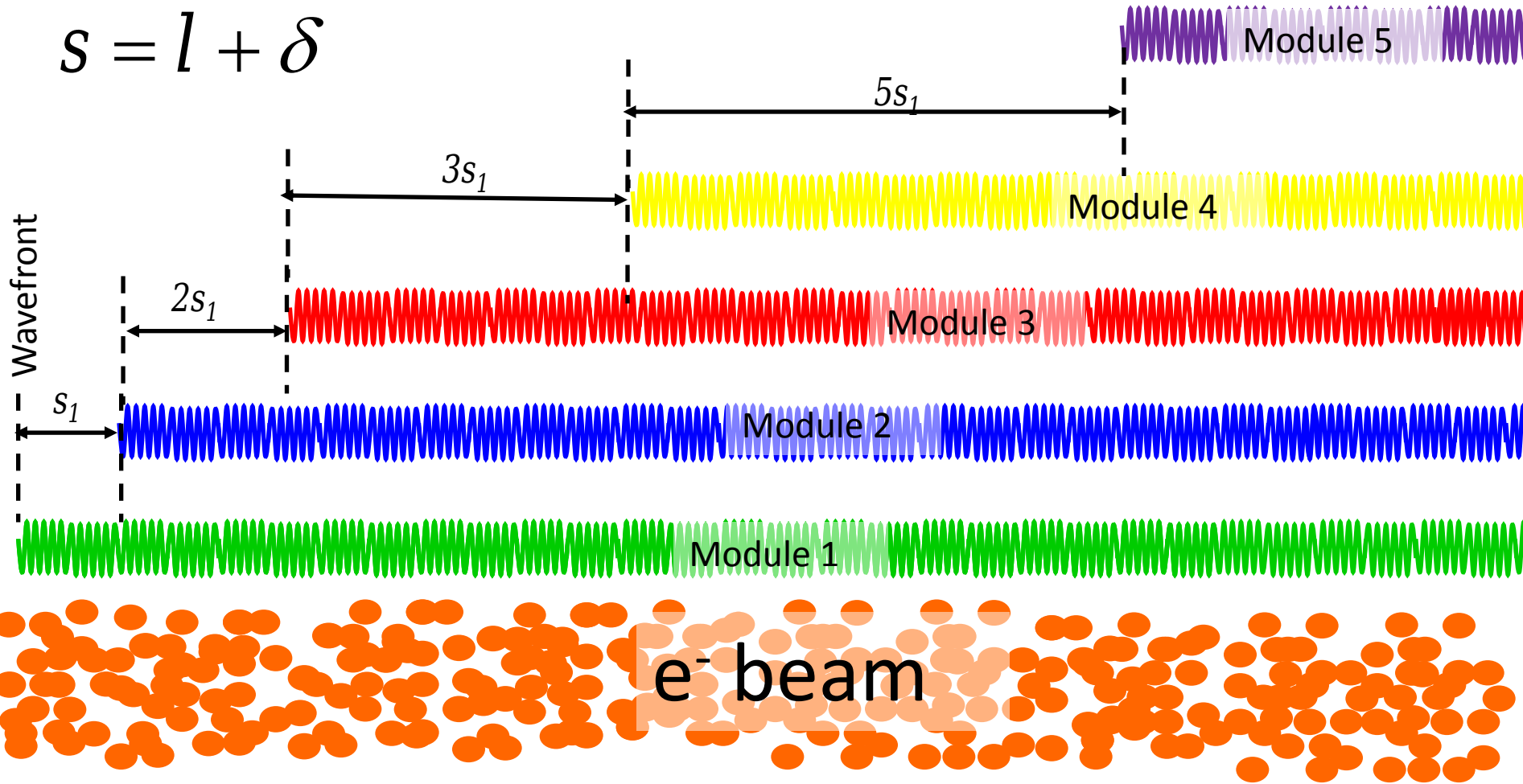
- ***no common supported sidebands between any two delays***

- The prime delay sequence is defined as

$$\bar{s}_n = \mathbb{P}_n \bar{s}_1 / 2 \quad \mathbb{P}_n \text{ is sequence of primes beginning with } \mathbb{P}_1 = 2$$

- Setting  $s_1$  scales the whole sequence.

# HB-SASE Mechanism I



Undulator modules have lengths  $l_g \lesssim 1$   
Radiation wavefronts then propagate  $\lesssim l_c$   
through electrons in each module

Due to extra slippage, no radiation wavefront propagates through electrons within local range  $l_c$  in successive undulators – **NO LOCALISED COOPERATIVE EFFECTS**

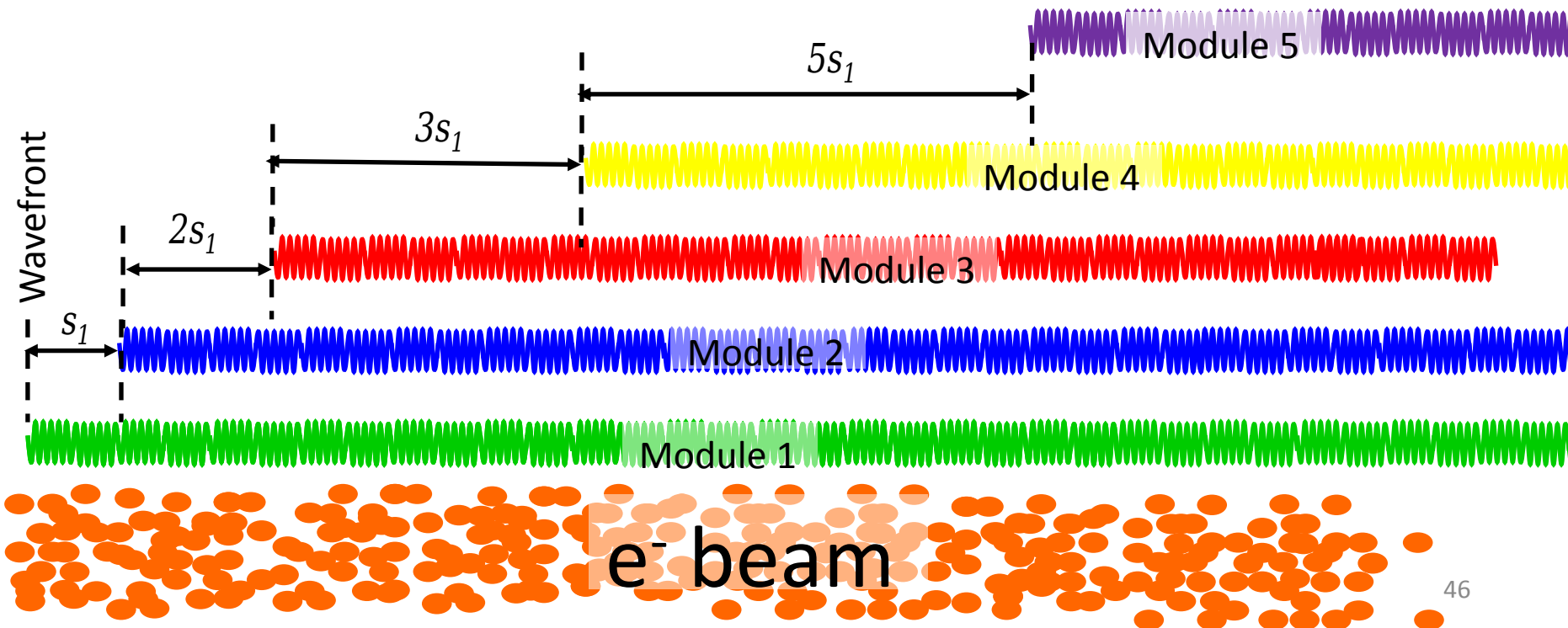
# HB-SASE Mechanism II

From Maxwell's wave equation:

$$\frac{da}{dz} = \langle \cos(\theta + \phi) \rangle, \quad \frac{d\phi}{dz} = -\frac{1}{a} \langle \sin(\theta + \phi) \rangle$$

The phase can adapt rapidly in linear regime due to the  $1/a$  term.

The phase coherence propagates rapidly at the enhanced slippage rate throughout the pulse



# HB-SASE: Simulation Results, Long Pulse, Scaled Units

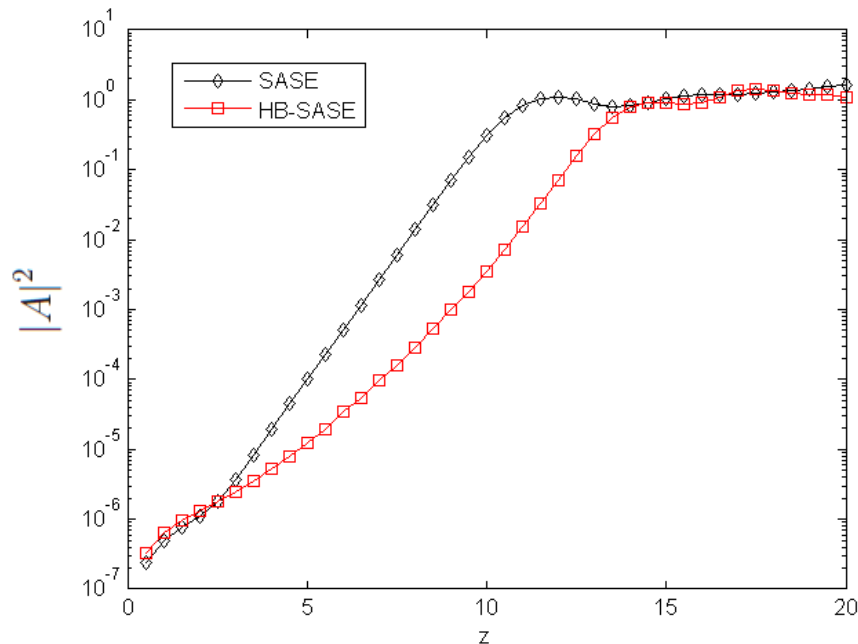
- Constant current,  $l_e = 4000$ , module length  $l = 0.5$ , delay sequence with  $s_1 = 4l$
- Coherence length calculated using:

$$\bar{l}_{coh} = \int |g(\bar{\tau}_1)|^2 d\bar{\tau}_1 \quad g(\bar{\tau}_1) = \frac{\langle A^*(\bar{z}_1)A(\bar{z}_1 + \bar{\tau}_1) \rangle}{\langle A^*(\bar{z}_1)A(\bar{z}_1) \rangle}$$

# HB-SASE: Simulation Results, Long Pulse, Scaled Units

- Constant current,  $l_e = 4000$ , module length  $l = 0.5$ , delay sequence with  $s_1 = 4l$
- Coherence length calculated using:

$$\bar{l}_{coh} = \int |g(\bar{\tau}_1)|^2 d\bar{\tau}_1 \quad g(\bar{\tau}_1) = \frac{\langle A^*(\bar{z}_1)A(\bar{z}_1 + \bar{\tau}_1) \rangle}{\langle A^*(\bar{z}_1)A(\bar{z}_1) \rangle}$$



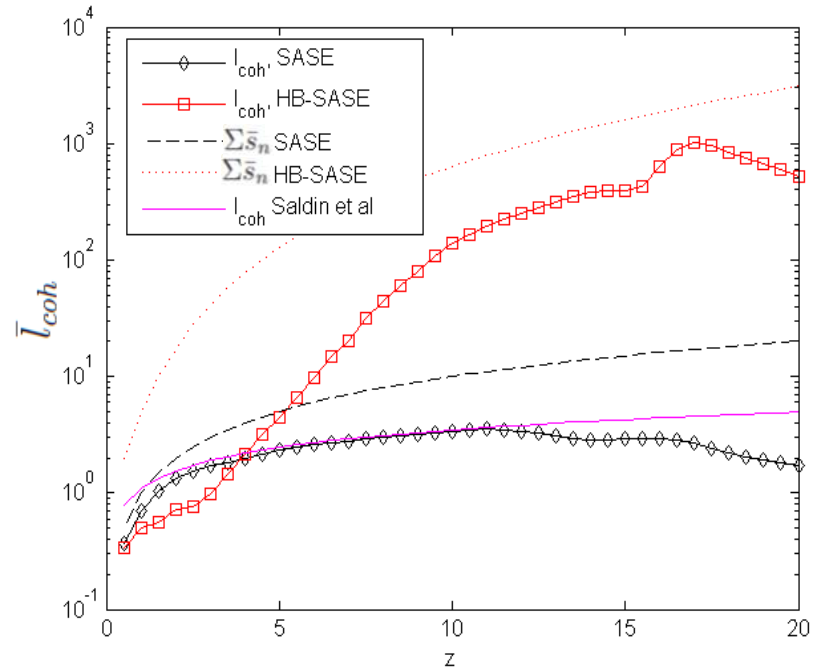
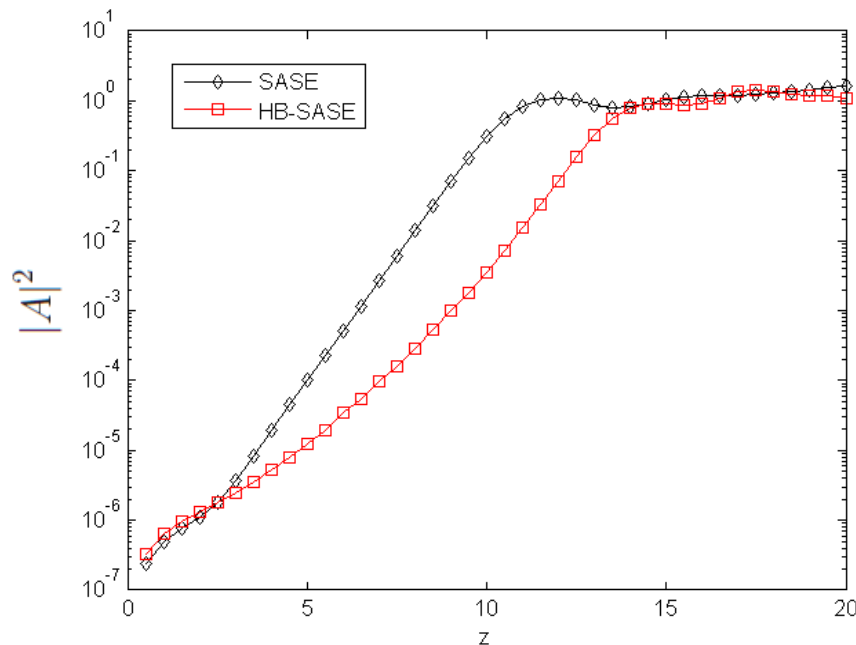


# HB-SASE: Simulation Results, Long Pulse, Scaled Units

- Constant current,  $l_e = 4000$ , module length  $l = 0.5$ , delay sequence with  $s_1 = 4l$
- Coherence length calculated using:

$$\bar{l}_{coh} = \int |g(\bar{\tau}_1)|^2 d\bar{\tau}_1$$

$$g(\bar{\tau}_1) = \frac{\langle A^*(\bar{z}_1)A(\bar{z}_1 + \bar{\tau}_1) \rangle}{\langle A^*(\bar{z}_1)A(\bar{z}_1) \rangle}$$

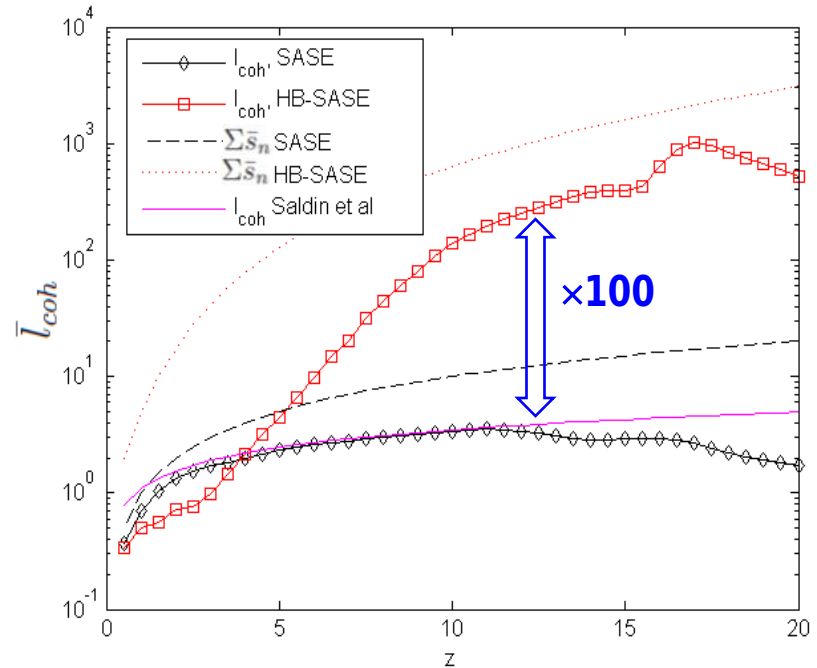
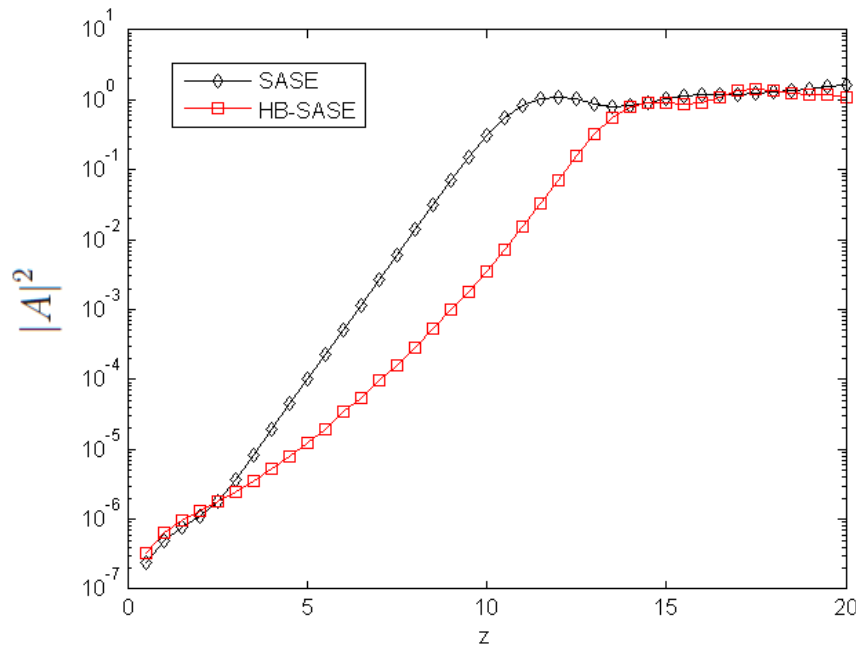


# HB-SASE: Simulation Results, Long Pulse, Scaled Units

- Constant current,  $l_e = 4000$ , module length  $l = 0.5$ , delay sequence with  $s_1 = 4l$
- Coherence length calculated using:

$$\bar{l}_{coh} = \int |g(\bar{\tau}_1)|^2 d\bar{\tau}_1$$

$$g(\bar{\tau}_1) = \frac{\langle A^*(\bar{z}_1)A(\bar{z}_1 + \bar{\tau}_1) \rangle}{\langle A^*(\bar{z}_1)A(\bar{z}_1) \rangle}$$

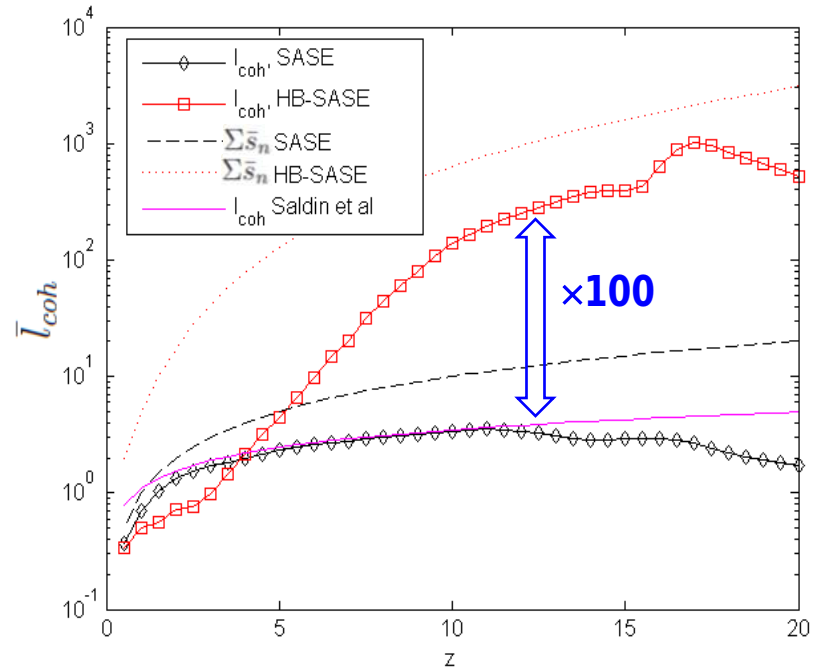
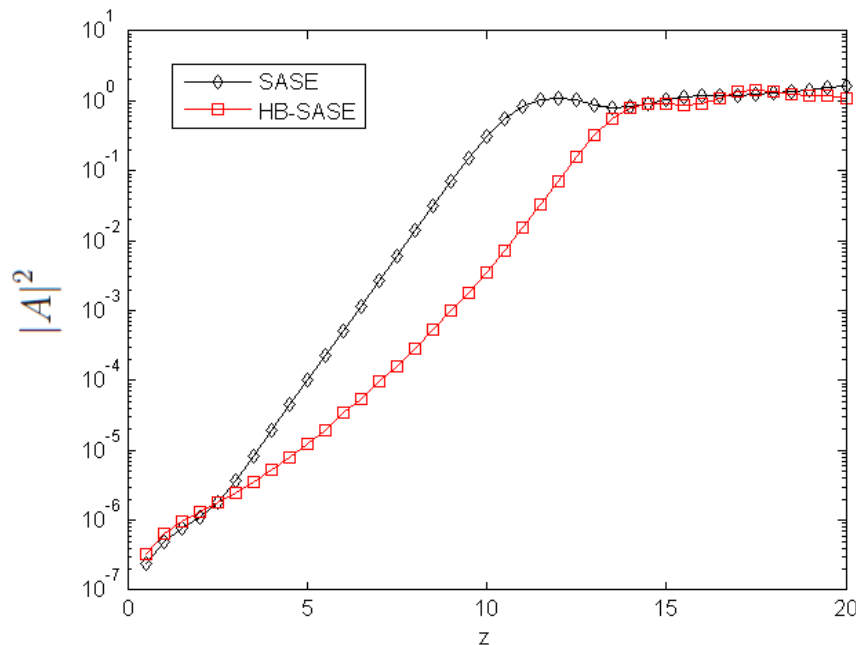


# HB-SASE: Simulation Results, Long Pulse, Scaled Units

- Constant current,  $I_e = 4000$ , module length  $l = 0.5$ , delay sequence with  $s_1 = 4l$
- Coherence length calculated using:

$$\bar{l}_{coh} = \int |g(\bar{\tau}_1)|^2 d\bar{\tau}_1$$

$$g(\bar{\tau}_1) = \frac{\langle A^*(\bar{z}_1)A(\bar{z}_1 + \bar{\tau}_1) \rangle}{\langle A^*(\bar{z}_1)A(\bar{z}_1) \rangle}$$



|                | $\bar{L}_{sat}$ | $\bar{l}_{coh}$ | $\bar{\sigma}_{\bar{\omega}}$ | $\bar{l}_{coh} \times \bar{\sigma}_{\bar{\omega}}$ |
|----------------|-----------------|-----------------|-------------------------------|--|
| <b>SASE</b>    | 12.0            | 3.4             | 0.5                           | 1.7 ( $\simeq \sqrt{\pi}$ )                        |
| <b>HB-SASE</b> | 14.5            | 393             | 0.0045                        | 1.8 ( $\simeq \sqrt{\pi}$ )                        |

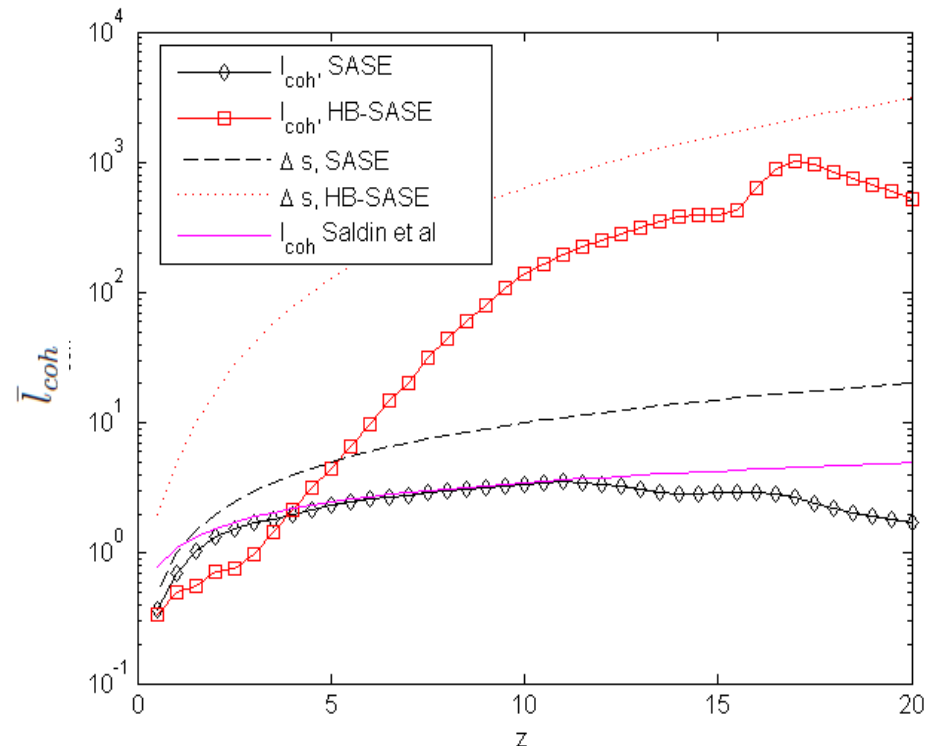
# HB-SASE Vs SASE: Comparison of Coherence Development

## ► SASE

- Coherence length evolves little after first three gain lengths, reaching half its saturation value by  $\bar{z} = 3$ , and always grows **more slowly** than the accumulated slippage

## ► HB-SASE

- Coherence length evolves more slowly for first three gain lengths, **then grows exponentially**



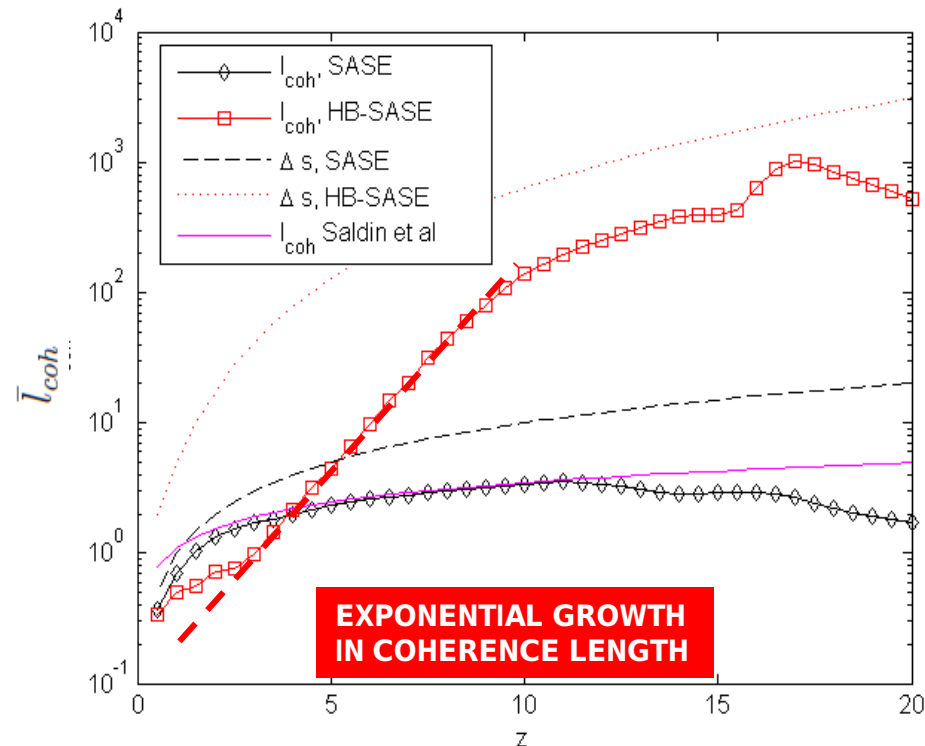
# HB-SASE Vs SASE: Comparison of Coherence Development

## ► SASE

- Coherence length evolves little after first three gain lengths, reaching half its saturation value by  $\bar{z} = 3$ , and always grows **more slowly** than the accumulated slippage

## ► HB-SASE

- Coherence length evolves more slowly for first three gain lengths, **then grows exponentially**



# HB-SASE Spectrum for simulation in soft X-ray at 1.24 nm\*

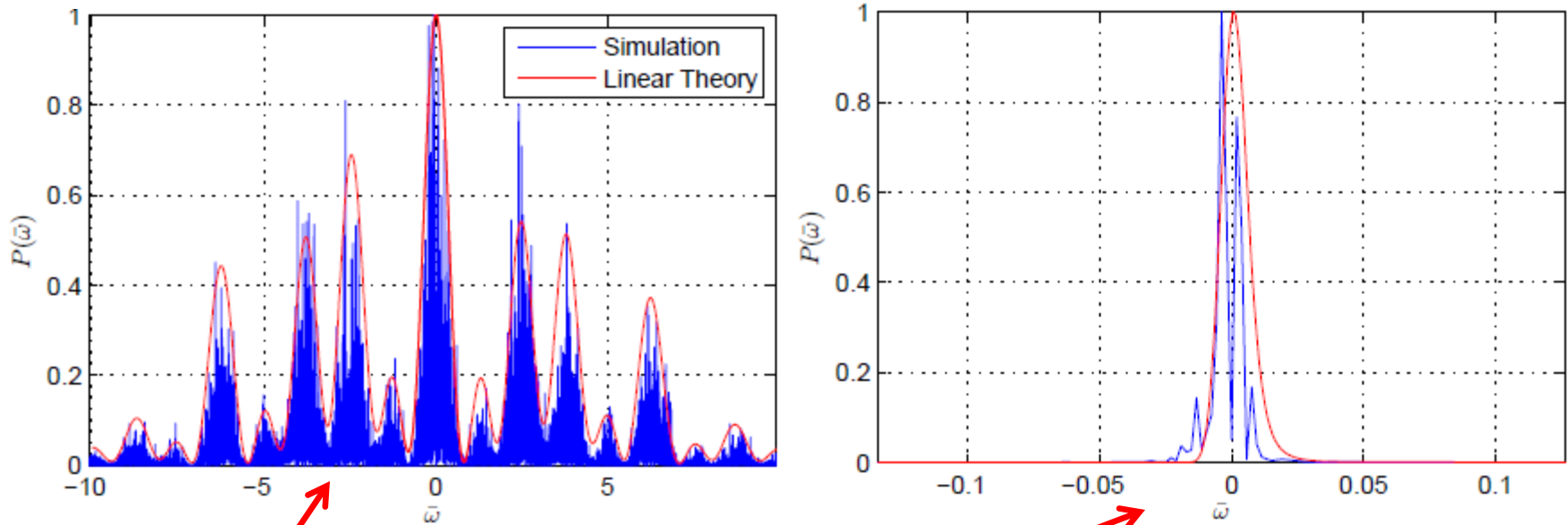


FIG. 3: Comparison of linear theory predictions of FEL spectra with simulation results, for the output after 3 modules (top) and 25 modules (bottom). Note the The  $x$ -axis range is adjusted on the bottom plot for clarity.

\*McNeil, Thompson and Dunning, Phys. Rev. Lett., **110**, 134802 (2013)

# HB-SASE Spectrum for simulation in soft X-ray at 1.24 nm\*

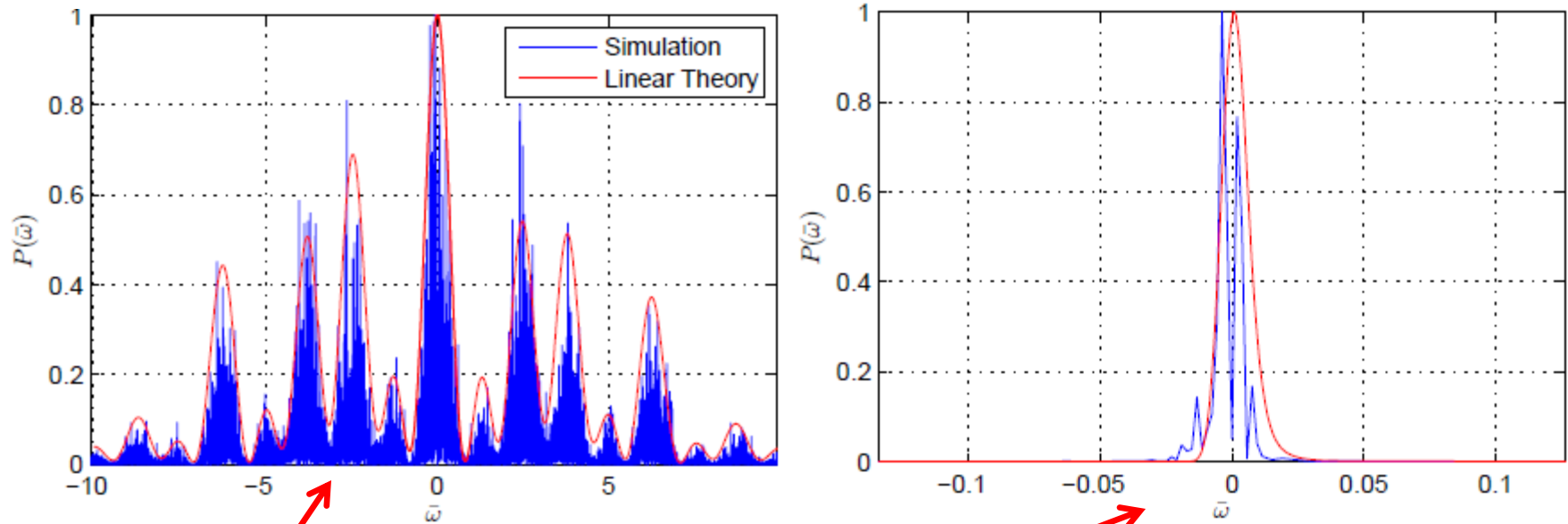


FIG. 3: Comparison of linear theory predictions of FEL spectra with simulation results, for the output after 3 modules (top) and 25 modules (bottom). Note the The  $x$ -axis range is adjusted on the bottom plot for clarity.

The system of shifts acts like a ‘distributed monochrometer’.

\*McNeil, Thompson and Dunning, Phys. Rev. Lett., **110**, 134802 (2013)

# SASE & HB-SASE comparison\*

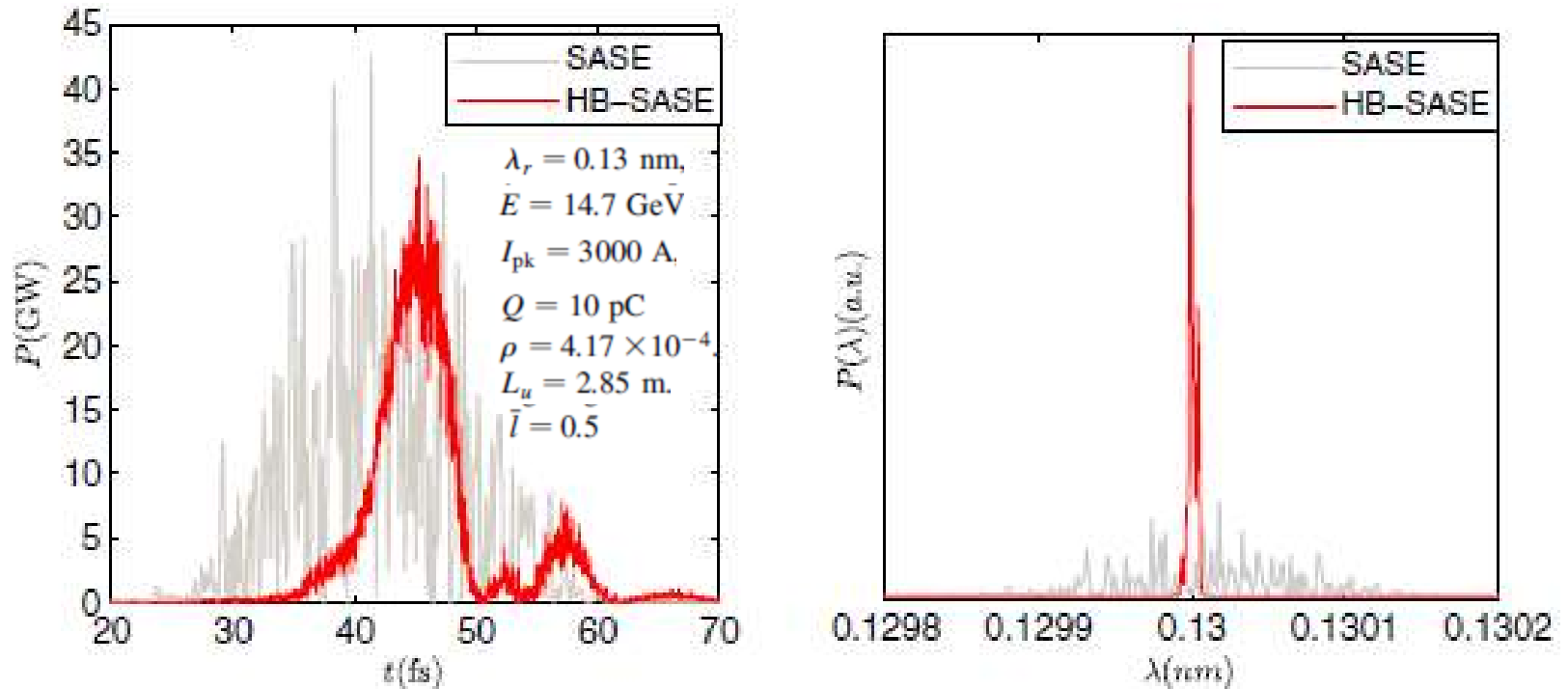


FIG. 3 (color online). Hard x-ray example at  $\lambda_r = 0.13$  nm: the pulse profiles and spectra of SASE and HB-SASE.

SASE:  $\Delta\nu\Delta t = 32$

Poor temporal coherence

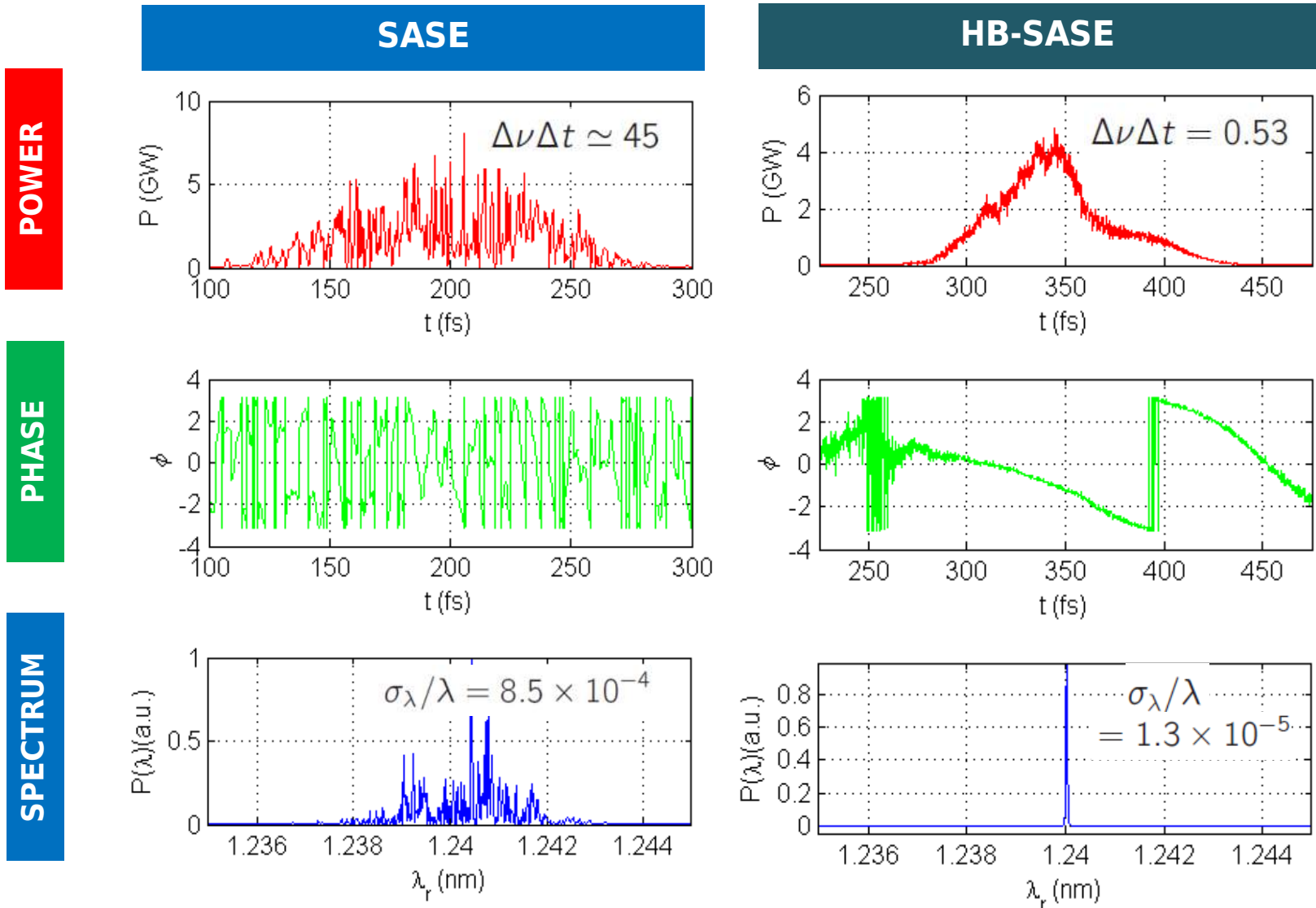
HB-SASE:  $\Delta\nu\Delta t = 0.85$

Excellent temporal coherence



# HB-SASE: 1.24nm Soft X-Ray Example

- **Parameters:**  $\lambda = 1.24\text{nm}$ ,  $E = 2.25\text{ GeV}$ ,  $I_{pk} = 1200\text{ A}$ ,  $Q = 200\text{ pC}$ ,  $\rho = 8.8 \times 10^{-4}$



# Very Related Research - iSASE

Proceedings of FEL2012, Nara, Japan

TUPD07

## GENERATION OF LONGITUDINALLY COHERENT ULTRA HIGH POWER X-RAY FEL PULSES BY PHASE AND AMPLITUDE MIXING\*

J. Wu<sup>#</sup>, SLAC, Menlo Park, CA 94025, USA

A. Marinelli, UCLA, Los Angeles, California 90095-1547, USA

C. Pellegrini, UCLA, Los Angeles, CA 90095-1547, USA, SLAC, Menlo Park, CA 94025, USA

- ***iSASE (Improved SASE)***
  - Chicanes used to delay electron bunches between undulator modules
  - Proposed a ***Geometric*** sequence of increasing delays
  - **Good temporal coherence (~constant phase) enables efficiently tapered undulator for ultra-high peak power – predict TW-level powers**
  - Proof-of-principle experiment on LCLS over a limited parameter range, using detuned undulators as delay sections, showed a threefold reduction in SASE linewidth, in agreement with expectation for the parameters used.
  - Demonstrated stability to electron beam energy jitter

# Very Related Research - iSASE

Proceedings of FEL2012, Nara, Japan

TUPD07

## GENERATION OF LONGITUDINALLY COHERENT ULTRA HIGH POWER X-RAY FEL PULSES BY PHASE AND AMPLITUDE MIXING\*

J. Wu<sup>#</sup>, SLAC, Menlo Park, CA 94025, USA

A. Marinelli, UCLA, Los Angeles, California 90095-1547, USA

C. Pellegrini, UCLA, Los Angeles, CA 90095-1547, USA, SLAC, Menlo Park, CA 94025, USA

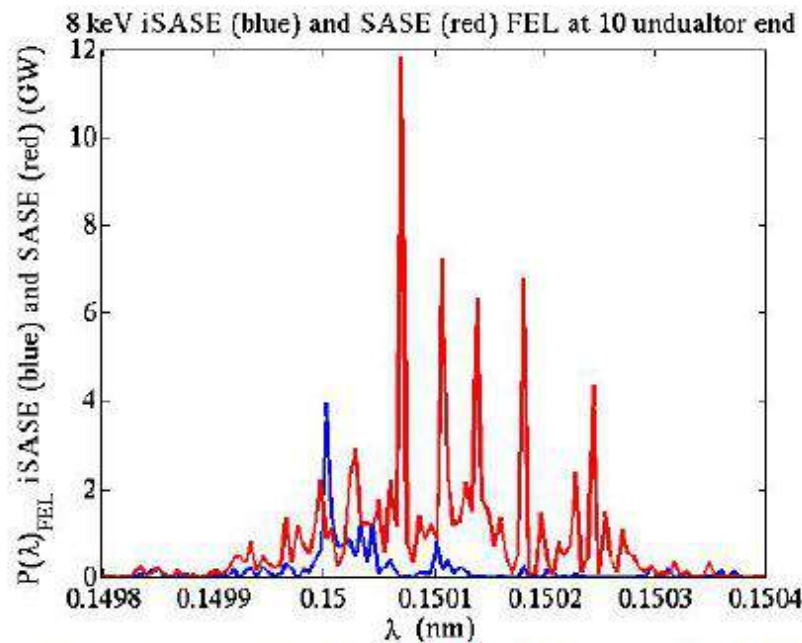


Figure 3: Spectrum of iSASE (blue) and SASE (red) radiation after 10 undulator modules. iSASE FWHM bandwidth is  $5.1\text{E-}05$ , compared to  $1.5\text{E-}03$  for SASE.

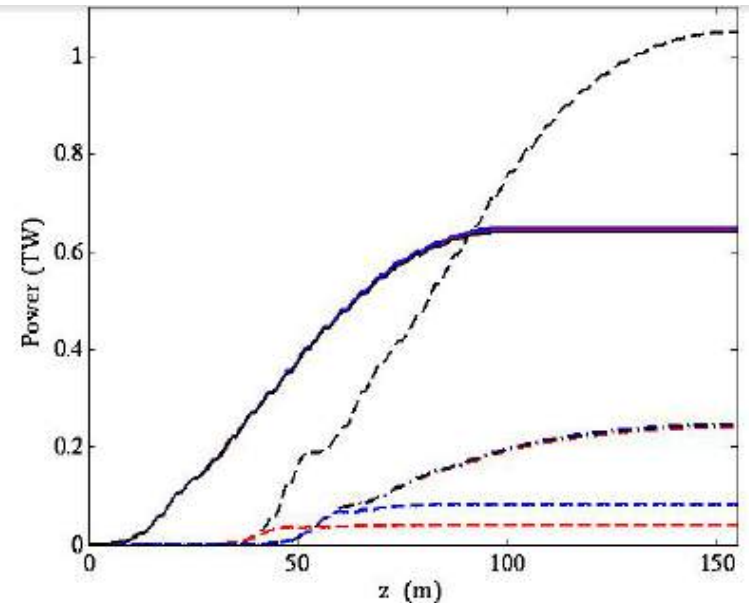


Figure 5: FEL power gain curve variation for a  $\pm 0.1\%$  energy jitter: on-energy (black),  $0.1\%$  (red), and  $-0.1\%$  (blue), and SASE (dash-dotted), iSASE (solid), and Self-seeding (dashed).

# Experiment!

WEODB101

Proceedings of IPAC2013, Shanghai, China

## X-RAY SPECTRA AND PEAK POWER CONTROL WITH ISASE\*

J. Wu<sup>†</sup>, C. Pellegrini, A. Marinelli, H.-D. Nuhn, F.-J. Decker, H. Loos, A. Lutman, D. Ratner, Y. Feng, J. Krzywinski, D. Zhang, D. Zhu, SLAC, Menlo Park, CA 94025, USA

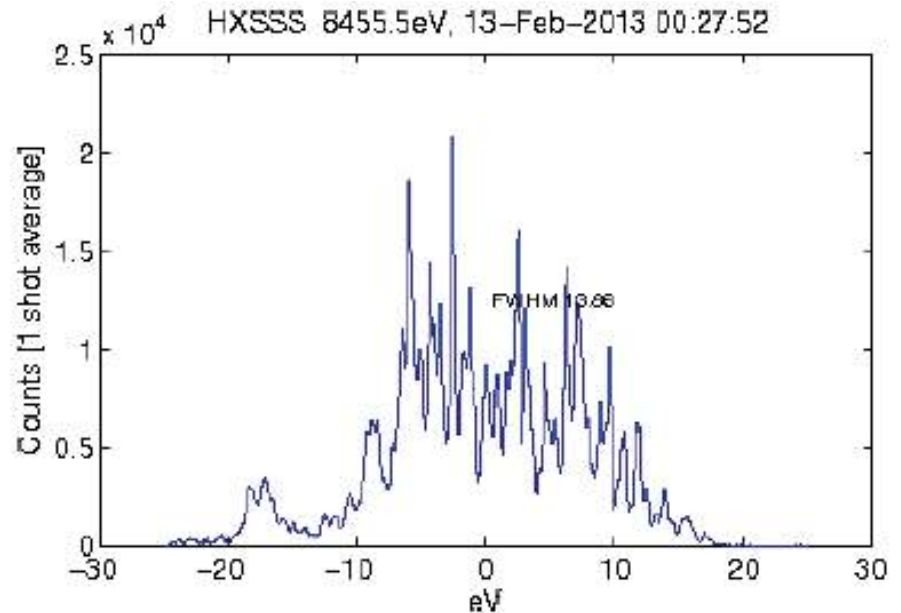
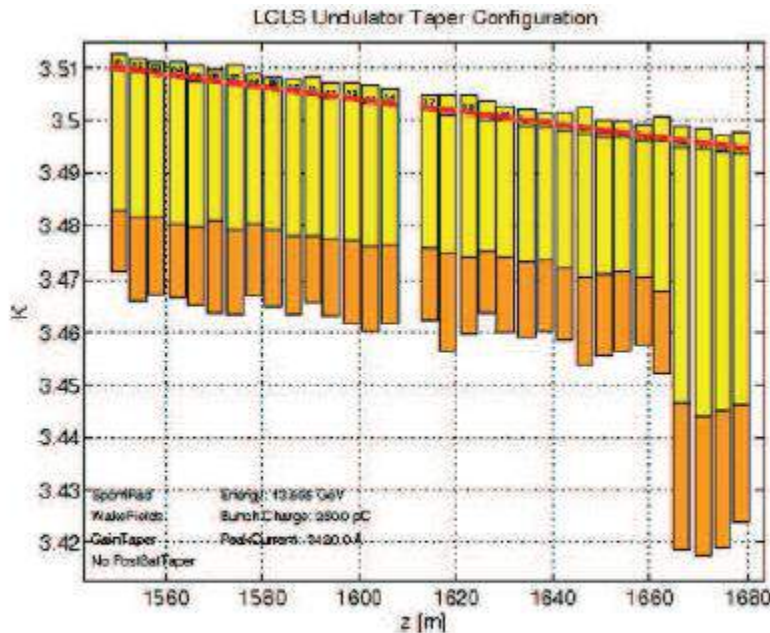


Figure 3: Undulator setup for SASE experiment at LCLS. Figure 4: A SASE FEL spectrum with undulator in Fig. 3.

**SASE**



# Experiment!

WEODB101

Proceedings of IPAC2013, Shanghai, China

## X-RAY SPECTRA AND PEAK POWER CONTROL WITH ISASE\*

J. Wu<sup>†</sup>, C. Pellegrini, A. Marinelli, H.-D. Nuhn, F.-J. Decker, H. Loos, A. Lutman, D. Ratner, Y. Feng, J. Krzywinski, D. Zhang, D. Zhu, SLAC, Menlo Park, CA 94025, USA

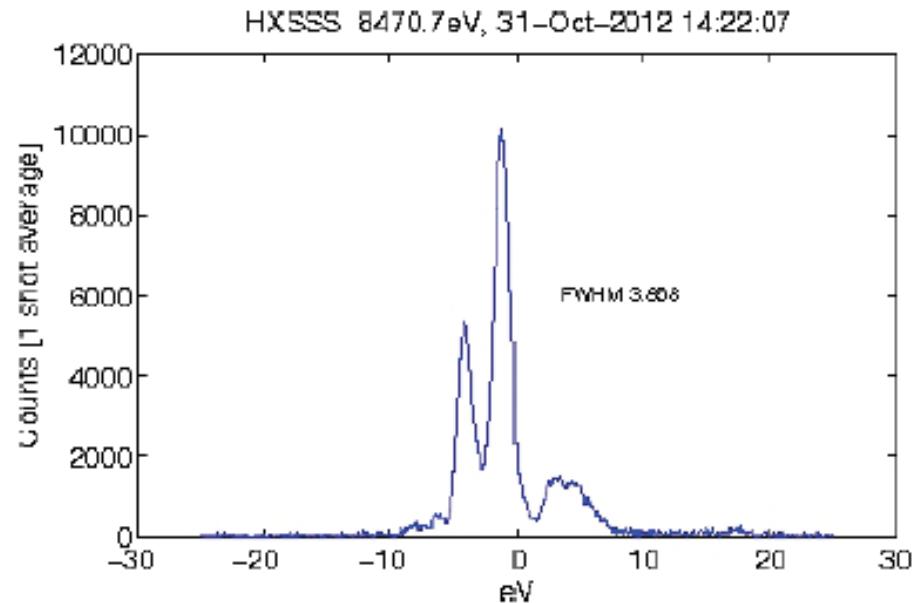
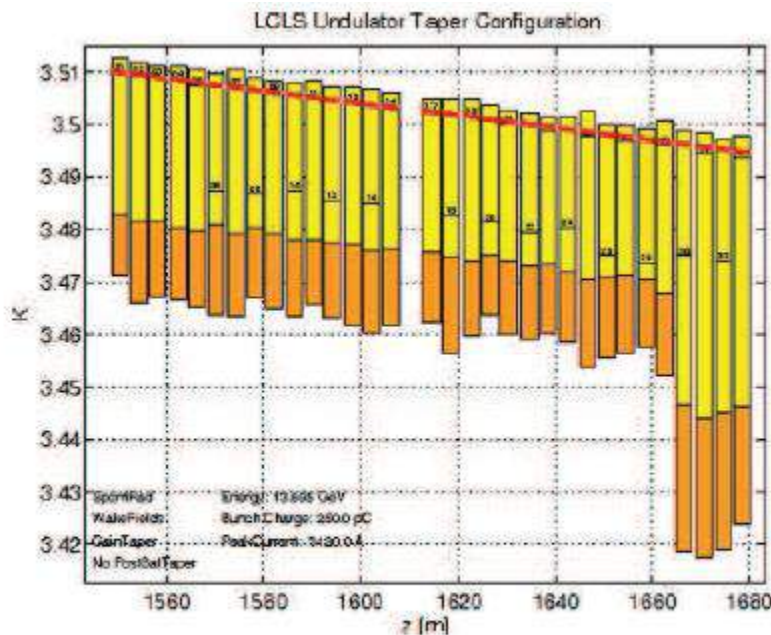


Figure 5: Undulator setup for iSASE experiment at LCLS. Figure 6: An iSASE FEL spectrum with undulator in Fig. 5.

iSASE



## Purified self-amplified spontaneous emission free-electron lasers with slippage-boosted filtering

Dao Xiang, Yuantao Ding, and Zhirong Huang

SLAC National Accelerator Laboratory, Menlo Park, California 94025, USA

Haixiao Deng

- ***pSASE (Purified SASE)***

- A few undulator sections (called slippage boosted sections – U2 below), resonant at a sub-harmonic of the FEL, are used in the middle stage of the exponential growth regime to amplify the radiation while simultaneously reducing the bandwidth

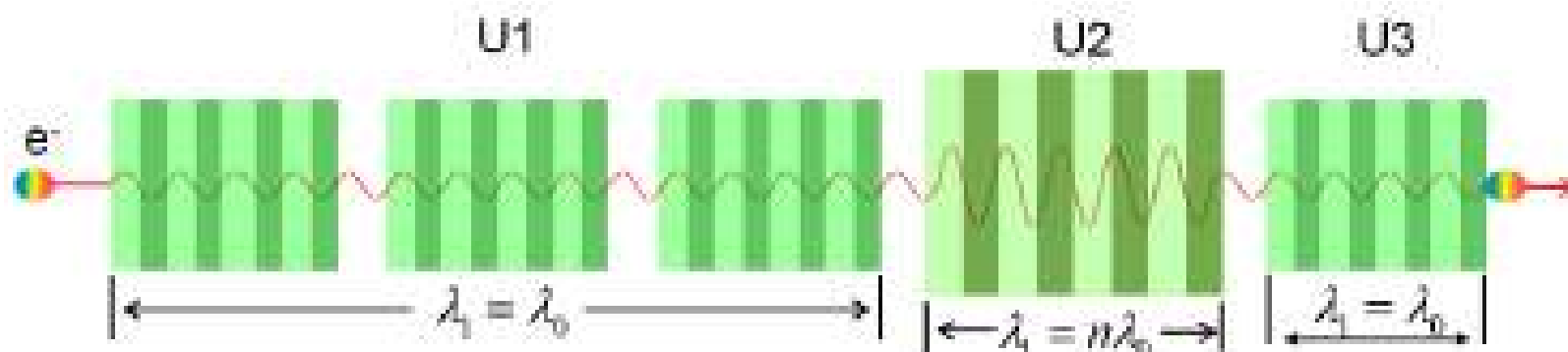
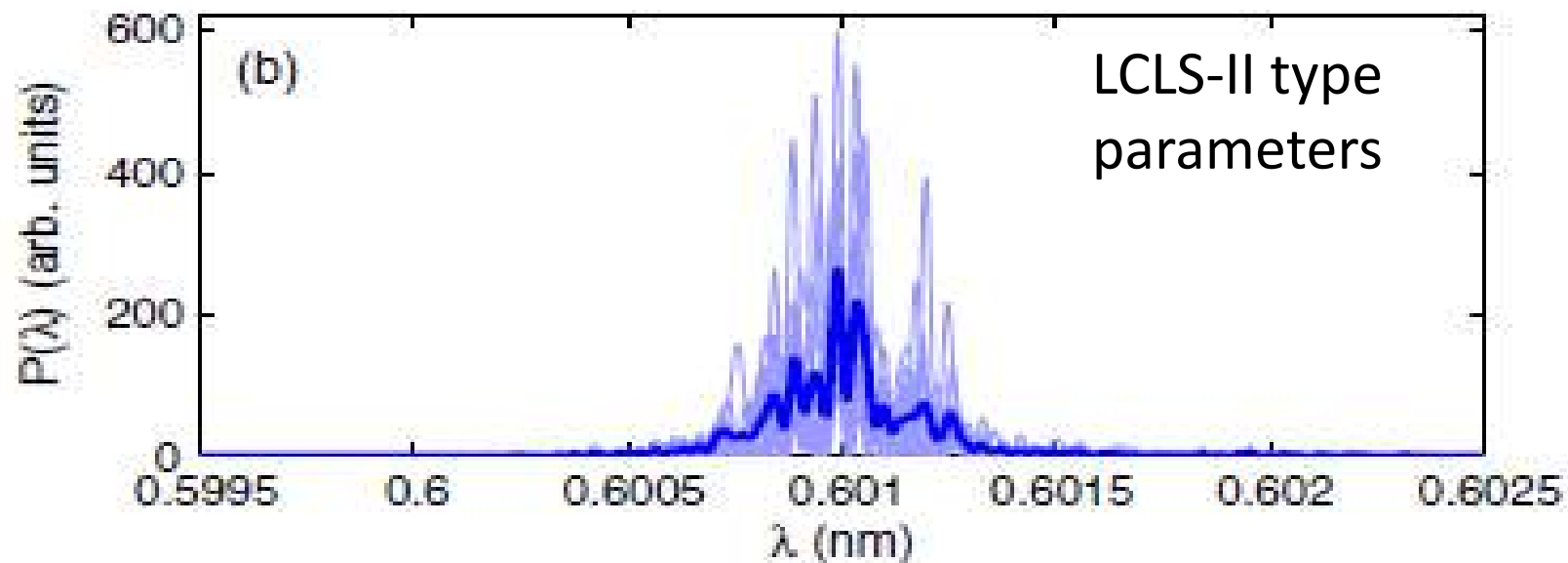
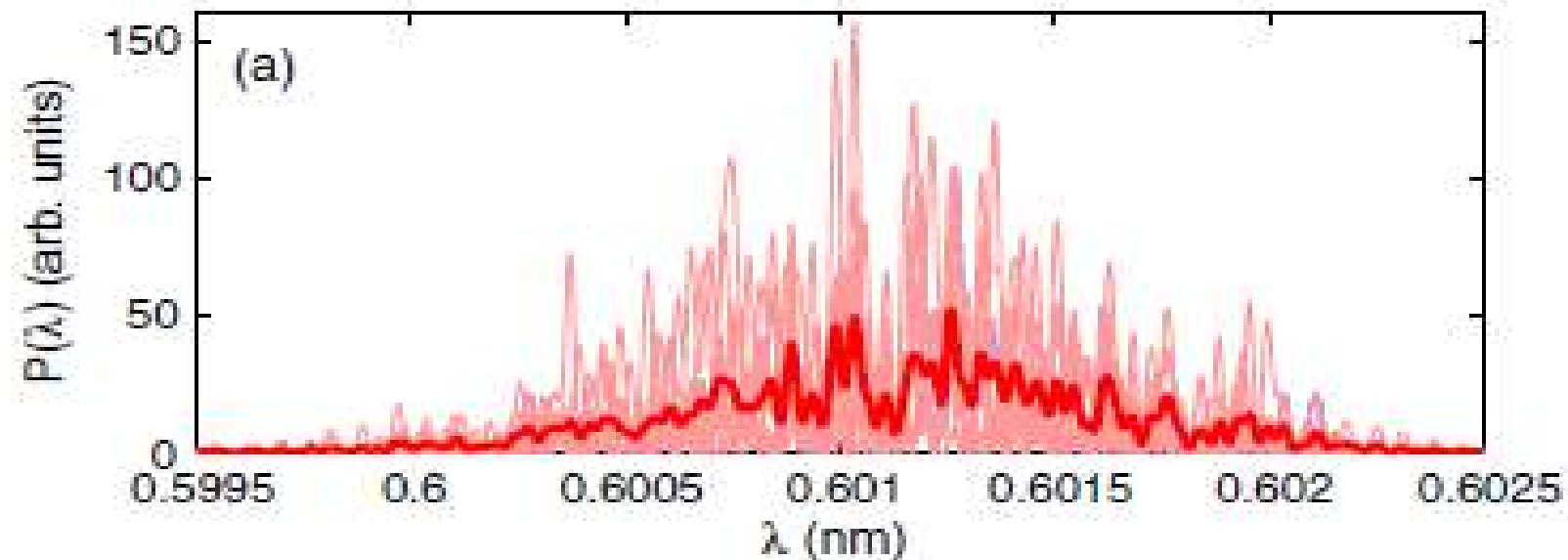


FIG. 2 Schematic layout of a pSASE FEL.



## Purified self-amplified spontaneous emission free-electron lasers with slippage-boosted filtering



# Practical Issues

- **Undulator module lengths**

- Undulator modules should ideally be less than a gain length to prohibit localised effect

| Scaled Undulator Length $\bar{l}$                | 0.5     | 1.0         | 2.0         |
|--|---------|-------------|-------------|
| Maximum $\frac{I_{coh}(HB-SASE)}{I_{coh}(SASE)}$ | $> 100$ | $\simeq 50$ | $\simeq 10$ |

- **Electron Beam Delays**

- Our work shown here uses isochronous chicanes which do not affect rate of electron microbunching
- Small deviation from non-isochronicity is OK. Simulation studies over limited parameter ranges have shown so far that the chicane must have  $R_{56} < 10\%$  of that of a standard 4-dipole chicane
- A design was developed at ASTeC\* that meets  $R_{56} < 10\%$  for the hard x-ray case shown here.
- For standard non-isochronous chicanes, increase in coherence length over SASE limited to **approximately  $\times 5$**
- An alternative might be to use standard dipole chicanes with correction in occasional negative  $R_{56}$  delays – yet to be investigated.....

- **Electron Beam Stability**

- For isochronous delays, if beam energy jitters the FEL wavelength will change but delay remain constant. This will destroy phase matching.
- For hard x-ray parameters shown here, for the largest delay to remain phase matched to  $\lambda/4$ , electron beam energy must jitter relatively by less than  $5 \times 10^{-5}$

\*J. K. Jones *et al.*, Proc. IPAC, TUPPP069 1759 (2012) .



# HB-SASE Summary

- **HB-SASE**
  - May be an alternative or additional method for improving the longitudinal coherence of SASE FELs.
  - **Requires no optics** and could in principle work at **any wavelength and repetition rate**.
  - May enable generation of transform limited X-ray FEL pulses
  - Delocalises the collective FEL interaction and breaks the dependence of the radiation coherence length on the FEL cooperation length
  - Exhibits exponential growth of radiation coherence length
  - Can be adapted for ML-SASE: equal chicanes → few-cycle pulse trains
- Work so far based on some analysis and one-dimensional simulations (but HB-SASE is a longitudinal effect, which is well modelled in 1D)
- Further study required to include 3D effects and full tracking through isochronous chicanes

# CLARA – a new UK test facility

# [Compact Linear Accelerator for Research and Applications]



PUBLISHED BY IOP PUBLISHING FOR SISSA MEDIALAB

RECEIVED: *January 21, 2014*

ACCEPTED: *March 25, 2014*

PUBLISHED: *May 9, 2014*

TECHNICAL REPORT

## CLARA conceptual design report

---

J.A. Clarke,<sup>a,b,\*</sup> D. Angal-Kalinin,<sup>a,b</sup> N. Bliss,<sup>a</sup> R. Buckley,<sup>a,b</sup> S. Buckley,<sup>a,b</sup> R. Cash,<sup>a</sup>  
P. Corlett,<sup>a,b</sup> L. Cowie,<sup>a,b</sup> G. Cox,<sup>a</sup> G.P. Diakun,<sup>a,b</sup> D.J. Dunning,<sup>a,b</sup> B.D. Fell,<sup>a</sup>  
A. Gallagher,<sup>a</sup> P. Goudket,<sup>a,b</sup> A.R. Goulden,<sup>a,b</sup> D.M.P. Holland,<sup>a,b</sup> S.P. Jamison,<sup>a,b</sup>  
J.K. Jones,<sup>a,b</sup> A.S. Kalinin,<sup>a,b</sup> W. Liggins,<sup>a,b</sup> L. Ma,<sup>a,b</sup> K.B. Marinov,<sup>a,b</sup> B. Martlew,<sup>a</sup>  
P.A. McIntosh,<sup>a,b</sup> J.W. McKenzie,<sup>a,b</sup> K.J. Middleman,<sup>a,b</sup> B.L. Militsyn,<sup>a,b</sup> A.J. Moss,<sup>a,b</sup>  
B.D. Muratori,<sup>a,b</sup> M.D. Roper,<sup>a,b</sup> R. Santer,<sup>a,b</sup> Y. Saveliev,<sup>a,b</sup> E. Snedden,<sup>a,b</sup>  
R.J. Smith,<sup>a,b</sup> S.L. Smith,<sup>a,b</sup> M. Surman,<sup>a,b</sup> T. Thakker,<sup>a,b</sup> N.R. Thompson,<sup>a,b</sup>  
R. Valizadeh,<sup>a,b</sup> A.E. Wheelhouse,<sup>a,b</sup> P.H. Williams,<sup>a,b</sup> R. Bartolini,<sup>c,d</sup> I. Martin,<sup>c</sup>  
R. Barlow,<sup>c</sup> A. Kolano,<sup>c</sup> G. Burt,<sup>b,f</sup> S. Chattopadhyay,<sup>b,f,g,h</sup> D. Newton,<sup>b,g</sup> A. Wolski,<sup>b,g</sup>  
R.B. Appleby,<sup>b,h</sup> H.L. Owen,<sup>b,h</sup> M. Serluca,<sup>b,h</sup> G. Xia,<sup>b,h</sup> S. Boogert,<sup>i</sup> A. Lyapin,<sup>i</sup>  
L. Campbell,<sup>j</sup> B.W.J. McNeil<sup>j</sup> and V.V. Paramonov<sup>k</sup>


CLARA – a new UK test facility

# [Compact Linear Accelerator Research and Development]



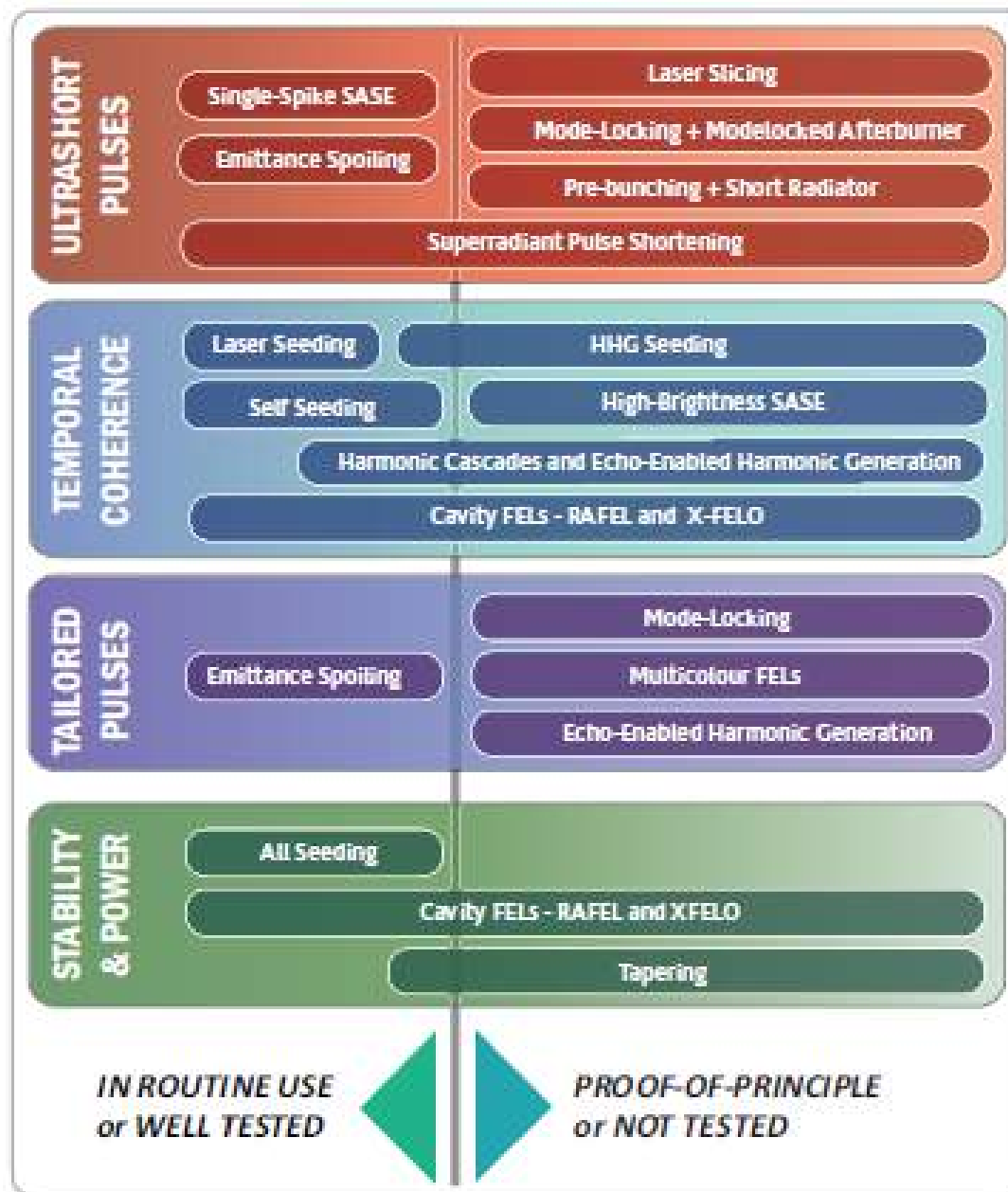
TECHNOLOGY

2014



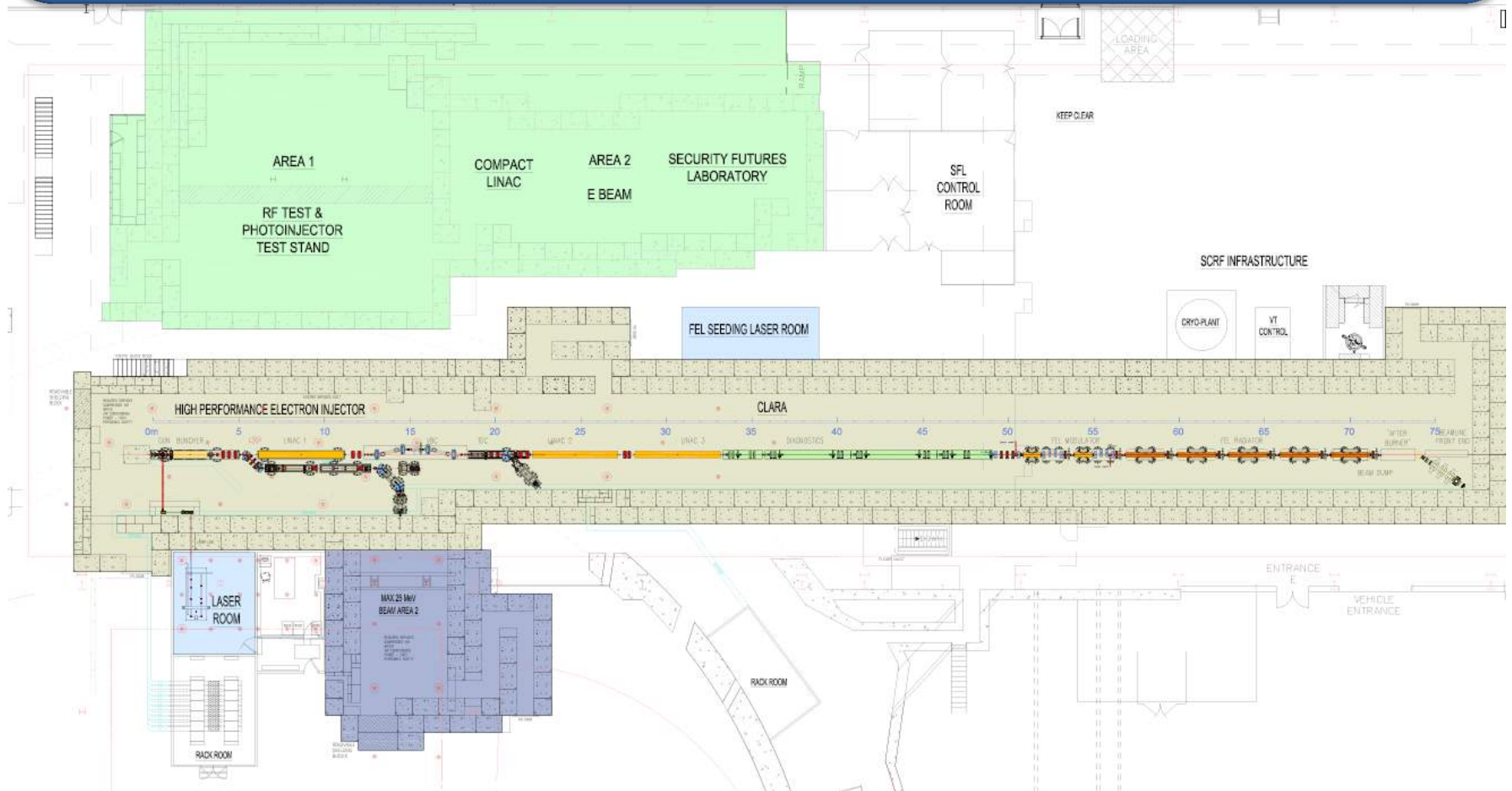
Clarastrasse

...y,<sup>a,b</sup> S. Buckley,<sup>a,b</sup> R. Cash,<sup>a</sup>  
...J. Dunning,<sup>a,b</sup> B.D. Fell,<sup>a</sup>  
...D.M.P. Holland,<sup>a,b</sup> S.P. Jamison,<sup>a,b</sup>  
...L. Ma,<sup>a,b</sup> K.B. Marinov,<sup>a,b</sup> B. Martlew,<sup>a</sup>  
...K.J. Middleman,<sup>a,b</sup> B.L. Militsyn,<sup>a,b</sup> A.J. Moss,<sup>a,b</sup>  
...R. Santer,<sup>a,b</sup> Y. Saveliev,<sup>a,b</sup> E. Snedden,<sup>a,b</sup>  
...M. Surman,<sup>a,b</sup> T. Thakker,<sup>a,b</sup> N.R. Thompson,<sup>a,b</sup>  
...Wheelhouse,<sup>a,b</sup> P.H. Williams,<sup>a,b</sup> R. Bartolini,<sup>c,d</sup> I. Martin,<sup>c</sup>  
...colano,<sup>c</sup> G. Burt,<sup>b,f</sup> S. Chattopadhyay,<sup>b,f,g,h</sup> D. Newton,<sup>b,g</sup> A. Wolski,<sup>b,g</sup>  
...oy,<sup>b,h</sup> H.L. Owen,<sup>b,h</sup> M. Serluca,<sup>b,h</sup> G. Xia,<sup>b,h</sup> S. Boogert,<sup>i</sup> A. Lyapin,<sup>i</sup>  
...mpbell,<sup>j</sup> B.W.J. McNeil<sup>j</sup> and V.V. Paramonov<sup>k</sup>

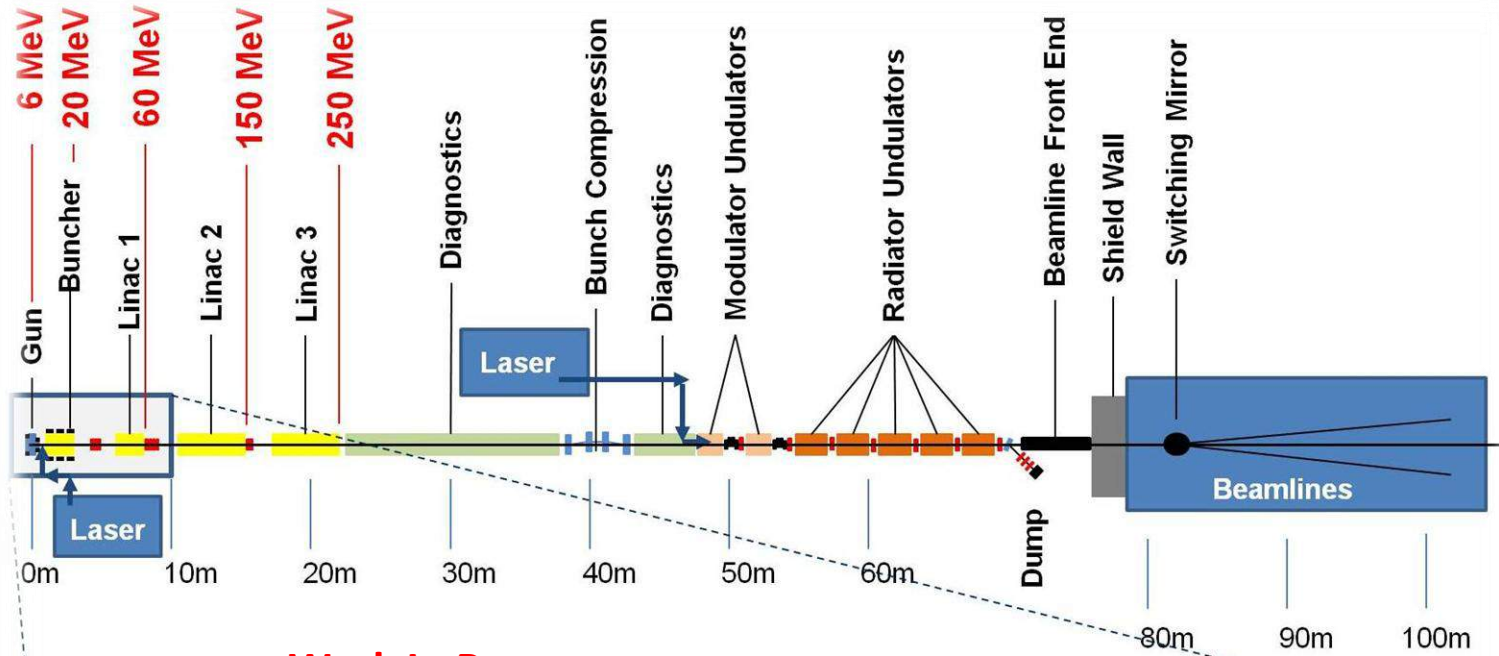


**Figure 1.2.** Schematic representation of the FEL landscape in terms of potential improvements to particular output properties against progress to date. 59

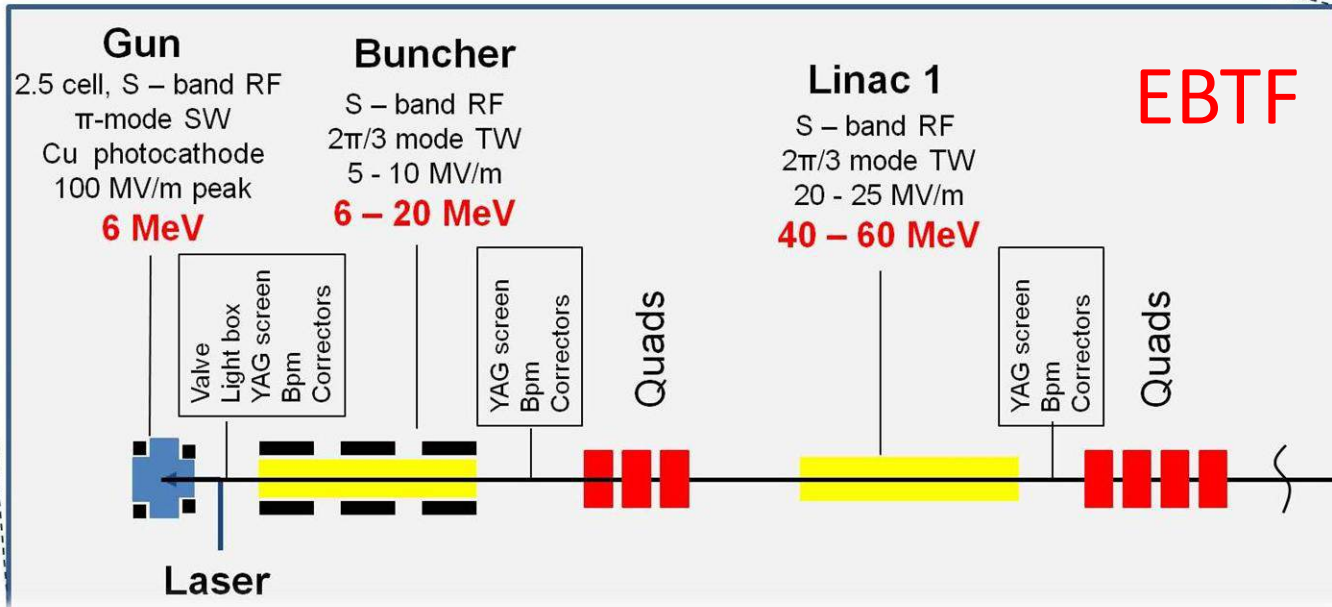
To develop a normal conducting test accelerator able to generate longitudinally and transversely bright electron bunches and to use these bunches in the experimental production of **stable, synchronised, ultra short** photon pulses of coherent light from a single pass FEL with techniques directly applicable to the future generation of light source facilities.

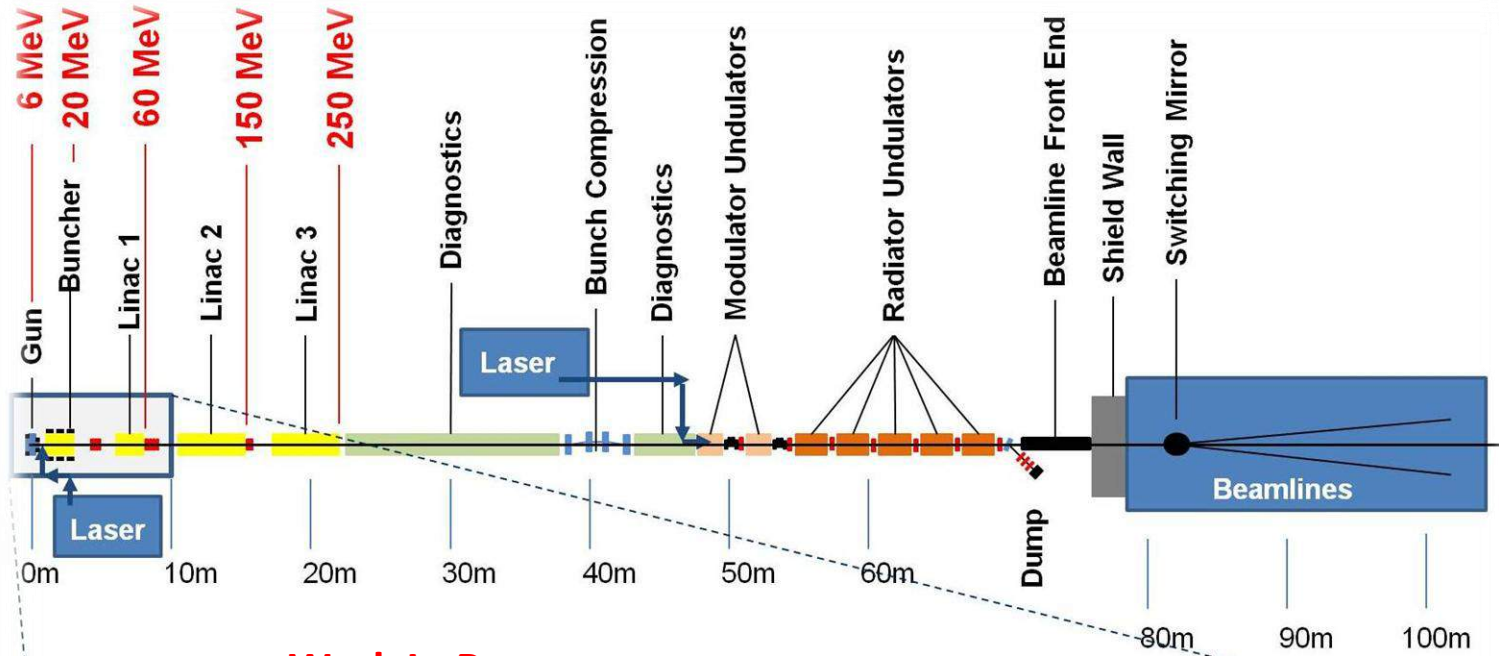






**Work In Progress**





Work In Progress

2.5 ce  
 $\pi$   
Cu  
10

**Now funded to**

**150 MeV!**

Laser

$\Gamma$  F

**Thank You!**